

**Three Dimensional Vascular Supply to Human Skeletal Muscles: An
Anatomical Analysis of Potential Donor Muscles for Segmental Muscle Transfer**

by

Khalid Mutlag Almutairi

**Submitted in partial fulfillment of the requirements
for the degree of Master of Science**

at

Dalhousie University

Halifax, Nova Scotia

March 2012

©Copyright by Khalid Mutlag Almutairi, 2012

DALHOUSIE UNIVERSITY

DEPARTMENT OF ANATOMY AND NEUROBIOLOGY

The undersigned hereby certify that they have read and recommend to the Faculty of Graduate Studies for acceptance a thesis entitled “Three Dimensional Vascular Supply to Human Skeletal Muscles: An Anatomical Analysis Of Potential Donor muscles for segmental muscle transfer” by Khalid Mutlag Almutairi in partial fulfillment of the requirements for the degree of Master of Science.

Dated: March 6, 2012

Supervisor:

Readers:

DALHOUSIE UNIVERSITY

DATE: March 6, 2012

AUTHOR: Khalid Mutlag Almutairi

TITLE: Three Dimensional Vascular Supply to Human Skeletal Muscles: An Anatomical Analysis of Potential Donor Muscles For Segmental Muscle Transfer

DEPARTMENT OR SCHOOL: Department of Anatomy and Neurobiology

DEGREE: MSc. CONVOCATION: MAY YEAR: 2012

Permission is herewith granted to Dalhousie University to circulate and to have copied for non-commercial purposes, at its discretion, the above title upon the request of individuals or institutions. I understand that my thesis will be electronically available to the public.

The author reserves other publication rights, and neither the thesis nor extensive extracts from it may be printed or otherwise reproduced without the author's written permission.

The author attests that permission has been obtained for the use of any copyrighted material appearing in the thesis (other than the brief excerpts requiring only proper acknowledgement in scholarly writing), and that all such use is clearly acknowledged.

Signature of Author

DEDICATION

To my parents Najat and Mutlag Almutairi for their unconditional love and support.

TABLE OF CONTENTS

LIST OF FIGURES	x
LIST OF TABLES	xv
ABSTRACT	xvii
LIST OF ABBREVIATIONS USED.....	xviii
ACKNOWLEDGMENTS	xxii
CHAPTER 1.0 INTRODUCTION	1
1.1 Historical Background	2
1.2 The Evolution of Angiography	3
1.3 Current Angiographic Techniques	4
1.4 Classification of Skeletal Muscles	5
1.5 Objectives	8
1.5.1 Phase I: Evaluating Mathes and Nahai's Classification.....	8
1.5.2 Phase II: Three Dimensional Analysis of Human Skeletal Muscles	8
1.5.2.1 Part (A) Animal Injection Study	9
1.5.2.2 Part (B) Cadaver Injection Study	9
1.5.2.3 Ethics statement	9

CHAPTER 2.0 EVALUATING MATHES AND NAHAI'S CLASSIFICATION

(PHASE I).....	10
Abstract: The Vascular Supply of Muscles of the Body.....	11
2.1 Materials and Methods.....	12
2.2 Results and Findings of Phase I.....	12
2.2.1 Muscles of the Head and Neck.....	13
2.2.2 The Trunk.....	19
2.2.2.1 Muscles of the Chest.....	19
2.2.2.2 Muscles of the Abdomen.....	24
2.2.2.3 Muscles of the Back.....	31
2.2.3 Upper Extremity.....	38
2.2.3.1 Muscles of the Shoulder.....	38
2.2.3.2 Muscles of the Arm.....	41
2.2.3.3 Muscles of the Forearm.....	48
2.2.3.4 Muscles of the Hand.....	70
2.2.4 Lower Extremity.....	78
2.2.4.1 Muscles of the Hip.....	78
2.2.4.2 Muscles of the Thigh.....	80

2.2.4.3 Muscles of the Leg.....	88
2.2.4.4 Muscles of the Foot.....	96
2.2.5 Discussion	102
2.2.6 Conclusion of Phase I	107
 CHAPTER 3.0 THREE DIMENSIONAL ANALYSIS OF THE VASCULAR ANATOMY (PHASE II)	
3.1 Introduction.....	109
3.1.1 History of Three Dimensional Imaging.....	109
3.1.2 Importance of Three Dimensional Imaging in Surgical Planning.....	110
3.2 Review of Current Popular Contrast Mixtures	112
3.2.1 Lead Oxide Gelatin Mixtures	112
3.2.2 Iodine Based Mixtures.....	112
3.2.3 Barium Based Mixtures	112
3.2.4 Gadolinium Based Mixtures.....	112
3.2.5 Discussion.....	113
3.2.6 Conclusion	114
3.3 Part (A) Animal Injection Study	115

Abstract A: A Novel Three Dimensional Technique for Imaging Vessels in Animals	115
3.3.1 Objectives	116
3.3.2 Materials and Methods	116
3.3.2.1 Animal Injection Protocol.....	116
3.3.2.2 Group A: Modified Lead Oxide with Gelatin.....	117
3.3.2.3 Group B: Modified Iodine with Gelatin.....	117
3.3.2.4 Group C: Barium Sulphate with Gelatin.....	118
3.3.2.5 Group D: Gadolinium with Gelatin	118
3.3.2.6 Computed Tomography Scanner Settings	118
3.3.2.7 Computer Aided Design and Data Analysis	121
3.3.3 Results.....	122
3.3.4 Discussion	128
3.3.5 Conclusion	128
CHAPTER 4.0 CADAVER INJECTION STUDY, PHASE II PART (B).....	129
Abstract B: Three Dimensional Analysis of Human Skeletal Muscles.....	130
4.1 Materials and Methods	131
4.2 Results and Discussion	132
4.2.1 Head and Neck.....	132

4.2.2 Trunk.....	140
4.2.3 Upper Extremity.....	148
4.2.4 Lower Extremity	161
CHAPTER 5.0 CONCLUSION	185
BIBLIOGRAPHY.....	190

List of Figures

Figure 1: Current Techniques in Angiography	6
Figure 2: Mathes and Nahai's Classification	7
Figure 3: Head and Neck Muscles	17
Figure 4: Muscles of the Chest	21
Figure 5: Serratus Anterior	22
Figure 6: Rectus Abdominis	26
Figure 7: Transverse Abdominis, Internal and External Oblique	27
Figure 8: Iliopsoas Muscle:	29
Figure 9: Right and left Latissimus Dorsi Muscle	35
Figure 10: The Angiographic Territories of Trapezius (also see Trapezius in 3D)	36
Figure 11: Vascular Territories of the Deltoid Muscle	40
Figure 12: Angiogram of Biceps Brachii	43
Figure 13: Angiogram of Coracobrachialis	44
Figure 14: Angiogram of Brachialis	45
Figure 15: Angiogram of Triceps Brachii	46

Figure 16: Pronator Teres	51
Figure 17: Palmaris Longus and Flexor Carpi Radialis	52
Figure 18: Flexor Carpi Ulnaris	53
Figure 19: Flexor Digitorum Superficialis	54
Figure 20: Flexor Digitorum Profundus and Flexor Pollicis Longus	55
Figure 21: Pronator Quadratus:	56
Figure 22: Brachioradialis:	59
Figure 23: Extensor Carpi Radialis Longus and Brevis:	60
Figure 24: Extensor Digitorum Communis and Extensor Digiti Minimi	62
Figure 25: Extensor Carpi Ulnaris and Anconeus	64
Figure 26: Extensor Pollicis Brevis, Abductor pollicis Longus and Supinator	66
Figure 27: Extensor Indicis and Extensor Pollicis Longus	68
Figure 28: Hypothenar Muscles	71
Figure 29: Thenar Muscles	73
Figure 30: Deep Intrinsic Muscles of the Hand	76
Figure 31: Gluteus Maximus, Medius and Minimus Muscles	79
Figure 32: Quadriceps Femoris Muscles	82

Figure 33: Muscles of Medial Thigh.....	84
Figure 34: Angiogram of Muscles of the Posterior Thigh.....	86
Figure 35: Angiogram of Muscles of Anterior Compartment of the Leg.....	89
Figure 36: Gastrocnemius and Soleus.....	91
Figure 37: Muscles of the Deep Compartment of the Posterior Leg.....	93
Figure 38: Intrinsic Muscles of the Foot.....	100
Figure 39: The Modified Mathes and Nahai’s classification.....	105
Figure 40: Vascular Pattern Distribution.....	106
Figure 41: CT sagittal view of a rabbit with a magnified pixel.....	120
Figure 42: Morphometric Data of Lead oxide injection group.....	124
Figure 43: Morphometric Data of Barium Gelatin injection group.....	125
Figure 44: Morphometric Data of Iodine Gelatin injection group.....	125
Figure 45: Morphometric Data of Gadolinium Gelatin injection group.....	126
Figure 46: Hounsfield Radiodensity Scale.....	126
Figure 47: Rabbit Injection study.....	127
Figure 48: Temporalis 3D Angiogram.....	133
Figure 49: Temporalis 3D-Capture and Dissection.....	134

Figure 50: Mean Contribution of each Vessel to Temporalis Volume in Percentage	135
Figure 51: Schematic Illustration of the Vascularity of Temporalis	136
Figure 52: Masseter 3D Angiogram	138
Figure 53: Masseter in 3D	139
Figure 54: Trapezius 3D Angiogram	142
Figure 55: Dorsal Scapular Artery	143
Figure 56: Latissimus Dorsi 3D Angiogram	146
Figure 57: Latissimus Dorsi Vascular territories	147
Figure 58: Coracobrachialis Three Dimensional Angiogram	149
Figure 59: Biceps Brachii 3D Angiogram	151
Figure 60: Brachialis 3D Angiograms	153
Figure 61: Abductor Pollicis Brevis	156
Figure 62: Flexor Pollicis Brevis	158
Figure 63: Thenar Muscles 3D Angiogram	160
Figure 64: Tensor Fascia Lata 3D Angiogram	162
Figure 65: TFL Perforator Flap in 3D	163

Figure 66: Sartorius 3D Angiogram	165
Figure 67: Medical Circumflex Femoral Artery (MCFA)	168
Figure 68: Gracilis 3D Angiogram	169
Figure 69: The Arterial Architecture of Gluteus Maximus	171
Figure 70: Gluteus Maximus and Medius 3D Angiogram	172
Figure 71: Arterial anatomy of Gastrocnemius	174
Figure 72: Gastrocnemius in 3D	175
Figure 73: Posterior surface of Soleus	177
Figure 74: Soleus in 3D	179
Figure 75: Extensor Digitorum Brevis	183
Figure 76: Foot 3D Angiogram	184
Figure 77: Anatomy of DCIA Bone Flap	187

List of Tables

Table 1: Summary of Angiograms of Muscles of the Head and Neck	18
Table 2: Summary of Angiograms of Muscles of the Chest.....	23
Table 3: Summary of Angiograms of Muscle of the Abdomen	30
Table 4: Summary of Angiograms of Muscles of the Back.....	37
Table 5: Summary of Angiograms of Shoulder and Upper Arm	47
Table 6: Summary of Angiograms of the Volar Antebrachial Muscles.....	57
Table 7: Summary of Angiograms of the Dorsal Antebrachial Muscles	69
Table 8: Summary of Angiorams of the Hand	77
Table 9: Summary of Angiograms of Muscles of The Hip and Thigh	87
Table 10: Summary of Angiograms of the Leg	95
Table 11: Summary of Angiograms of the Foot.....	101
Table 12: Range of Vascular Variation per Body Region.....	104
Table 13: Vascular Patterns per Body Region	104
Table 14: Optimal CT Scanner Setting for All Groups.....	120
Table 15: Vascular Radiodensities in Select Tissues	124

Table 16: Three Dimensional Analysis of Temporalis.....	135
Table 17: Three Dimensional Analysis of Masseter.....	139
Table 18: Three Dimensional Analysis of Trapezius.....	144
Table 19: Three Dimensional Analysis of Latissimus Dorsi.....	146
Table 20: Three Dimensional Analysis Data Coracobrachialis.....	149
Table 21: Three Dimensional Analysis of Biceps Brachii.....	151
Table 22: Three Dimensional Analysis of Brachialis.....	154
Table 23: Summary of Three Dimensional Analysis of Thenar Muscles.....	159
Table 24: Mean lengths of Lateral Circumflex Femoral Vascular tree.....	162
Table 25: Three Dimensional Analysis of Sartorius.....	165
Table 26 Three Dimensional Analysis of Gracilis.....	168
Table 27: Three Dimensional Analysis of Gluteus Maximus.....	171
Table 28: Three Dimensional Analysis of Gastrocnemius.....	174
Table 29: Three Dimensional Analysis of Soleus.....	178
Table 30: Three Dimensional Analysis of the Foot Muscles.....	182

Abstract

Functional muscle transfer requires a donor muscle with reliable vascularity. The goal of functional muscle transfer is to restore active motion. The main focus of this project was on potential donor muscles for functional muscle transfer.

We hypothesized that muscles are supplied by a consistent number of predictable vascular pedicles that originated from defined number of source arteries (angiosomes).

The literature was reviewed, and 2339 angiograms from 40 cadavers were analyzed. Seven cadavers were injected utilizing a modified lead oxide injection technique. Twenty skeletal muscles selected based on surgical suitability were studied. Vascular pedicles with diameters ≥ 0.5 mm were measured from dissections, and measurements from stereolithography models. Mean muscle surface area, volume, length and diameters of each vessel were recorded.

In conclusion, our hypothesis that skeletal muscles have a consistent and predictable blood supply held true, and the three dimensional models provided valuable qualitative and quantitative anatomical data.

List of Abbreviations Used

ACHA	Anterior circumflex humeral artery
ADM	Adductor digiti minimi
ADTA	Anterior Deep Temporal Artery
ALT	Anterior Lateral thigh
APB	Abductor pollicis Brevis
APM	Adductor pollicis muscle
CSA	Circumflex scapular artery
DCIA	Deep circumflex iliac artery
DCM	Digital Imaging and Communications in Medicine
DIEA	Deep Inferior Epigastric Artery
DIOM	Dorsal Interosseus Muscle
DMA	Deep Masseteric Artery
DMCA	Dorsal Metacarpal Artery
DPA	Deep Plantar arch, Deep Palmar Arch
DSA	Dorsal Scapular Artery

DTCA	Deep Transverse Cervical Artery
ECRB	Extensor Carpi Radialis Brevis
ECRL	Extensor Carpi Radialis Longus
ECU	Extensor Carpi Ulnaris
EDC	Extensor Digitorum communis
EDM	Extensor Digiti Minimi
FCAT	Federative Committee on Anatomical Terminology
FDP	Flexor Digitorum Profundus
FDS	Flexor Digitorum Superficialis
FHL	Flexor Hallucis Longus
FPB	Flexor Pollicis Brevis
FPL	Flexor Pollicis Longus
GPU	Graphics processing unit
IGA	Inferior Gluteal Artery
IMA	Inferior Masseteric Artery
KCL	Potassium chloride
LCFA	Lateral Circumflex Femoral Artery

LPA	Lateral Plantar Artery
LTA	Lateral Thoracic Artery
MIMICS	Materialise's Interactive Medical Image Control System
MI	Myocardial Ischemia/Infarction
MPA	Medial Plantar Artery
MRI	Magnetic resonance imaging
MTA	Middle Temporal Artery
OPM	Opponens Pollicis Muscle
PCHA	Posterior Circumflex Humeral artery
PDTA	Posterior Deep Temporal Artery
PICA	Posterior Intercostal Arteries
PIOM	Palmar Interossei Muscles
PMA	Palmar Metacarpal Artery
PPA	Princeps Pollicis Artery
PVD	Peripheral Vascular Disease
RIA	Radialis Indicis Artery
SMA	Superior Masseteric Artery

SSA	Suprascapular Artery
STA	Superficial Temporal Artery
STCA	Superficial Transverse Cervical Artery
STL	Standard Tessellation Language
TCA	Transverse Cervical Artery
TDA	Thoracodorsal Artery
TDAP	Thoracodorsal Artery Perforator
TFL	Tensor Fascia Lata
TLP	Thoracolumbar Perforators
TRAMP	Transverses Rectus Abdominis Muscle Perforator

Acknowledgments

I would like to thank my supervisor Dr. Steven Morris not only for his guidance and support, but also for being my inspiration to pursue this project. Many thanks to my friend Dr. Maolin Tang for his support and contribution. I would like to thank Dr. Kazue Semba, and my thesis committee members Dr. William Baldrige, Dr. Boris Kablar, and Dr. Frank Smith. Finally, I would like to thank my good friend Michael Butler for his continuous support and keen interest in anatomy.

“Not everything that can be counted counts, and not everything that counts can be counted”

Albert Einstein

Chapter 1.0 Introduction

In reconstructive microsurgery, large soft tissue defects in the body are reconstructed using tissues transferred from other regions of the body. The soft tissue defects may result from trauma, limb amputation, congenital causes or after the removal of large tumors. The techniques utilized to reconstruct these wounds have evolved over the past few decades. Skeletal muscle has been used in reconstructive surgery in two major areas: soft tissue coverage and functioning muscle transfer.

In soft tissue (skin, fat, muscle) reconstruction using skeletal muscle, the muscle may be transferred as a pedicled transfer (still attached to its origin or insertion) or as a free microvascular tissue transfer (muscle is transplanted and reattached with microvascular anastomoses of the artery and vein and sometimes nerve). The most common mechanisms of muscle injury are direct trauma to the muscle compartment, ischemic paralysis, nerve injury, and tumor resection.¹ It is critical to understand the three-dimensional neurovascular intramuscular anatomy of the skeletal muscles of the body in order to optimize the results of muscle transfer and in particular, determine the most suitable muscle for a segmental or whole muscle transfer.

The objective of this thesis project is to comprehensively document the three-dimensional vascular anatomy of muscles of the body. This information will be used to customize clinical procedures for segmental or whole muscle microsurgical transfer.

1.1 Historical Background

The quest for functional restoration of areas of head, neck, upper and lower extremities by means of free functioning muscle transfers has spanned several continents and several decades. Substitution of functional loss by microneurovascular transfer of a muscle from its donor site to the face or the extremities is the goal of free functioning muscle transfer procedures.

Muscle transfer for restoration of function is a complex procedure that requires a donor muscle with reliable and suitable anatomy and appropriate dynamic structure to meet the functional needs of the recipient site. The goal of functional muscle transfer is to restore active motion and satisfy a patient's particular functional need. The success of such procedures is dependent on the ability of the surgeon to select the most appropriate muscle. The muscle selected must be well vascularized. Anatomical dissections and dye injections have been used to demonstrate anatomical variations.² Ariyan in 1980, stressed the territorial nature of blood supply to muscle flaps.³ In 1981, Mathes and Nahai published their classification of muscle circulation based on their 10 year experience with dissections and angiographic studies. Their classification remains the cornerstone used to determine the usefulness of muscle as surgical flaps.⁴⁻⁶ Tobin expanded on the work of Mathes and Nahai and studied some common muscle flaps and their intramuscular neurovascular anatomy. Tobin demonstrated in the latissimus dorsi of humans and dogs the presence of muscular subunits that could be manipulated surgically.^{7,8}

Manketlow and Zuker described functional muscle transfers based on their neurovascular studies of the pectoralis and gracilis muscle. These flaps were segmental and transferred as free flaps for hand reconstruction.⁹⁻¹²

Cormack and Lamberty described the arterial supply to muscles in their comprehensive text.¹³ In 1987, Taylor and Palmer introduced the Angiosome concept. Based on their two dimensional angiographic studies, they proposed that the body is a three-dimensional jigsaw made up of composite blocks of tissues supplied by named source arteries.¹⁴ Taylor and colleagues categorized individual muscles based on their most common mode of innervation, the classification does not take into account the intramuscular patterns of innervation.¹⁵

In 1970, Tamai and colleagues provided electrophysiological evidence of muscle contraction after the successful transfer of a rectus femoris muscle to a forelimb in a canine model. Three years later, microsurgions at the Sixth People's Hospital in Shanghai successfully transferred the lateral portion of the pectoralis major muscle in a patient with Volkmann's ischemic contracture.¹⁶ This was the first successful clinical application of functioning muscle transfer. Harii and colleagues demonstrated the role of functioning muscle transplantation for the rehabilitation of facial paralysis in 1976.¹⁷ In 1996, Kubo and colleagues demonstrated the normal histological appearance of muscle after its microsurgical transfer.¹⁸

1.2 The Evolution of Angiography

The utility of radiographic contrast material in mapping the arterial supply to skeletal muscles was described almost a hundred years ago. The first angiogram was produced by Hascheck in 1986.¹⁹ Angiographic techniques have continued to evolve and currently the gold standard method for 2 dimensional angiograms is the lead oxide gelatin technique.²⁰⁻²²

Knowledge of the three dimensional vascular anatomy is crucial to optimize the result of free tissue transfer.²³⁻²⁸ Several authors have utilized this technology to answer questions relevant to their daily practice. In 2007 Tregaskiss et al. described a method for imaging microvascular anatomy in three dimensions. Their study produced very low quality images and most importantly lacked quantitative analysis of the anatomy.²⁶ Tregaskiss employed his technique to study the anatomy of the anterior abdominal wall and described the unique vascular anatomy of the deep inferior epigastric artery (DIEA) to explain the ischemia-related morbidity observed with DIEA-based perforator flaps. They concluded that preservation of superficial epigastric perforators adjacent to the costal margin during abdominoplasty will likely improve abdominal wall perfusion and reduce donor-site morbidity.²⁹

In a recent study Saint-Cyr et al. described the use of three dimensional imaging in planning the anterolateral thigh (ALT) flap and noted the difference in outcomes in thinned ALT flaps between Caucasian and Asian populations.^{30, 31} In a separate study, Schaverien et al. was also able to demonstrate the safety of thinning the thoracodorsal artery perforator flap (TAP) using the same technique.³²

1.3 Current Angiographic Techniques

Optimal results are obtained when cadavers are injected with lead oxide and then radiographed. However, the lead oxide produces significant artefact when computed tomography is used. Ideally, a CT scan of the injected cadaver should be obtained to provide three-dimensional models of the injected cadaver. However, current techniques do not allow the high-resolution angiograms that the lead oxide injection technique provides in three dimensions due to the CT artefact issue. A recent literature review of

post-mortem angiography outlined the need for future studies to look at the optimal injection mixture for computed tomography when three dimensional models are to be considered.³³ Figure 1 demonstrates the artefacts associated with conventional techniques.

1.4 Classification of Skeletal Muscles

Muscles can be classified in variety of ways, and there are many physiological and morphological classifications. The utility of each classification system depends on the field of study. In reconstructive surgery success is predicated upon the availability of robust blood supply and effective venous drainage, and therefore a muscle classification system based on vascularity provides an excellent framework to facilitate the selection of a muscle for local or distant transfer.

The only classification based on the vascular supply to skeletal muscles was introduced by Mathes and Nahai.⁴ This classification is widely accepted among reconstructive surgeons. The classification was reported following a single cadaver dissection in 1981, yet this classification has been very useful for surgeons to conceptualize the vascularity of muscles and plan surgeries.³⁴ This classification is based on the "pattern" of vascular supply to skeletal muscles. Figure 2 illustrates the five patterns of blood supply to skeletal muscles as described by Mathes and Nahai.

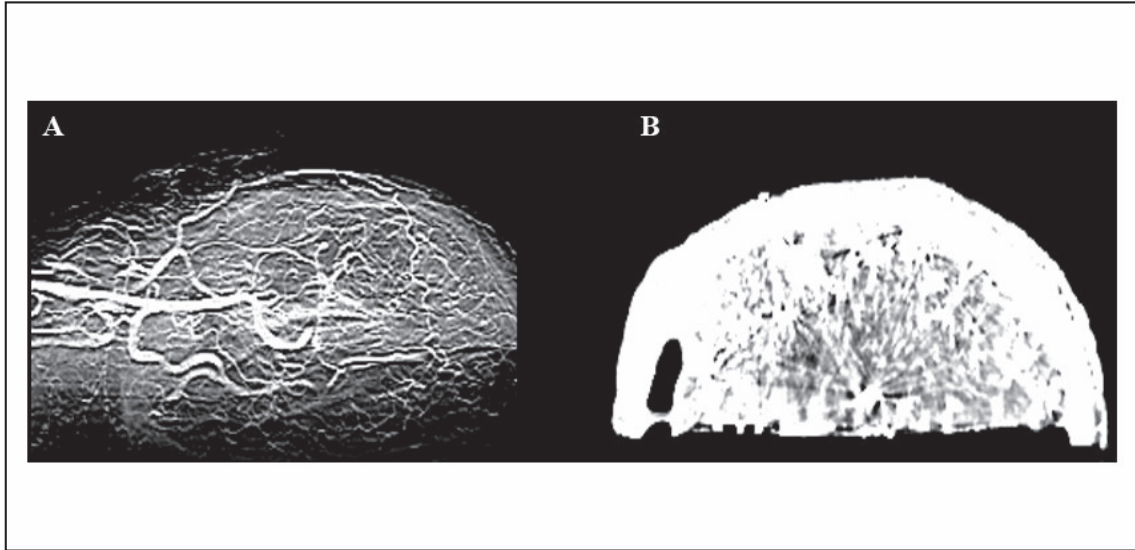


Figure 1: Current Techniques in Angiography

A. Cross sectional X-ray Image of a lead oxide injected cadaver; note the fine details of vasculatures; B. Axial cross section of CT scanned cadaver with heavy artifacts generated by the lead oxide technique.

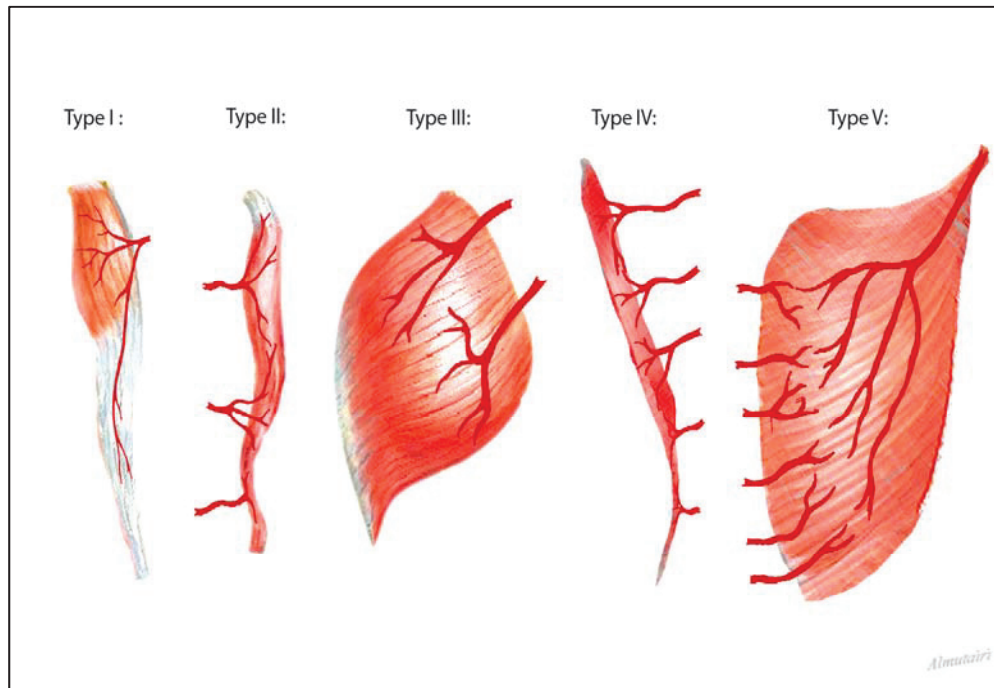


Figure 2: Mathes and Nahai's Classification

I- Muscles that receive only one major pedicle.

II- Muscles that receive major pedicle(s) and minor pedicle(s) that belong to the same trunk.

III- Muscles that receive two or more dominant pedicles, with both pedicles from a different arterial source or on the opposite side of each other.

IV- Muscles that receive segmental supply in which no segment provides larger supply to the muscle than any of the other segments supplying the muscle.

V- Muscles that receive a single dominant pedicle and several segmental blood vessels supplying the muscle. The segmental blood vessels are capable of supplying the muscle on their own and the source of these segmental vessels is different than the major pedicle.⁴

1.5 Objectives

This thesis project is a two-phase study. The objective of the preliminary phase of this thesis was to document the vascular supply to skeletal muscles and to clarify the classification of muscles according to their pattern and origin of blood supply.

1.5.1 Phase I: Evaluating Mathes and Nahai's Classification

In Phase One of this thesis, data from 40 fresh cadavers that were previously injected with the lead oxide, gelatin and water arterial injection technique were analyzed. Angiograms and dissections were reviewed to document the observed pattern of vascular supply to skeletal muscles. In addition, a comprehensive review of the literature pertaining to the vascular anatomy of skeletal muscles was undertaken. The objective of this study was to compare the Mathes and Nahai's classification to a large series of muscle injection studies.

1.5.2 Phase II: Three Dimensional Analysis of Human Skeletal Muscles

The objective of this phase was to comprehensively document vascular anatomy to a selected group of surgically accessible muscles using a novel three-dimensional technique. This was a two-part study. Part A was a pilot study conducted to select the best injection mixture that will produce the highest quality three-dimensional models. In Part B, 7 cadavers with whole body injection and CT scans were analyzed using a novel three-dimensional technique.

1.5.2.1 Part (A) Animal Injection Study

In Part A, a series of modified injection techniques were performed using an animal model to optimize the 3-dimensional CT scanning of anatomical specimens in order to use this technique in human cadavers to obtain 3-D imaging of the arterial anatomy of skeletal muscles. The objectives of Part A was (i) to define the best injection protocol for 3D evaluation of the vascular anatomy, (ii) to reduce artifacts and noise by defining the appropriate CT Scanner Settings, and (iii) to determine the smallest vessel caliber traceable with this technique

1.5.2.2 Part (B) Cadaver Injection Study

In Part B, 7 cadavers were dissected and the three dimensional vascular anatomy was studied. The objectives of Part B was (i) to measure, in 2 dimensions, the muscle surface area supplied by each pedicle reported in percentage and average surface area cm^2 , (ii) to measure the average volume in cm^3 of each muscle, (iii) the percentage of volume supplied by each vascular pedicle, (iv) to document average pedicle lengths, extra and intramuscular arterial diameters, and (v) to define surface landmarks of entry points of vessels to facilitate their surgical harvest.

1.5.2.3 Ethics statement

Strict adherence to the Dalhousie University ethical guidelines was practiced. Ethics approval for both studies was obtained from Dalhousie University research ethics board, and additional ethics approval for the animal study was obtained from the University council on laboratory animals.

Chapter 2.0 Evaluating Mathes and Nahai's Classification (Phase I)

K Almutairi, M Tang, SF Morris. The Vascular Supply of Muscles of the Body.

Plastic and Reconstructive Surgery. 121: 98, 2008. (Published Abstract)

Abstract: The Vascular Supply of Muscles of the Body

Knowledge of the vascular anatomy of skeletal muscles is of great importance to the reconstructive surgeon. Mathes and Nahai originally presented their classification in 1981 based on the pattern of vascular supply to individual muscles, and today this classification is very popular. ⁴

The objective of this study was to review the pattern of vascular supply to skeletal muscles of the human body in a series of 40 cadavers.

The lead oxide, gelatin and water arterial injection technique was utilized in a series of 40 cadavers. A total of 2339 muscles were individually dissected, and two-dimensional angiograms were obtained. The angiograms were scanned, and the vascular supply to each muscle was classified according to the five groups described by Mathes and Nahai. The variability of muscle vascular supply was assessed.

A total of 72% of all muscles studied could be classified according to the Mathes and Nahai classification. We found that many muscles had variable patterns of vascular supply, and a significant number of muscles (28%) exhibited a pattern of vascular supply that did not fit the Mathes and Nahai's classification.

In conclusion, this study demonstrates the excellent quality of angiograms produced by the lead oxide injection technique. As well, we observed significant vascular variability in skeletal muscle, which can produce variable clinical results.

2.1 Materials and Methods

The lead oxide, gelatin and water arterial injection technique was utilized in a series of 40 cadavers.^{20, 22, 33} All cadavers were obtained via the Dalhousie University Donor program. None of the cadavers had any peripheral vascular disease or any other pathology that could impair our dissection or angiographic studies. Prior to dissection, all cadavers were injected with lead oxide and then radiographed. The dissection process involved step by step photography of muscles and their arterial pedicles.

A total of 2339 muscles were individually dissected, and two-dimensional angiograms were obtained. The angiograms were scanned, and the vascular supply to each muscle was classified according to the five groups described by Mathes and Nahai. In addition, the literature related to the 126 skeletal muscles was reviewed from the early 1900's. The variability of muscle blood supply patterns was assessed.

2.2 Results and Findings of Phase I

In this section we present the most comprehensive review of angiographic studies documented to date. Forty cadavers were dissected and 2339 muscle angiograms from 126 different skeletal muscles were studied.

The body was studied in a regional fashion, starting with the head and neck followed by the trunk, upper and lower extremities. The vascular anatomy in these angiograms was also compared to findings of Mathes and Nahai as well as the work of many other contributors to the field.

2.2.1 Muscles of the Head and Neck

Temporalis:

The temporalis takes origin from the temporal lines of the parietal bones and inserts on the coronoid process. The temporalis is supplied by three major pedicles, the anterior and posterior deep temporal arteries from the internal maxillary artery, and the superficial temporal artery.³⁴⁻³⁶ Temporalis is currently a type III muscle; this review confirmed this pattern in all 14 muscles. Figure 3A shows the typical vascular pattern of this muscle.

Orbicularis Oculi:

The orbicularis oculi muscle is a three-part muscle, composed of palpebral, lacrimal and orbital parts. The origin is the frontal and lacrimal bones and the insertion is the palpebral raphae. This muscle is supplied by multiple dominant pedicles. Inferiorly it is supplied the infraorbital and infratrochlear artery. Superiorly it receives the supratrochlear and supraorbital arteries. Laterally it receives branches from the frontal branch of the superficial temporal artery and medially it receives supply from the angular artery. Although this muscle was not previously classified,^{37, 38} this muscle was found to have the arterial pattern of a type III muscle in all 13 muscles (Figure 3B).

Masseter:

The masseter originates from the zygoma and maxilla, and inserts on the ramus and angle of the mandible. It is supplied by the deep masseteric artery via the internal maxillary artery, as well segmental blood supply by the facial artery via the inferior and superior masseteric arteries.^{35, 39} The masseter muscle was not previously classified and the pattern in 11 angiograms did not fit into any of the 5 patterns described by Mathes and Nahai. It has both 2 dominant pedicles in addition to a segmental pattern. It is worth noting that this muscle receives its blood supply from 2 different angiosomes; the facial and internal maxillary artery angiosomes. The dominant blood supply is via the facial artery. Figure 3C shows the territories of the four vessels; premasseteric, inferior, superior, and deep arteries supplying this muscle.

Orbicularis Oris:

The orbicularis oris muscle originates from the perioral maxilla and mandible, and inserts onto the labial skin, it is supplied by the facial artery and its superior and inferior labial artery connections.³⁴ All 14 muscles conformed to the current classification as type III.

Tongue:

The tongue consists of intrinsic and extrinsic musculature. The skeletal muscles of the tongue are the genioglossus, the hyoglossus, the styloglossus and the palatoglossus. The tongue is held in place by the retractors the hyoglossus and the palatoglossus.

Blood supply to the tongue muscles is mainly by the lingual artery and its branches the dorsal lingual artery, deep lingual artery, sublingual artery and suprahyoid artery. In review of 12 angiograms of the tongue muscles all were found to exhibit a type I circulation. Each tongue muscles receives one major pedicle.^{40, 41}

Mylohyoid:

This muscle originates from the mylohyoid line and inserts on the hyoid and the median raphe, it receives its arterial supply from a number of sources. First the sublingual branch of the lingual artery, second the maxillary artery via the mylohyoid branch of the inferior alveolar artery, and third the submental branch of the facial artery.

The main blood supply to the floor of the mouth and the mylohyoid is from the submental artery. Mylohyoid has 2 dominant pedicles, the superficial aspect is supplied by submental artery and the deep surface is supplied by the sublingual and mylohyoid artery of the inferior alveolar artery.⁴²

Digastric:

The posterior belly is supplied by the posterior auricular artery and occipital artery. The anterior belly is supplied by the submental artery and gives off 3 branches to the muscle. The first branch at the posterior border of the anterior belly is the dominant pedicle. Anteriorly there are two minor branches that supply the muscle. In review of 3 angiograms the digastric muscle exhibited a type II circulation, this finding was supported by the literature review.⁴³⁻⁴⁷

The submental artery branches at the level of the submandibular gland and runs towards the chin below the mandible. It supplies the surrounding musculature and anastomoses with the mylohyoid branch of the inferior alveolar artery and the sublingual branch of the lingual. At the chin it bifurcates into superior and deep branches, which anastomose with the mental and inferior labial arteries.

Omohyoid:

The superior thyroid supplies this muscle proximally by a dominant pedicle. Distally it receives minor branches from the inferior thyroid artery pedicles.⁴⁸ All 5 angiograms demonstrated a type II muscle.

Platysma:

The platysma receives its dominant pedicle from the submental artery proximally. The superior thyroid artery provides multiple branches to the muscle in the middle part blood supply to this muscle and the transverse cervical artery provides the distal part with a dominant pedicle.^{34, 49-51} Four out of 5 muscles were type III; only one angiogram exhibited a type II circulation.

Sternocleidomastoideus

The sternocleidomastoideus is supplied by 2 major pedicles; the occipital artery and the superior thyroid artery. It is supplied by 2 minor pedicles; inferiorly by the suprasternal artery a branch the suprascapular artery and superiorly by the posterior auricular artery.^{44, 52-71} Nine muscles were reviewed, and they were all type II muscles.

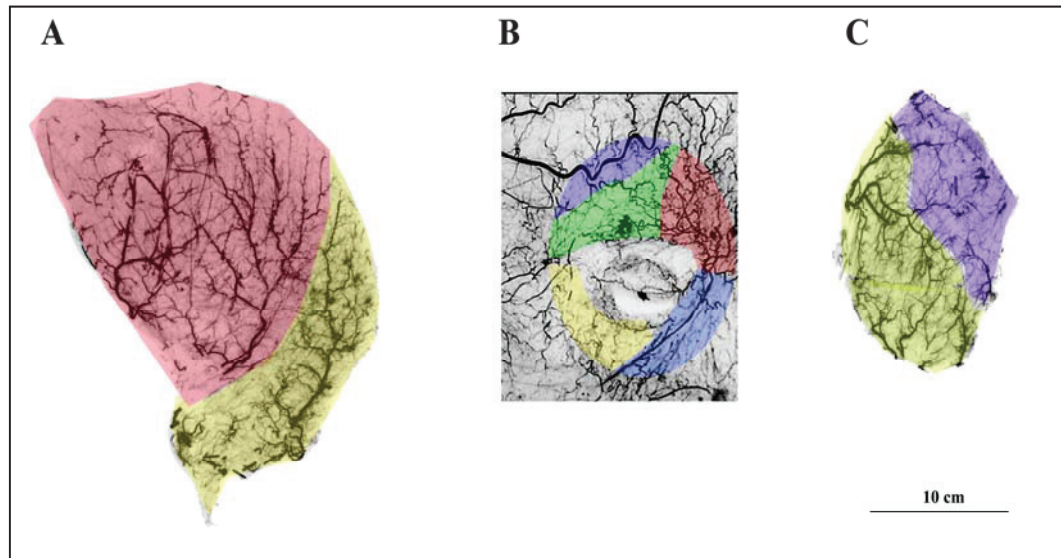


Figure 3: Head and Neck Muscles

A. Temporalis. The yellow zone outlines the territory of the superficial temporal artery, and the red zone highlights the territory of the deep temporal arteries; **B. Orbicularis Oculi.** The superior blue zone is the territory of the superficial temporal artery. The green zone is the territory of the supraorbital artery. The supratrochlear artery territory is represented by the red zone. The yellow zone represents the territory of the infraorbital artery, and the caudal blue zone represents the territory of the muscle supplied by the angular artery; **C. Masseter.** The yellow zone represents of the territory supplied by the facial artery (transverse facial and facial arteries). The blue zone represents the deep masseteric arteries from the internal maxillary angiosome.

Table 1: Summary of Angiograms of Muscles of the Head and Neck

	Type I	Type II	Type III	Type IV	Type V	Total	Current Dominant Type	Muscles Conforming to current classification %	Observed Type	Observed Dominant Type %
Head and Neck										
Occipitalis	0	12	0	0	0	12	II	100	II	100%
Frontalis	0	12	0	0	0	12	II	100	II	100%
Orbicularis oculi	0	0	13	0	0	13	Not classified	Not classified	III	100%
Nose muscles										
Temporalis	0	0	14	0	0	14	III	100	III	100%
Masseter	0	0	0	0	11	11	II	0%	V	100%
Orbicularis oris	0	14	0	0	0	14	Not classified	Not classified	II	100%
Tongue	12	0	0	0	0	12	Not classified	Not classified	I	100%
Digastric	0	3	0	0	0	3	II	100%	II	100%
Sternohyoid	0	8	0	0	0	8	II	100%	II	100%
Omothyoid	0	5	0	0	0	5	II	100%	II	100%
Platysma	0	1	4	0	0	5	II	25%	III	75%
Sternocleidomasto	0	9	0	0	0	9	II	100%	II	100%
Total						118				

2.2.2 The Trunk

2.2.2.1 Muscles of the Chest

Pectoralis Major:

This muscle receives its dominant blood supply from the thoracoacromial artery via the pectoral artery. The lateral thoracic artery supplies the muscle with a minor pedicle, and it receives segmental blood supply from the first intercostal spaces via the internal thoracic artery. In all 44 angiograms this muscle constantly had a type V circulation.^{34, 72-74} Figure 4A demonstrates the typical vascular pattern of this muscle.

Pectoralis Minor:

The pectoralis minor has 2 dominant pedicles, the pectoral branch of the thoracoacromial artery, and a branch from the lateral thoracic artery. It also receives a minor pedicle from the axillary artery.⁷⁵ Only 3 out of 30 angiograms had a type II circulation, the rest of the angiograms demonstrated a muscle that had a type III muscle. Figure 4B, C demonstrates the typical vascular pattern of this muscle.

Serratus Anterior:

The serratus anterior principally derives its arterial supply from the branches of the axillary artery, the lateral thoracic artery course along the anterior border of the muscle and gives off branches to the upper 4-5 slips of serratus anterior. The lower half of the muscle is supplied by the serratus branch of the thoracodorsal artery, there are few reports in the literature that describes variability related to the thoracodorsal artery branch to serratus, however the reported variability was related to the origin of the angular

branch to serratus either from the thoracodorsal or subscapular system (higher origin).⁷⁶

This however was not observed in our angiographic review or dissections.⁷⁷ Ten out of 33 muscles had a type II circulation the remaining 23 muscles exhibited a type III circulation. Figure 5 demonstrates the typical vascular pattern of this muscle.

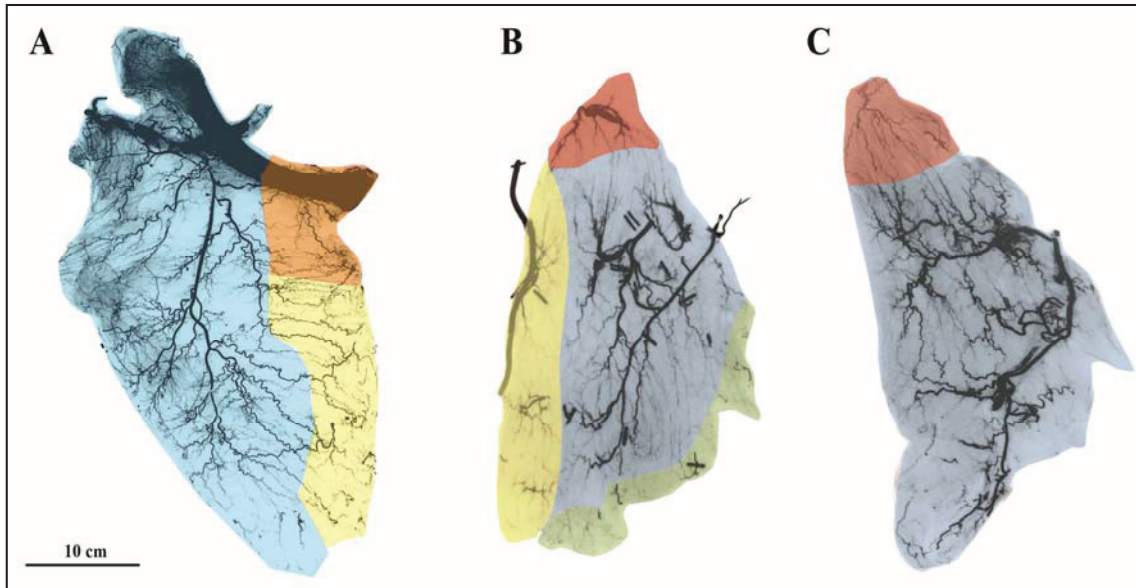


Figure 4: Muscles of the Chest

A. Pectoralis Major. The yellow zone outlines the territory of blood supply by the internal thoracic artery; the blue zone shows the major blood supply via the pectoral branches of the thoracoacromial artery, in addition there is a highly variable and inconstant branch from the highest thoracic artery to this muscle (orange zone).

B. Pectoralis Minor. The yellow zone indicates the contribution of the lateral thoracic artery to this muscle. The blue zone is the major territorial supply to the muscle via branches of the thoracoacromial artery. The green zone outlines the minor contribution to this muscle by the intercostal perforators, and a minor independent branch from the axillary artery (red zone). **C. Pectoralis minor** only receives blood supply from the thoracoacromial artery, and a minor independent branch from the axillary artery (red zone).

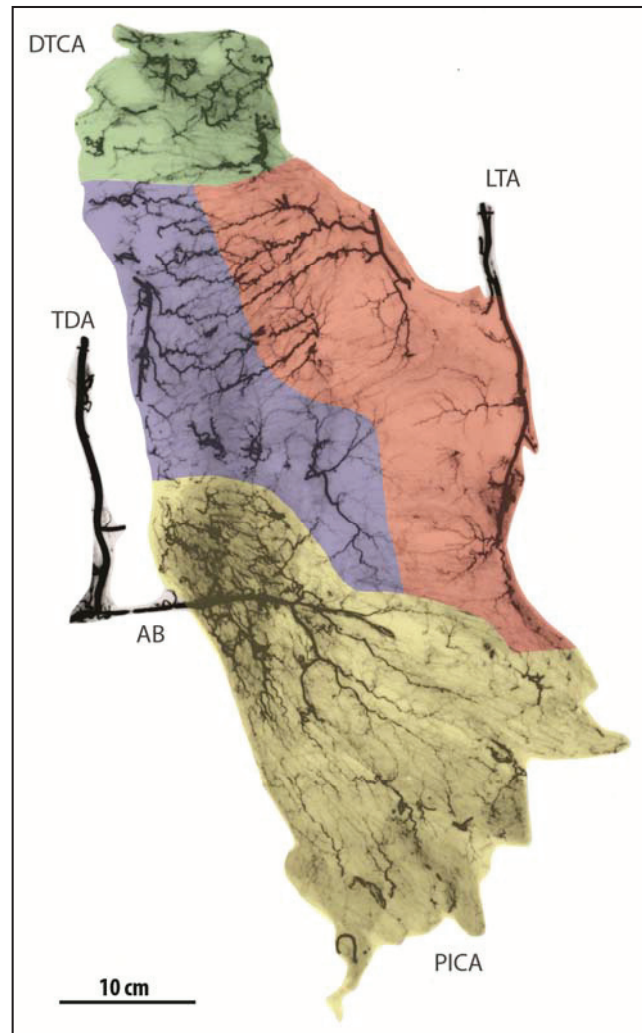


Figure 5: Serratus Anterior

The green zone outlines the minor blood supply to the superior part of the muscle from the descending branches of the transverse cervical artery (DTCA). The red zone outlines the dominant blood supply to the upper slips of serratus from the lateral thoracic artery (LTA). The blue zone outlines the contribution of posterior intercostals to the muscle, and the yellow zone outlines the dominant blood supply to the lower slips of serratus by the angular branch (AB) of the thoracodorsal artery (TDA).

Table 2: Summary of Angiograms of Muscles of the Chest

Chest	Type I	Type II	Type III	Type IV	Type V	Total	Current Dominant Type	Muscles Conforming to current classification %	Observed Type	Observed Dominant Type%
Pectoralis Major	0	0	0	0	44	44	V	100%	V	100%
Pectoralis Minor	0	3	27	0	0	30	III	90%	III	90%
Serratus Anterior	0	10	23	0	0	33	III	69%	III	69%
Total						107				

2.2.2.2 Muscles of the Abdomen

Rectus Abdominis:

Rectus abdominis is supplied by the internal thoracic artery superiorly and by the deep epigastric artery inferiorly, as well as subcostal and intercostal segmental minor pedicles. The muscle is currently classified as a type III muscle, the pattern of supply to this muscle in 10 out of 40 angiograms could be grouped with type V; given the segmental nature of the blood supply from the subcostal and intercostal arteries or with type II as the collective contribution of blood supply by the segmental intercostal and subcostal arteries was a major contributor to the blood supply to this muscle.^{4, 34, 78} Thirty five angiograms had the arterial pattern of a type III muscle, and 5 angiograms with type II pattern. Figure 6 demonstrates the different arterial zones of this muscle.

External Oblique:

The external oblique muscle derives its arterial supply from the lower 6-7 posterior intercostal arteries (T6-12). In 35 angiograms, the blood supply to the external oblique was derived from the lower 6 or 7 posterior intercostal arteries. The vessels course between the transversus abdominis and internal oblique muscles and supplies the external oblique muscle via perforating branches.^{79, 80} The ascending branch of the deep circumflex iliac artery (DCIA) and lateral branches of the deep inferior epigastric artery (DIEA) give perforating branches to the muscle. This muscle has a segmental blood supply type IV. Figure 7A demonstrates the different arterial zones of this muscle.

Internal Oblique:

The blood supply to the internal oblique has a unique pattern. In all 30 angiograms, this muscle received its blood supply from 4 sources. The major blood supply to this muscle is based on the arterial arcade of the deep iliac artery. The deep circumflex artery (branch of the external iliac system) and the iliac branch of the iliolumbar artery (branch of the posterior division of the internal iliac artery) provide this muscle with its major arterial supply. The rest of the muscle is supplied medially by lateral branches of the deep inferior epigastric artery, superiorly by the subcostal artery and its posterolaterally by segmental branches from the four lumbar arteries.^{81, 82} The muscle was previously classified as a type V muscle. Figure 7B demonstrates the different arterial zones of the internal oblique muscle.

Transversus Abdominis:

The transversus abdominis blood supply is poorly defined; it receives its blood supply from multiple perforating branches of the lateral intercostal arteries through the plane between the transversus abdominis and internal oblique. Laterally the muscle is supplied by the lateral collateral branches of the deep inferior epigastric artery, and distally it receives branches from the deep circumflex iliac artery.⁸³ None of the 29 angiograms was compatible with any of the patterns of Mathes and Nahai's Classification. (Figure 7 C) demonstrates the different arterial zones of this muscle.

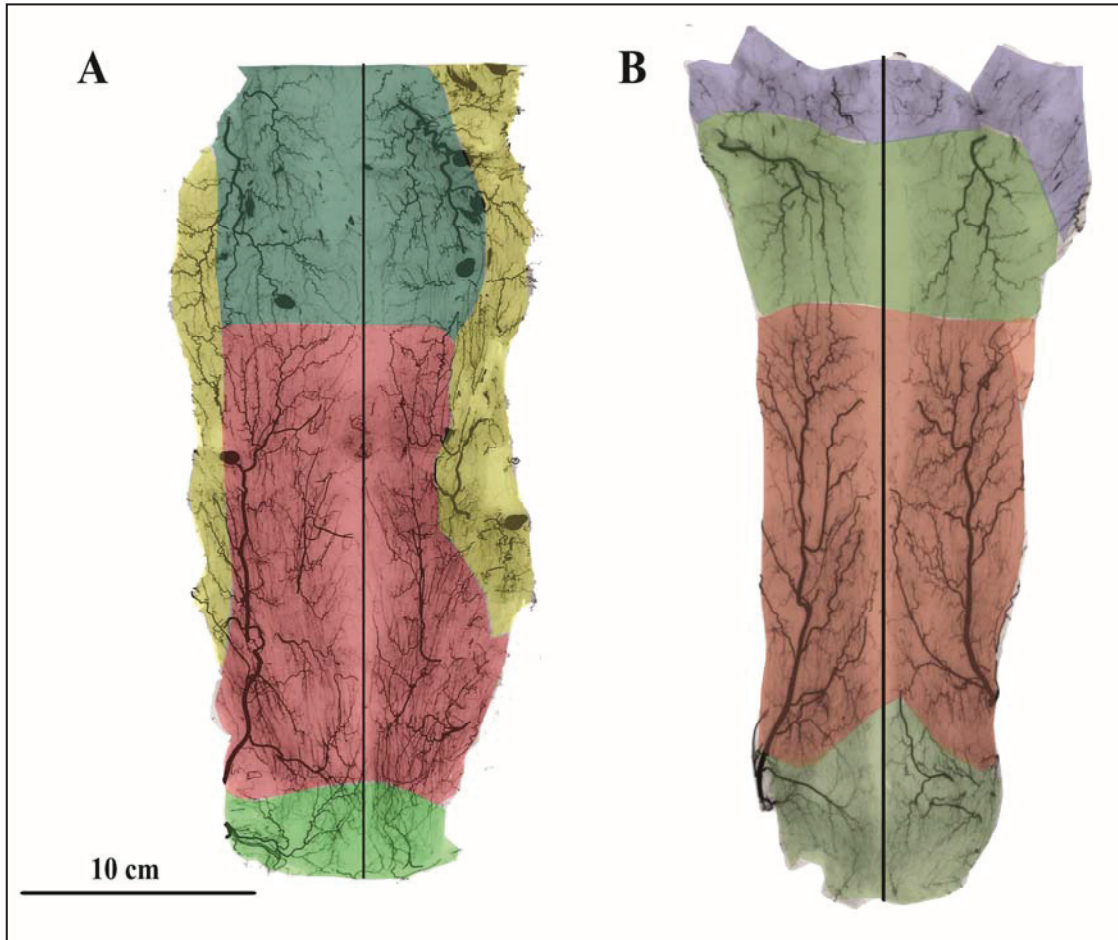


Figure 6: Rectus Abdominis

A. Right and left rectus abdominis. In red the major blood supply via the deep inferior epigastric artery (DIEA). The yellow zone showing considerable contribution to the muscles via the subcostal and 7-8 intercostal arteries, in light green is the area of muscle supplied by the superficial external pudendal arteries. **B. Right and left rectus abdominis** with the major blood supply from the DIEA, with the other 3 territories supplying the muscle to a lesser extent.

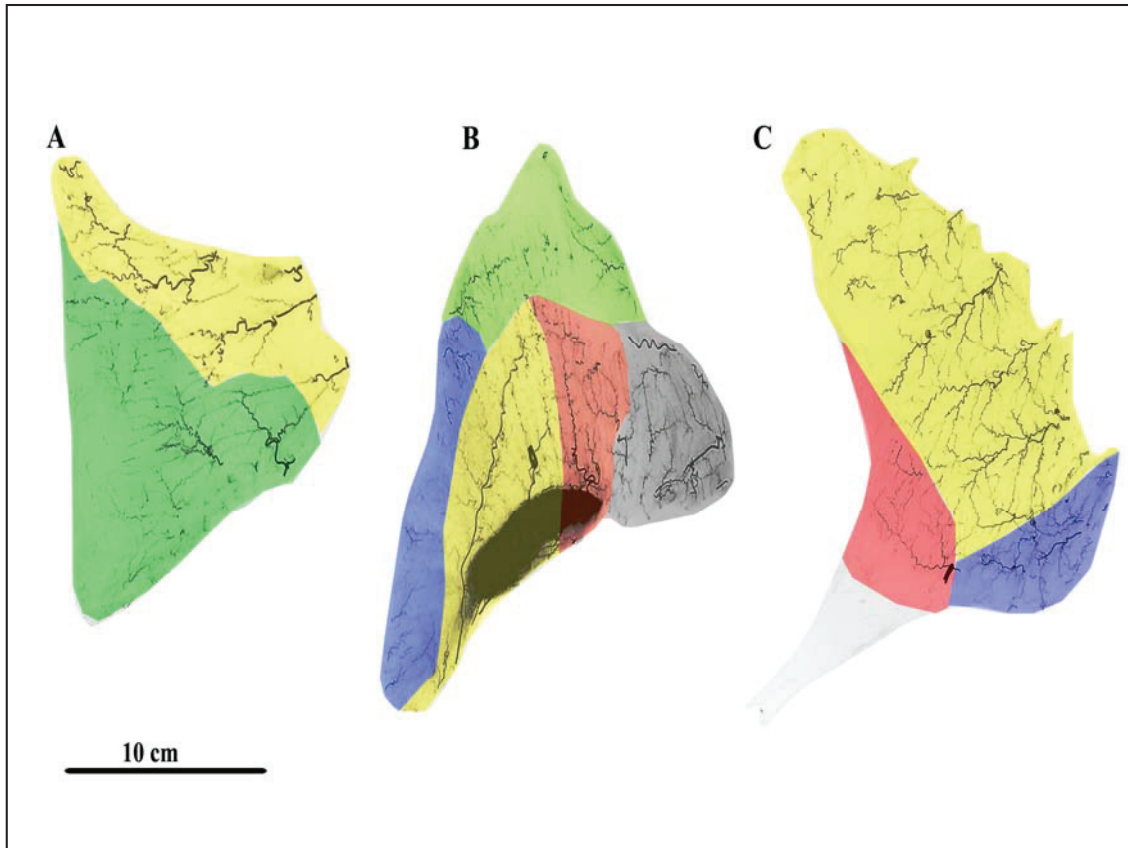


Figure 7: Transversus Abdominis, Internal and External Oblique

A. Transversus Abdominis, with the green zone indicating the blood supply from perforators the transverse and ascending branches deep circumflex iliac artery. The yellow zone highlights the contribution of perforators from the subcostal and lumbar arteries. **B. Internal oblique muscle**, the red and yellow zone highlights the arterial supply via the DCIA and iliolumbar arteries respectively. The medial most is the blue zone with contribution to the aponeurosis of the muscle from the lateral branches of the DIEA. The grey and green zone laterally and posteriorly highlight the territories of the lumbar and subcostal arteries. **C. External oblique**, the three zones are the red, yellow and blue with the blood supply derived from perforating branches of the DCIA, posterior intercostal and lumbar arteries respectively.

Iliacus:

This muscle receives its blood supply via a major pedicle from the iliolumbar artery, and a minor pedicle from the deep circumflex iliac artery.⁸⁴ All of the 18 angiograms exhibited a type II muscle (Figure 8 A).

Psoas Major:

This muscle receives segmental branches from the first four trunks of the lumbar arteries, as well as a dominant branch from the deep circumflex artery.⁸⁴ The external iliac provide segmental branches to the muscle proximal to the inguinal ligament. In all 9 angiograms this muscle exhibited a type V vascular pattern (Figure 8B).

Psoas Minor:

Six angiograms were studied. The psoas minor is a Type IV muscle that receives blood supply from the first four trunks of the lumbar arteries (Figure 8 C).⁸⁴

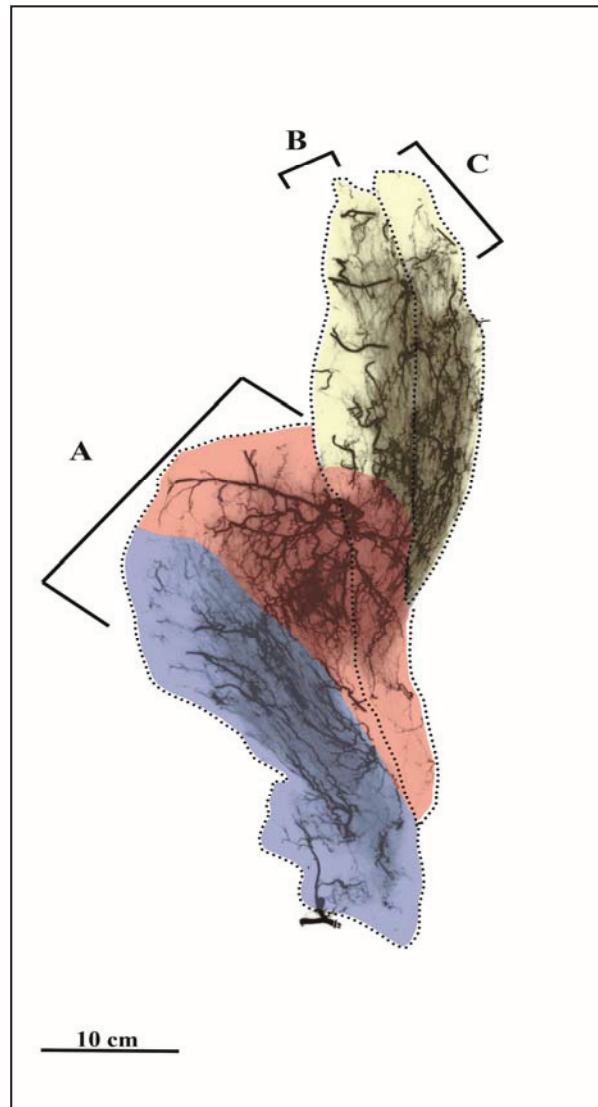


Figure 8: Iliopsoas Muscle:

The iliopsoas is a collective term for the Iliacus (A), psoas major (B) and psoas minor muscles. Note the arterial perfusion zones to these muscles; the iliacus (A) perfused by the deep circumflex iliac artery (blue zone), and the iliolumbar artery (red zone). Psoas major (A) receives its blood supply from both the iliolumbar artery (red zone), and lumbar arteries (yellow zone). The lumbar arteries (yellow zone) also supply the psoas minor muscle (C).

Table 3: Summary of Angiograms of Muscle of the Abdomen

	Type I					Type II					Type III					Type IV					Type V					Total	Current Dominant Type	Muscles Conforming to current classification %	Observed Type	Observed Dominant Type%			
	Type I	Type II	Type III	Type IV	Type V	Type I	Type II	Type III	Type IV	Type V	Type I	Type II	Type III	Type IV	Type V	Type I	Type II	Type III	Type IV	Type V	Type I	Type II	Type III	Type IV	Type V								
Abdomen																																	
Rectus Abdominus	0	5	35	0	0	0	5	35	0	0	0	0	0	0	0	0	0	0	0	0	0	0	0	0	0	0	0	0	40	III	88%	III	88%
External Oblique	0	0	0	35	0	0	0	0	35	0	0	0	0	0	0	0	0	0	0	0	0	0	0	0	0	0	0	0	35	IV	100%	III	100%
Internal Oblique	0	0	0	0	0	0	0	0	0	0	0	0	0	0	0	0	0	0	0	0	0	0	0	0	0	0	0	0	30	V	100%	V	100%
Transvers Abdominus	0	0	0	0	0	0	0	0	29	0	0	0	0	0	0	0	0	0	0	0	0	0	0	0	0	0	0	0	29	IV	100%	IV	100%
Iliacus	0	18	0	0	0	0	18	0	0	0	0	0	0	0	0	0	0	0	0	0	0	0	0	0	0	0	0	18	Not classified	Not classified	II	100%	
Psoas Major	0	0	0	3	0	0	0	0	3	6	0	0	0	0	0	0	0	0	0	0	0	0	0	0	0	0	0	9	Not classified	Not classified	V	66%	
Psoas Minor	0	0	0	0	0	0	0	0	0	0	0	0	0	0	0	0	0	0	0	0	0	0	0	0	0	0	0	6	Not classified	Not classified	IV	100%	
Total																												167					

2.2.2.3 Muscles of the Back

Splenius Capitis:

In 2 angiographic studies the major pedicle to splenius capitis was from the occipital artery, and with minor blood supply from the vertebral artery and deep cervical artery. This is a type II muscle.

Latissimus Dorsi:

The latissimus dorsi is a three-territory muscle.^{85,86} In 44 angiograms this muscle always received its dominant blood supply by the thoracodorsal artery, the intercostal and lumbar perforators accounting for the three previous territories as well as an additional small but important contribution from the arcade formed by the dorsal scapular and descending branch of the circumflex artery at the inferior angle of the scapula (Figure 9). The thoracodorsal artery is the dominant arterial supply and enters the proximal part of the muscle, supplying over half of the proximal part of the muscle. The lower and posterior parts are supplied by 4-6 posterior intercostal arteries and lumbar perforators. The thoracodorsal artery anastomoses with intercostal, lumbar perforators and the arcade formed by the dorsal scapular and descending branch of the circumflex artery at the inferior angle of the scapula within the muscle. This muscle is a type V.

Trapezius:

There are many conflicting reports in the literature regarding the arterial anatomy of the trapezius muscle. Inconsistent nomenclature and the presence of anatomical

variability in the origin of both the transverse cervical artery and the dorsal scapular artery explain the difficulty in understanding the vascular anatomy of this muscle.

According to the Federative Committee on Anatomical Terminology (FCAT) the dorsal scapular artery is an old term.⁸⁷ The transverse cervical artery (TCA) in their definition divides into a superficial and deep branches and the deep branch, according to FCAT, is the dorsal scapular artery in some literature.

Despite this explanation, the confusion in the literature and textbook remains, the FCAT describes a deep branch of the transverse cervical artery arising from the subclavian artery in 67 % of the case; to describe the dorsal scapular artery as a deep branch of the transverse cervical is not accurate since it implies a more superficial course of the source artery, as the dorsal scapular artery travels deep to the rhomboids muscle prior to sending its superficial branch to trapezius on the other hand, the transverse cervical artery only travels deep to trapezius and is more superficial to the dorsal scapular artery.

According to few but well conducted anatomical studies; the transverse cervical artery arises most of the time of the thyrocervical trunk (77%).^{88, 89} In 20 % of the cases the transverse cervical artery arose as a branch of the dorsal scapular artery. This was confirmed by our review, and is further illustrated in phase II of this thesis. (Chapter 4 page 140).

In 44 angiograms the trapezius muscle was a type II muscle with superior, lower and middle zones. The muscles is supplied by the occipital artery (OA), deep cervical artery, transverse cervical artery (TCA) deep and superficial branches, superficial branch

of the dorsal scapular artery (DSA), vertebral radicular perforators and the posterior intercostal arteries (PICA).

The smallest zone of perfusion is near the muscle's occipital origin and is supplied by branches of the occipital artery, and deep cervical artery. The part around the root of the neck and the posterior shoulder is the largest zone of perfusion, and is supplied mostly by the deep branch of the transverse cervical artery, and the superficial branch of TCA supplies the muscle and the overlying skin medial to the posterior shoulder. The suprascapular artery supplies a small area laterally near the acromion. We confirm that the transverse cervical artery is the dominant arterial supply.⁹⁰⁻⁹²

The dorsal scapular artery descends along the medial border of the scapula and sends a superficial perforating branch that supplies the middle third of the muscle on its deep surface. The vertebral radicular perforators supply the muscle medially around the spine. The posterior intercostal arteries supply the muscle constantly in its lower and lateral parts (Figure 10).

Levator Scapula:

Twenty angiograms were reviewed revealing a type II muscle with the major pedicle from the descending branch of the transverse cervical trunk or dorsal scapular artery. The minor pedicle was via the costocervical trunk near the muscle's origin.

Rhomboids:

The rhomboids receive its blood supply from the main vessels that course to supply the trapezius muscle. In 20 angiograms, the pattern of arterial supply was segmental type IV.

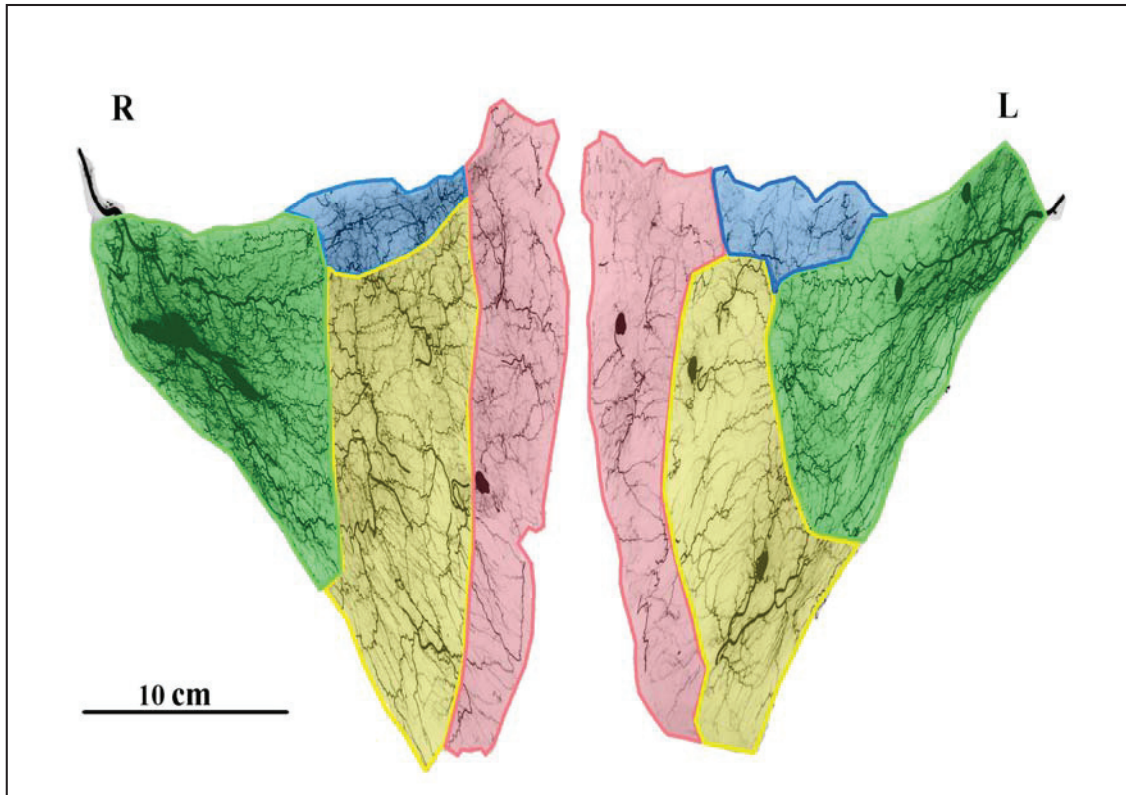


Figure 9: Right and left Latissimus Dorsi Muscle

The latissimus dorsi muscle with its four territories as outlined in this figure. The green zone outlines the territory supplied by the thoracodorsal artery. The yellow zone outlines the intercostal contribution to the latissimus dorsi. The red zone highlights the area supplied by the vertebral arteries, and finally the fourth zone in blue color outlining the blood supply to this muscle from the arcade formed by the descending branch of the circumflex scapular artery and the dorsal scapular artery.

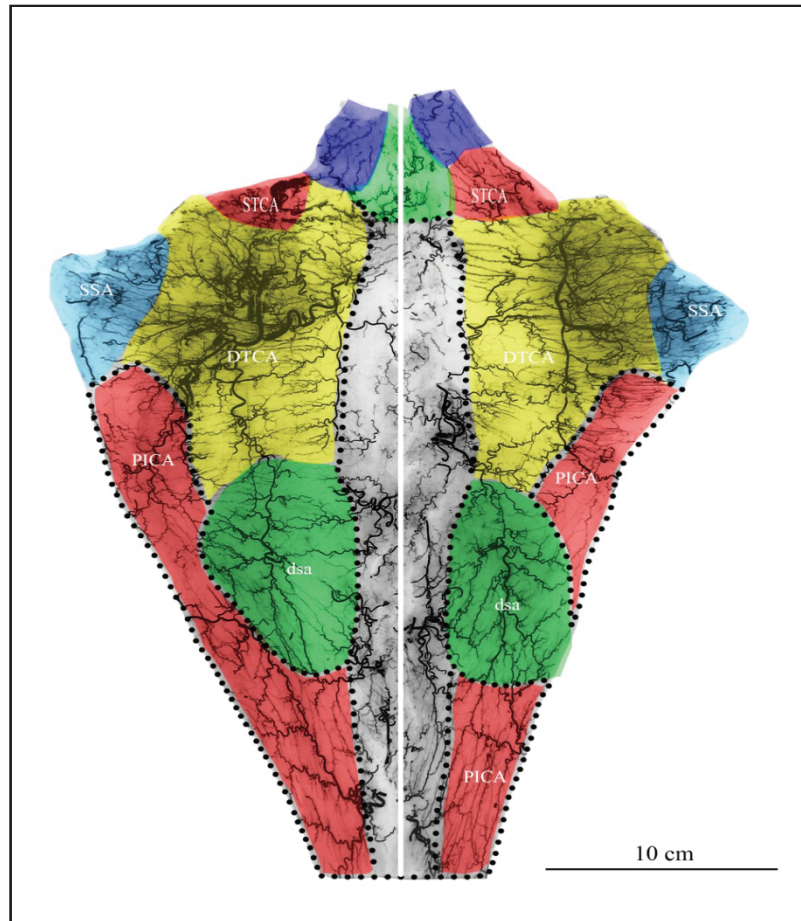


Figure 10: The Angiographic Territories of Trapezius (also see Trapezius in 3D)

Proximally and cephalically, the blue zone illustrates the contribution of the posterior occipital artery, the small green zone superiorly in the midline is the zone supplied by the deep cervical artery perforators. The transverse cervical artery supplies the muscle mainly by its deep branch in the yellow zone, and its superficial branch in red superiorly (TCA). The distal and caudal large in green is the area supplied by the dorsal scapular artery (DSA). The posterior intercostals supply the lateral aspect of trapezius, in red, and the gray area in the midline is the territory supplied by the vertebral radicular perforators.

Table 4: Summary of Angiograms of Muscles of the Back

	Type I					Type II					Type III					Type IV					Type V					Total	Current Dominant Type	Muscles Conforming to current classification %	Observed Type	Observed Dominant Type %
	Type I	Type II	Type III	Type IV	Type V	Type I	Type II	Type III	Type IV	Type V	Type I	Type II	Type III	Type IV	Type V	Type I	Type II	Type III	Type IV	Type V	Type I	Type II	Type III	Type IV	Type V					
Back																														
Splenius Capitis	0	2	0	0	0	0	0	0	0	0	0	0	0	0	0	0	0	0	0	0	0	0	0	0	0	2	II	100%	100%	
Latissimus Dorsi	0	0	0	0	0	0	0	0	0	0	0	0	0	0	0	0	0	0	0	0	0	0	0	0	0	44	V	100%	100%	
Trapezius	0	44	0	0	0	0	0	0	0	0	0	0	0	0	0	0	0	0	0	0	0	0	0	0	0	44	II	100%	100%	
Levator Scapula	0	20	0	0	0	0	0	0	0	0	0	0	0	0	0	0	0	0	0	0	0	0	0	0	0	20	II	100%	100%	
Rhomboid	0	0	0	0	0	0	0	0	0	0	0	0	0	0	0	0	0	0	0	0	0	0	0	0	0	20	IV	100%	100%	
Total																										130				

2.2.3 Upper Extremity

2.2.3.1 Muscles of the Shoulder

Deltoid:

In 44 angiograms this muscle received its dominant blood supply via the posterior circumflex humeral artery (Figure 11).⁹³⁻⁹⁶ Additional supply is provided anteriorly by the deltoid branch of the thoracoacromial artery, and the anterior circumflex humeral artery. Superiorly it receives blood supply from the acromial branch of the thoracoacromial artery, and inferiorly by the brachial and profunda brachii artery. This is a type II muscle.

Supraspinatus:

The suprascapular artery is the dominant blood supply. The suprascapular artery provides single long pedicle the supplies the muscle. The minor supply is segmental via dorsal scapular artery. In 33 angiograms this muscle was type V.

Infraspinatus:

In 25 angiograms this muscle received segmental blood supply from the suprascapular, dorsal scapular and circumflex scapular arteries. This muscle is type IV.

Subscapularis:

The subscapularis muscle receives its blood supply inferiorly either directly from the subscapular artery or from the thoracodorsal artery, this branch is consistent and the only variation is whether the vessel originated higher from the subscapular or more distal from the thoracodorsal artery. The laterally and superiorly the muscle receive a branch

from the anterior circumflex humeral artery, and medially the muscle receives multiple branches from the dorsal scapular artery. In 35 angiograms this muscle was type V.

Teres Major:

Teres major receives its blood supply via the circumflex scapular artery, the suprascapular artery (SSA), and dorsal scapular artery (DSA). The CSA is the dominant blood supply; the suprascapular artery and dorsal scapular artery provide the muscle with segmental blood supply.^{97,98} In 30 angiograms this muscle was a type V.

Teres Minor:

Teres minor had multiple small contributions from posterior circumflex humeral artery (PCHA), the circumflex scapular artery (CSA), and the suprascapular artery (SSA). In 38 angiograms this muscle was a type IV.

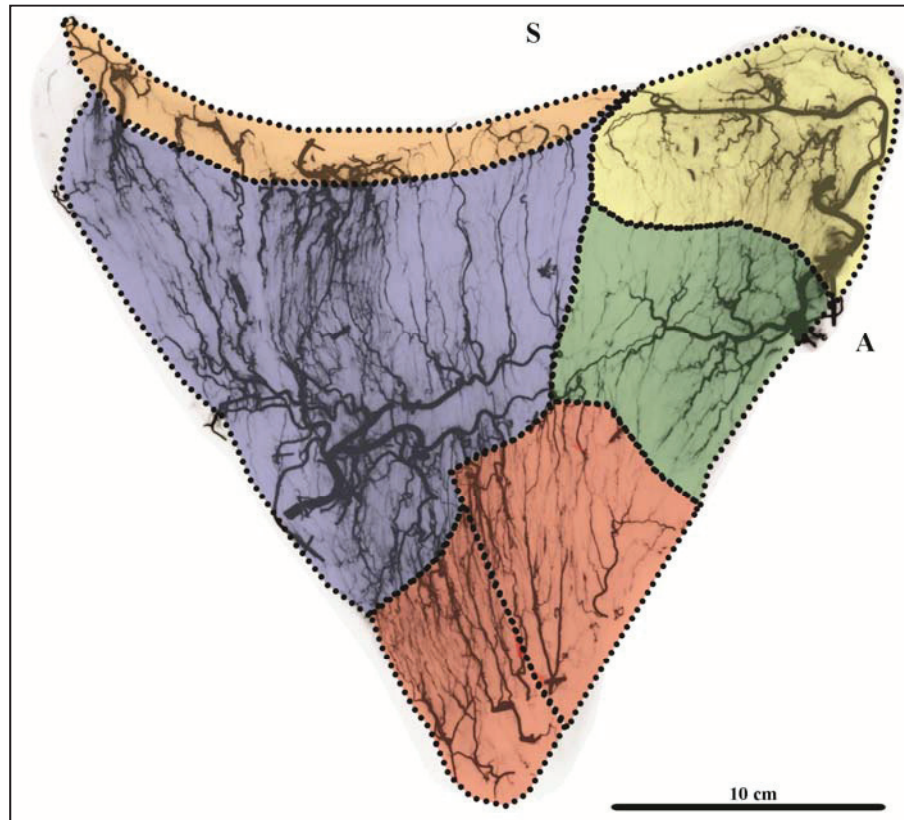


Figure 11: Vascular Territories of the Deltoid Muscle

The deltoideus has 6 vascular territories: The first territory is the superior part of the anterior fibers (yellow zone); this area is supplied by the acromial and deltoid branches of the thoracoacromial artery. The anterior circumflex humeral artery (ACHA) supplies the largest surface area of the anterior fibers of this muscle (green zone); (A=anterior). The brachial artery and profunda brachii artery supply the lower part of the deltoid fibers (red divided zone). The bulk of the muscle is supplied by the posterior circumflex humeral artery (PCHA) (blue zone). The orange zone is a small part of deltoideus near its superior and posterior attachment (S= superior), which is supplied by the anastomosing branches of the suprascapular artery.

2.2.3.2 Muscles of the Arm

Biceps Brachii:

The major supply to this muscle is via two large branches from the brachial artery in the middle mass of the muscle. It also receives small branches caudally from the ulnar collateral artery and profunda brachii artery.⁹⁹⁻¹⁰² In 43 angiograms, this muscle could be classified as a type III or II muscle (Figure 12). Please refer to the discussion section to for the modified classification, which eliminates the differences in classifying muscles with such blood supply.

Coracobrachialis:

In 12 angiograms coracobrachialis received a dominant pedicle from the axillary artery proximally and minor branches from the thoracoacromial artery. Midway it receives segmental blood supply along its medial aspect via the brachial artery.^{99, 103} This muscle is a type V (Figure 13).

Brachialis:

Brachialis is supplied from its medial surface by the brachial artery where it receives 2-3 branches with the proximal vessel being the dominant pedicle. The ulnar recurrent distally supplies a small part of the muscle as well as the radial collateral artery.⁹⁹ In 37 angiograms, this muscle was always a type II muscle (Figure 14).

Triceps Brachii:

In 28 angiograms the dominant supply to this muscle was via a proximal branch from the profunda brachii, the minor pedicles are also mostly from the profunda brachii. It also receives contribution from the posterior circumflex humeral artery proximally and the superior ulnar collateral distally.⁹⁹ This is a type II muscle (Figure 15).

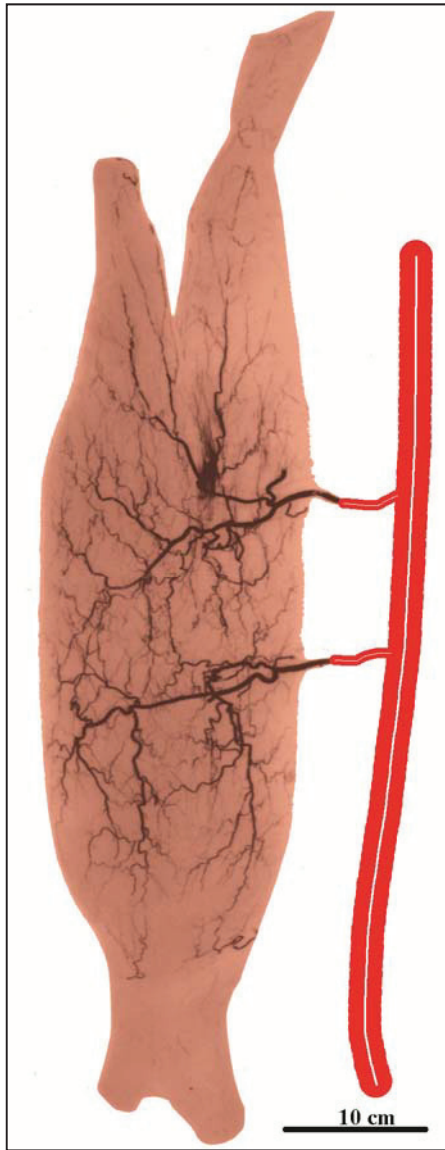


Figure 12: Angiogram of Biceps Brachii

Note the 2 main vessels feeding the biceps brachii muscle. The sources is the brachial artery, therefore the muscle blood supply is directly from a single angiosome (brachial artery angiosome). However, both vessels are equally dominant. This muscle could be classified either as a type II or III.



Figure 13: Angiogram of Coracobrachialis

Typical angiogram of coracobrachialis showing the source of blood supply to this muscle, the territory around the muscle's proximal attachment (yellow zone) is commonly supplied by the its major pedicle; the coracobrachialis branch of the axillary artery. The medial aspect receives its blood supply via a branch of the thoracoacromial artery (red zone). The distal part of the muscle (blue zone) is supplied by segmental branches of the brachial artery.

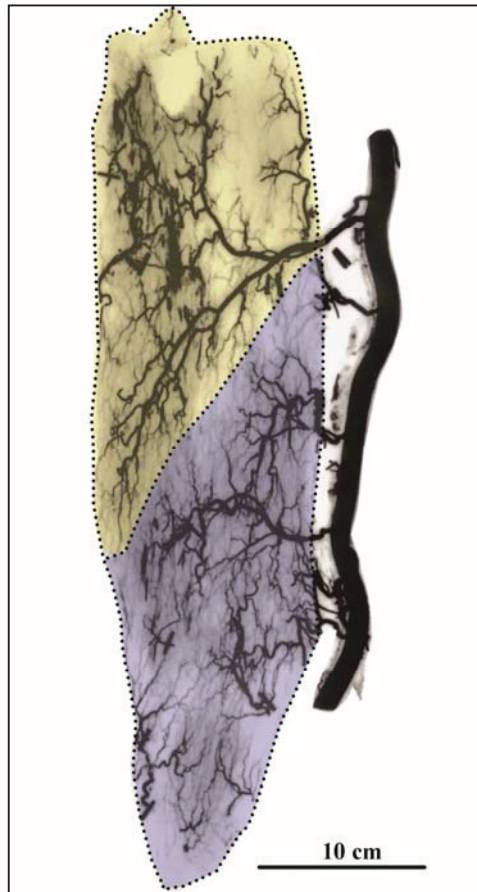


Figure 14: Angiogram of Brachialis

Brachialis is supplied by multiple branches from the brachial artery, with the most proximal branch being the dominant pedicle (yellow). The rest of the muscle is supplied by smaller branches along the course of the brachial artery (blue).

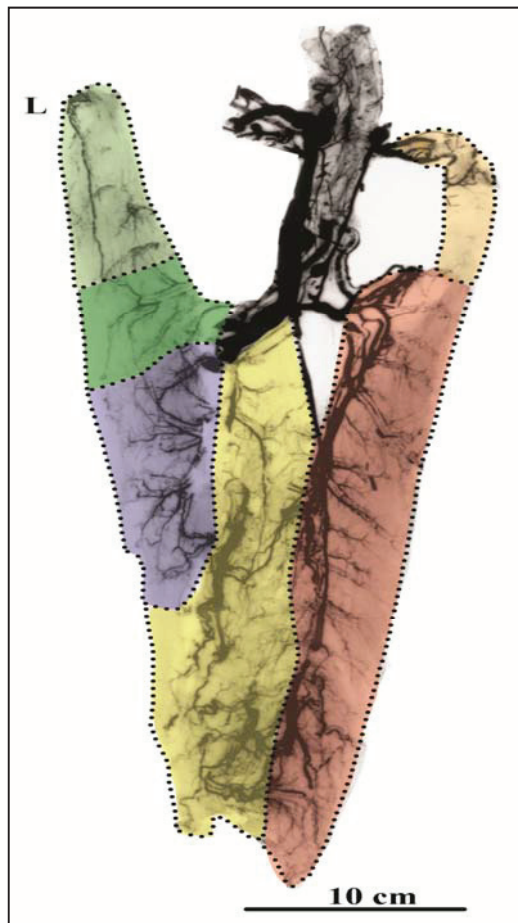


Figure 15: Angiogram of Triceps Brachii

The long head of the triceps brachii (L) receives its blood supply proximally via a branch from the circumflex scapular artery (light green). The middle aspect of the long head receives its blood supply via branches of the posterior circumflex humeral artery (dark green). The distal aspect of the long head receives its blood supply via the radial collateral (blue) and profunda brachii (yellow). The medial head receives its blood supply via branches of profunda brachii (yellow). The lateral head receives its blood supply via the ulnar collateral artery and profunda brachii (red).

Table 5: Summary of Angiograms of Shoulder and Upper Arm

Upper Extremity	Muscles	Type I	Type II	Type III	Type IV	Type V	Total	Current Dominant Type	Muscles Conforming to current classification %	Observed Type	Observed Dominant Type %
		Type I	Type II	Type III	Type IV	Type V	Total				
Scapular Muscles											
	Deltoid	0	43	0	0	0	43	II	100%	II	100%
	Infraspinatus	0	0	0	25	0	25	Not classified	Not classified	IV	100%
	Supraspinatus	0	0	33	0	0	33	Not classified	Not classified	III	100%
	Subscapularis	0	0	0	0	35	35	Not classified	Not classified	V	100%
	Teres Major	0	0	0	0	30	30	I	0%	V	100%
	Teres Minor	0	0	0	38	0	38	Not classified	Not classified	IV	100%
	Total						204				
Upper Arm											
	Biceps brachii	0	0	34	0	0	34	III	100%	III	100%
	Coracobrachialis	0	0	0	0	12	12	V	100%	V	100%
	Brachialis	0	37	0	0	0	37	II	100%	II	100%
	Tricepsbrachii	0	28	0	0	0	28	II	100%	II	100%
	Total						111				

2.2.3.3 Muscles of the Forearm

Volar Antebrachial muscles

Pronator Teres:

Pronator teres has two heads; it is supplied by segmental fashion from the inferior ulnar collateral proximally at its site of proximal attachment. The brachial artery provides supply prior to splitting into ulnar and radial arteries. The common ulnar Interosseus artery gives a branch to the muscle. Finally the muscle receives few small branches at the site of its distal attachment.^{1, 104} The most common configuration of this muscle is outlined in (Figure 16). In 16 angiograms, pronator teres was a type IV muscle.

Flexor Carpi Radialis:

Flexor carpi radialis receives its blood is supplied primarily by the radial artery. It receives a branch at it proximal attachment from the anterior ulnar recurrent artery, and a small contribution from the anterior interosseus artery. The radial artery provides the major branch those courses through the muscle as well as another 2-3 segmental branches that directly anastomose with the first major branch of the radial artery making, in 21 angiograms this muscle was a type V muscle (Figure 17A).¹⁰⁵

Palmaris Longus:

Palmaris longus is supplied via the anterior recurrent ulnar artery, as well as minor branches from the ulnar artery distally.^{1, 104} In 12 angiograms this muscle was a type II muscle (Figure 17B).

Flexor Carpi Ulnaris:

Flexor carpi ulnaris is supplied proximally and from its posterior attachment by a branch of posterior ulnar recurrent artery, the anterior ulnar recurrent also gives off a branch to this muscle at its anterior attachment. The ulnar artery is the major supplier to this muscle via several branches to the muscle. The first and second branches of the ulnar artery are usually small. The third is usually the largest of all these branches and is the dominant vascular pedicle to this muscle.^{1, 34, 105} This muscle has one major pedicle, three minor pedicles and several segmental branches. This muscle is grouped with type II muscle although it has some segmental blood supply along its course 18 of 24 muscles reviewed had the same pattern. Only six muscles had different arterial patterns (Figure 18).

Flexor Digitorum Superficialis:

The flexor digitorum superficialis receives its blood supply via four major vessels that. They all contribute to it in a segmental fashion. The anterior ulnar recurrent artery proximally, median artery from the deep and central surface, the ulnar artery medially and the radial artery laterally.^{1, 104, 105} In 21 angiograms this muscle was a type IV muscle (Figure 19).

Flexor Digitorum Profundus:

The posterior ulnar recurrent artery supplies this muscle proximally. The major blood supply to it is from the anterior interosseus artery, which supplies this muscle from its deep aspect, the anterior interosseus sends several branches, and usually the second

branch is the largest and is considered a major supplier of the muscle. The ulnar artery supplies the proximal part of the muscle from its lateral border with one to two branches and the distal part with one or two smaller branches from its medial border. The pattern of supply in 29 angiograms was type V (Figure 20).^{1, 104, 105}

Flexor Pollicis Longus:

The flexor pollicis longus is supplied by the anterior interosseus artery from its medial border, and the radial artery from its lateral border. The segmental supply by the anterior interosseus provides larger supply to this muscle. This muscle has segmental type IV picture (Figure 20).

Pronator Quadratus:

The deep and superficial heads of pronator quadratus receive their major supply by direct branches off the anterior interosseus artery,^{1, 104} it also receives some minor segmental contribution from both radial and ulnar arteries. The vascular supply was constant in 22 angiograms; the pattern of supply is type V (Figure 21).

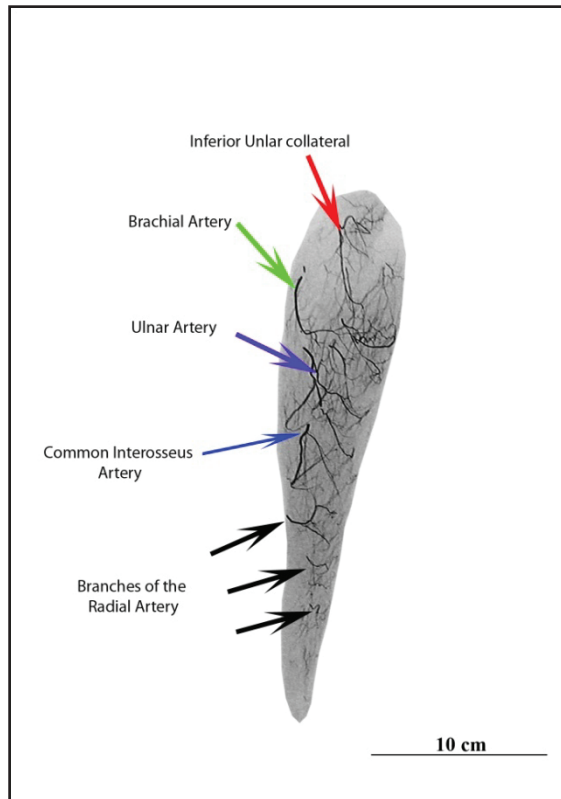
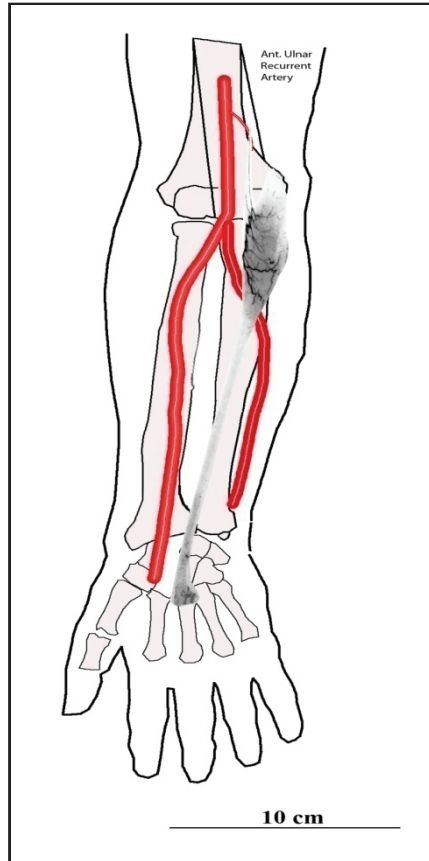


Figure 16: Pronator Teres

Pronator teres has two heads; it is supplied by segmental fashion from the inferior ulnar collateral proximally at its site of proximal attachment. The brachial artery provides supply prior to splitting into ulnar and radial arteries. The common ulnar interosseus artery gives a branch to the muscle. Finally, the muscle receives few small branches at the site of its distal attachment.

A) Palmaris Longus



B) Flexor Carpi Radialis

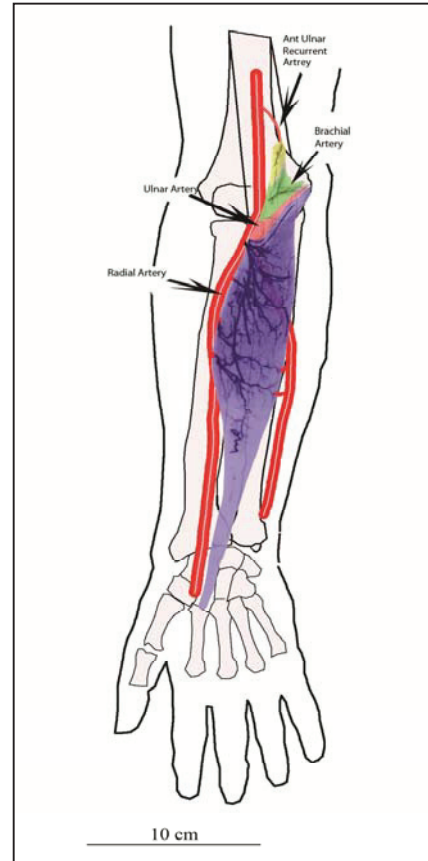


Figure 17: Palmaris Longus and Flexor Carpi Radialis

A. Palmaris longus is supplied via the anterior recurrent ulnar artery and some minor branches from the ulnar artery distally. This is a type II muscle. **B. Flexor Carpi Radialis**, this muscle receive its blood is supply primarily by the radial artery. It receives a branch at it proximal attachment from the anterior ulnar recurrent artery, and a small contribution from the Anterior Interosseus artery. The radial artery provides a major branch that courses through the muscle as well as 2-3 other segmental branches that directly anastomose with the first major branch of the radial artery making this muscle a Type V muscle.

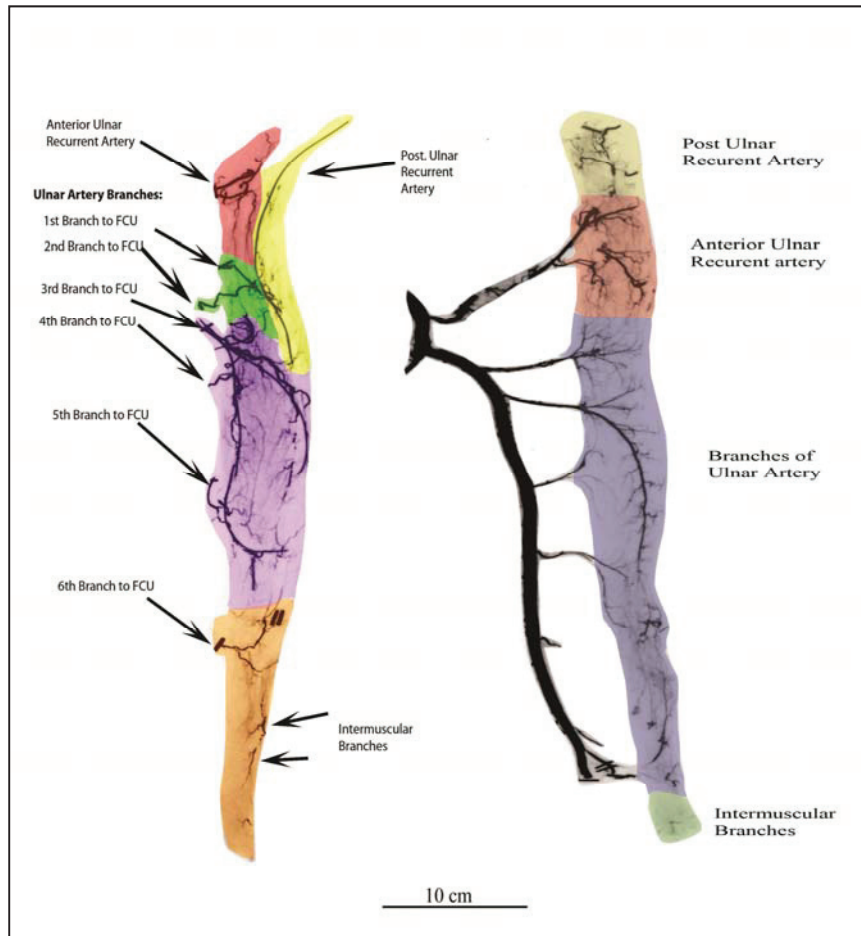


Figure 18: Flexor Carpi Ulnaris

Flexor carpi ulnaris is supplied proximally and from its posterior attachment by a branch of posterior ulnar recurrent artery, the anterior ulnar recurrent also gives off a branch to this muscle at its anterior attachment. The ulnar artery is the major arterial supply to this muscle. The first and second branches of the ulnar artery are usually small. The third is most often the largest of all these branches and is the dominant vascular pedicle to this muscle. This muscle has one major pedicle, 2-3 minor pedicles, and several segmental branches. This muscle is considered a type II albeit having segmental blood supply along its course.

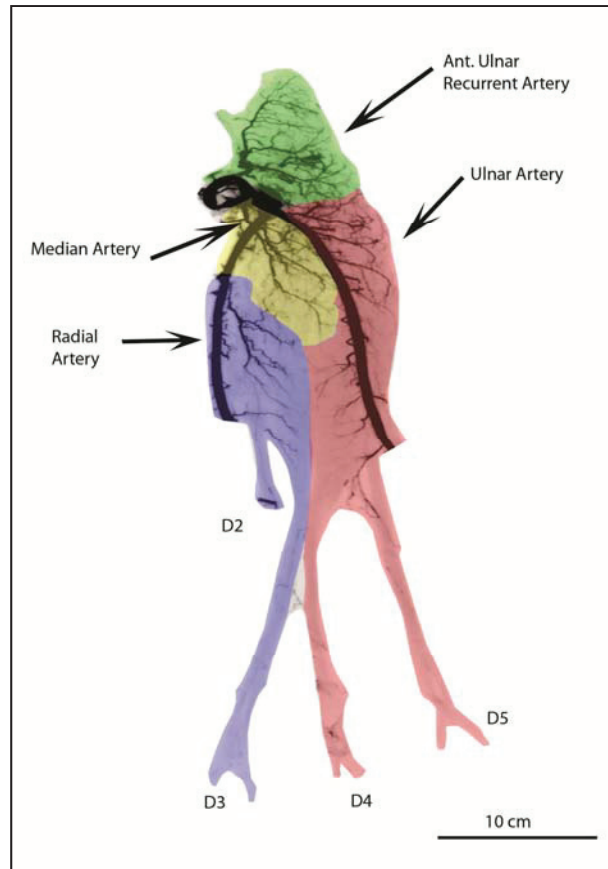


Figure 19: Flexor Digitorum Superficialis

There are four vessels that supply this muscle; proximally the anterior ulnar recurrent artery supplies the muscle, medially the ulnar artery is the major contributor to this muscle. Laterally the radial artery supplies FDS by 2-3 branches with the most proximal branch being the largest in caliber. The median artery supplies the muscle from the deep and central surfaces. FDS has 3 minor pedicles and several segmental but major supplies from the ulnar artery. This muscle is type IV.

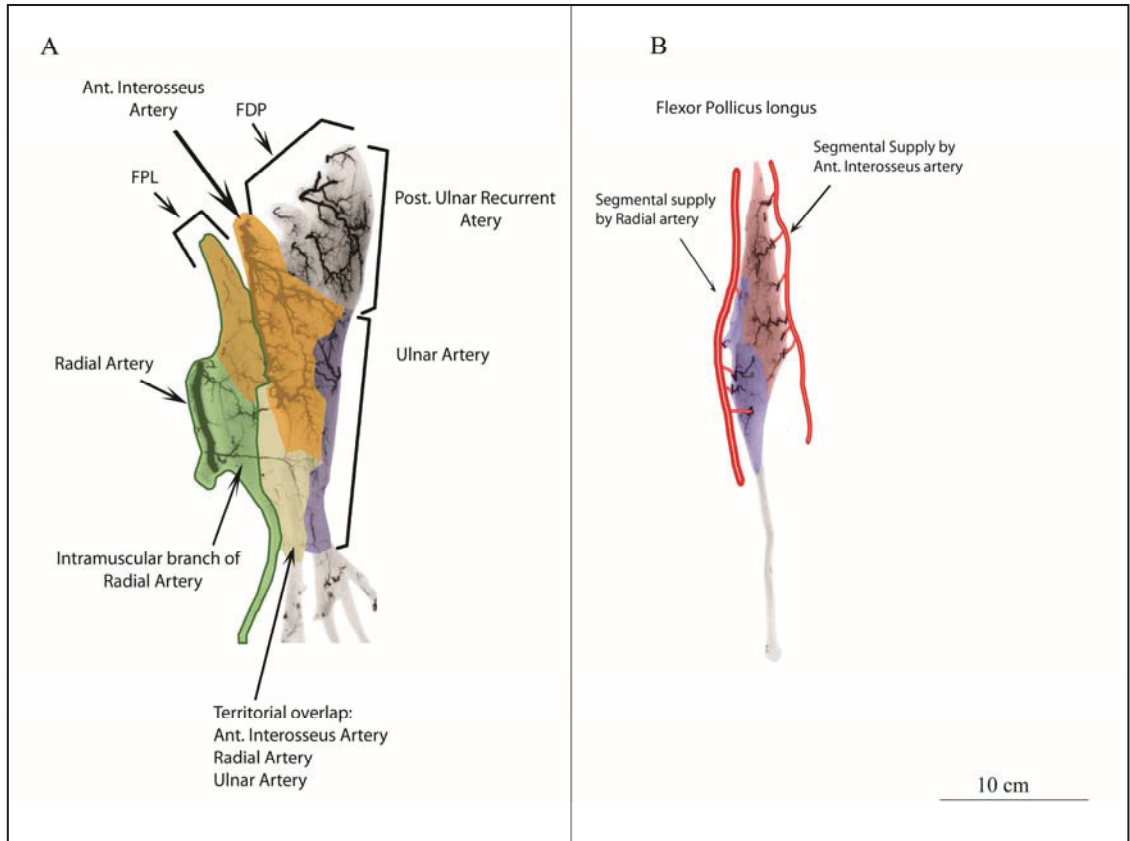


Figure 20: Flexor Digitorum Profundus and Flexor Pollicis Longus

A: Single Angiogram of FDP and FPL

B: Single Angiogram of FPL

The major blood supply to FDP is from the anterior interosseus artery, which supplies this muscle from its lateral border, the anterior interosseus sends several branches, and usually the second branch (or the third) is the largest and is considered a major supplier of the muscle. Proximally this muscle is supplied by the posterior ulnar recurrent artery, and the ulnar artery, which supplies the proximal part from its lateral border with 1-2 branches. The ulnar artery also supplies the distal part of the muscle medially with one or two smaller branches. The pattern of supply is type V.

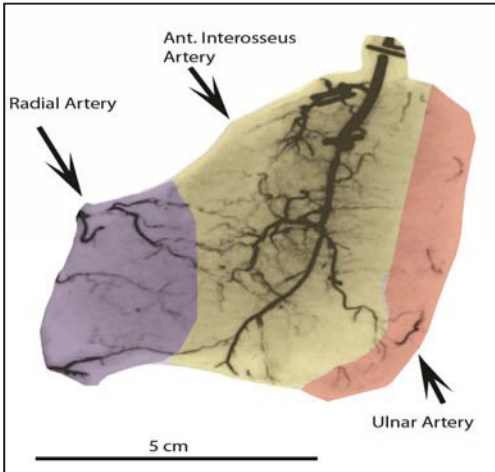


Figure 21: Pronator Quadratus:

Pronator quadratus is a three-territory muscle with its blood supply from the anterior interosseus artery (green) supplying the central and largest part of this muscle. The ulnar (red) and radial artery (blue) respectively supply the ulnar and radial attachments of pronator quadratus.

Table 6: Summary of Angiograms of the Volar Antebrachial Muscles

	Type I	Type II	Type III	Type IV	Type V	Total	Current Dominant Type	Muscles Conforming to current classification %	Observed Type	Observed Dominant Type %
The Volar Antebrachial Muscles										
Pronator teres	0	0	0	16	0	16	IV	100%	IV	100%
Flexor carpi radialis	0	0	0	0	21	21	V	100%	V	100%
Palmaris longus	0	12	0	0	0	12	II	100%	II	100%
Flexor carpi ulnaris	0	18	0	3	3	24	II	75%	II	75%
Flexor digitorum superficialis	0	0	0	21	0	21	IV	100%	IV	100%
Flexor digitorum profundus	0	0	0	0	29	29	IV	100%	V	100%
Flexor pollicis longus	0	0	0	25	0	25	III	0%	III	100%
Pronator quadratus	0	0	0	0	22	22	IV	0%	IV	100%
Total						170				

The Dorsal Antebrachial Muscles

Brachioradialis:

Brachioradialis is supplied proximally by a major pedicle from the radial collateral artery.

A branch the radial recurrent artery supplies the middle part. The radial artery provides

the middle and distal part of the muscle with multiple branches.^{104, 106, 107} In 36

Angiograms the pattern of blood supply to this muscle was type II (Figure 22).

Extensor Carpi Radialis Longus and Brevis:

The radial collateral artery supplies the proximal part of the ECRL. The radial recurrent

artery supplies the bulk of the muscle. The radial recurrent artery gives ECRL an average

of 2-3 Branches with the most distal branch being the largest.^{1, 104} The radial recurrent

artery also supplies the ECRB via intermuscular branches from ECRL. In 38 angiograms,

the pattern for ECRL is type II; ECRB is a type IV muscle due to its intermuscular

segmental supply (Figure 23).

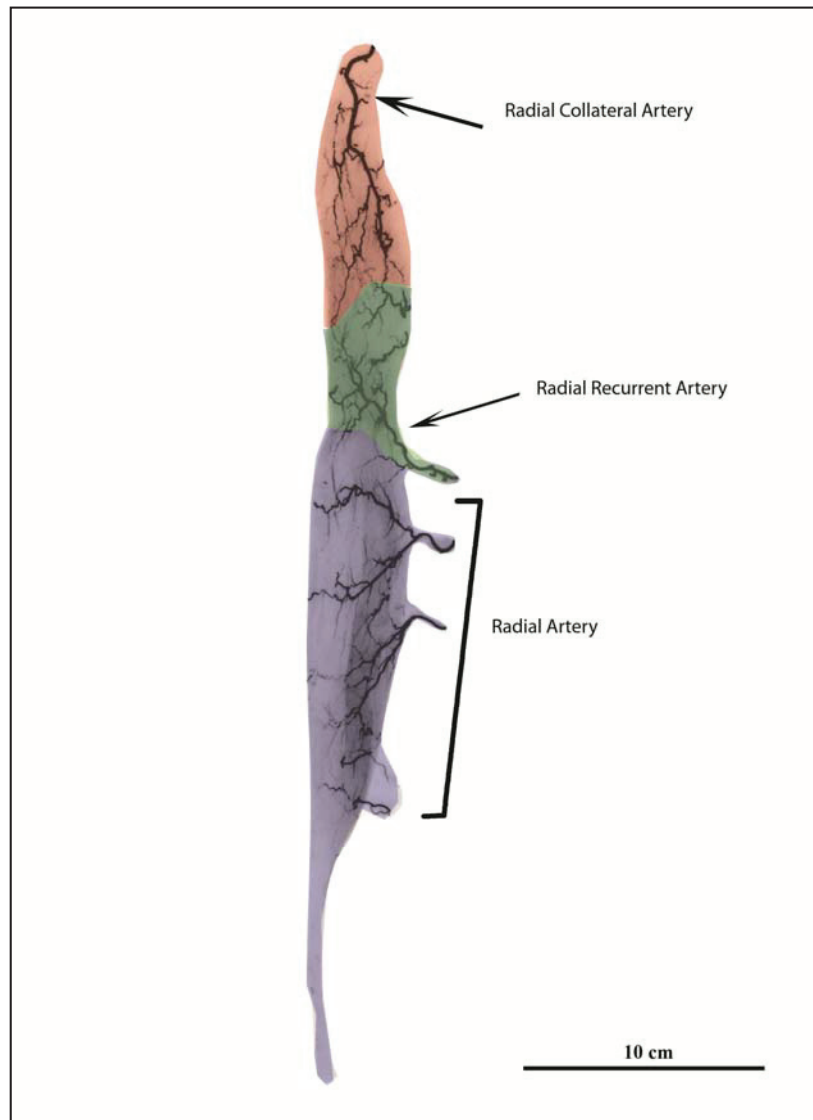


Figure 22: Brachioradialis:

The brachioradialis muscle receives its entire blood supply through the radial artery angiosome. The proximal part (red zone) is supplied by the radial collateral artery, the middle part is supplied by the radial recurrent artery (green zone) and the distal half is supplied by segmental branches from the radial artery (blue zone).

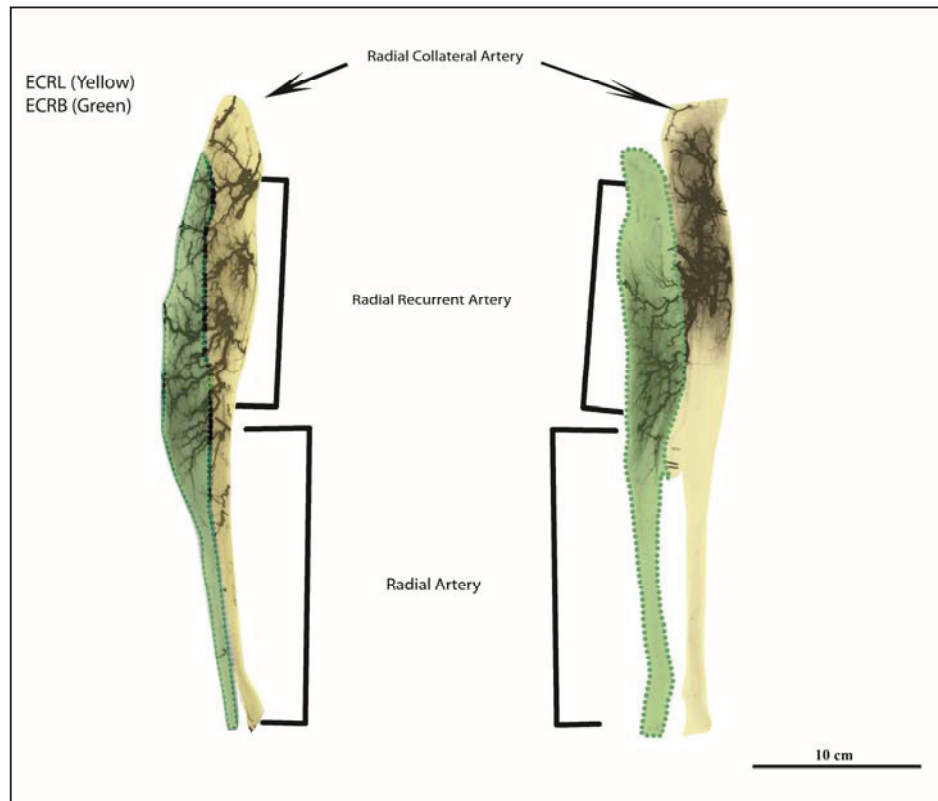


Figure 23: Extensor Carpi Radialis Longus and Brevis:

To the left ECRB and ECRL are shown compared to ECRL and ECRB on the right, despite the difference in the arterial architecture of the supply on the two angiograms a common feature is the constant intermuscular branches from ECRL to ECRB, this is noted to be the dominant blood supply to the ECRB muscle. This muscle does not fit any of the Mathes and Nahai's classes.

Extensor Digitorum Communis:

This muscle is supplied proximally by the Radial recurrent artery and Interosseus recurrent artery.^{1, 104} The dominant supply is by the posterior interosseus artery. This muscle has a type II pattern (Figure 24A).

Extensor Digiti Minimi:

This muscle receives its blood supply proximally by the interosseus recurrent artery. The major supply to this muscle is by the posterior interosseus in a segmental fashion.^{1, 104} The anterior interosseus artery supplies the distal end of the muscle via a perforating branch. In review of 17 angiograms this muscle is Type IV (Figure 24B).

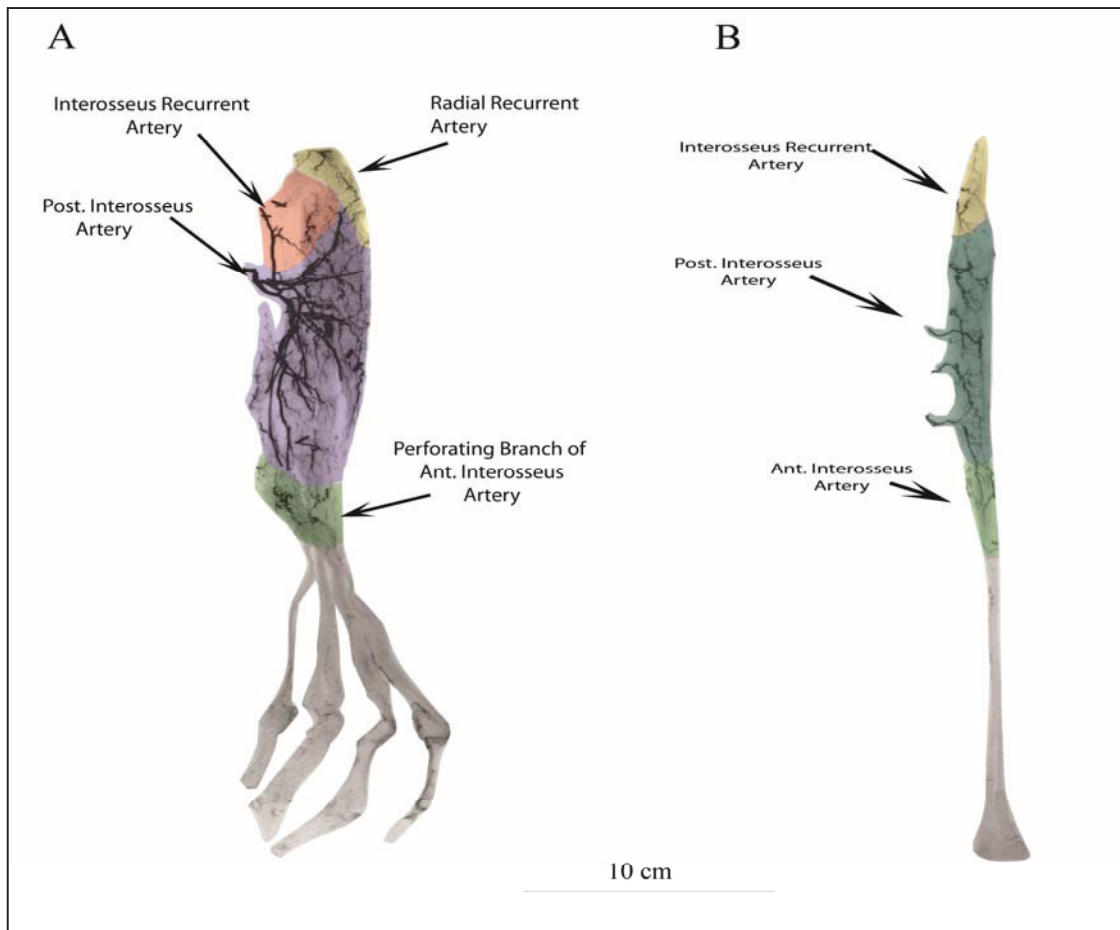


Figure 24: Extensor Digitorum Communis and Extensor Digiti Minimi

A. Extensor digitorum communis (EDC) receives its dominant blood supply from the posterior interosseus artery (blue); at its origin the muscle receives minor contribution from both the radial recurrent artery (yellow) and the interosseus recurrent artery (red). Distally the muscle receives an important contribution from the anterior interosseus artery; this allows survival of this muscle on the anterior interosseus artery in case of surgical or traumatic division of the posterior interosseus artery. **B.** Extensor digiti minimi (EDM) receives its major blood supply from the posterior interosseus artery (blue), proximally at its origin it receives minor contribution from the interosseus recurrent artery (yellow), and distally and important contribution from the anterior interosseus artery (green).

Extensor Carpi Ulnaris:

The proximal part of this muscle is supplied by the Interosseus recurrent artery.¹⁰⁴
The major supply to this muscle is by the posterior interosseus artery via segmental branches. In 22 angiograms this muscle is type IV. (Figure 25 A)

Anconeus:

This muscle is supplied from its deep surface by a major branch of the posterior interosseus recurrent artery. Proximally and laterally it receives minor supply from the posterior branch of the radial collateral artery. Proximally and medially it receives a branch of the medial collateral artery.^{34, 104, 108} Anconeus was previously classified as type I, but in 12 angiograms it was a type II muscle (Figure 25B).

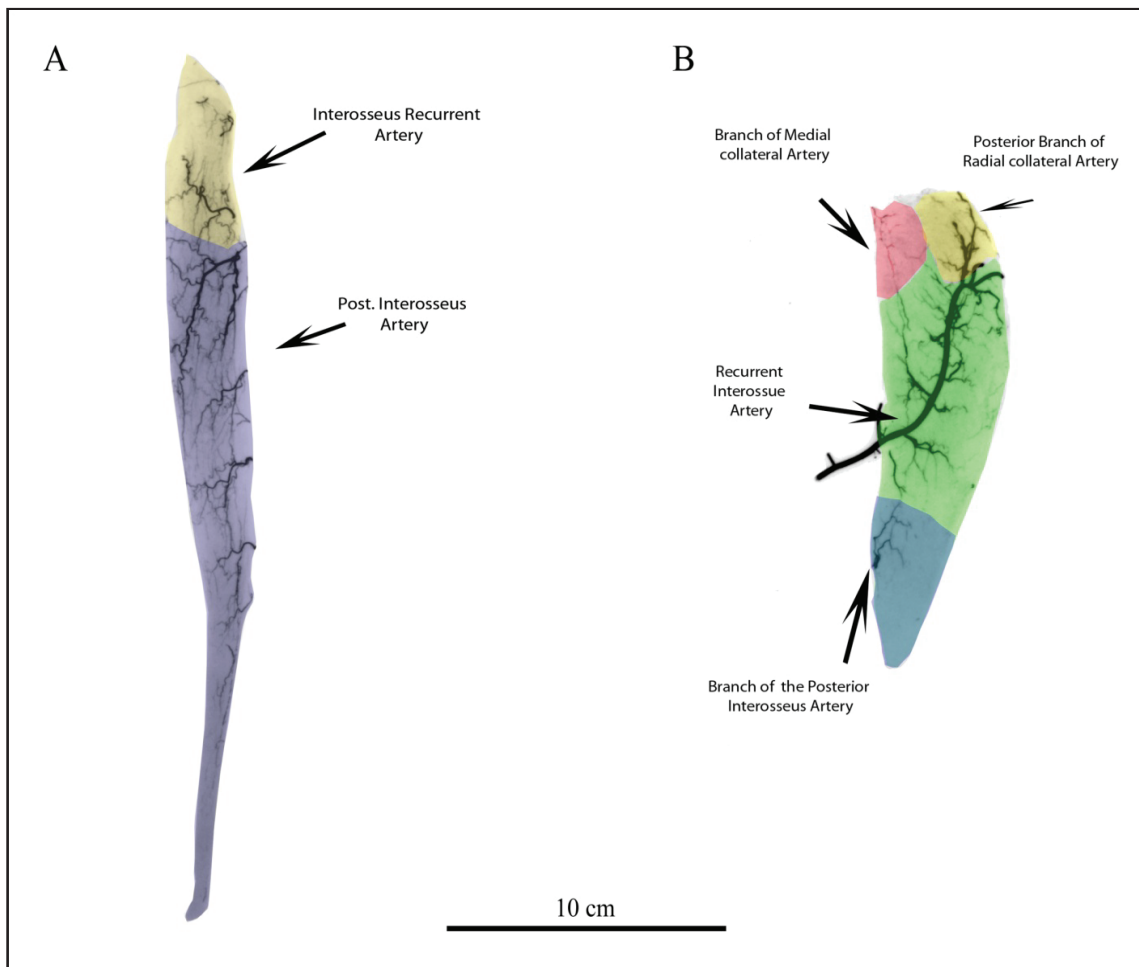


Figure 25: Extensor Carpi Ulnaris and Anconeus

A. Extensor Carpi Ulnaris (ECU) receives its major blood supply by segmental branches of the posterior interosseus artery, and proximally it receives a minor contribution from the interosseus recurrent artery. **B.** Anconeus receives its major blood supply from the recurrent interosseus artery and proximally receives a minor contribution from the medial collateral artery (branch of profunda brachii), and the radial collateral artery. The distal part of the muscle receives its blood supply from the posterior interosseus artery.

Supinator:

The supinator receives its arterial supply from the radial collateral artery on the volar surface and from both the posterior interosseus artery and recurrent interosseus artery on the dorsal surface. The major pedicle to this muscle is from the recurrent interosseus artery.¹⁰⁴ In 5 angiograms this is a type V muscle.

Abductor Pollicis Longus:

Abductor pollicis longus receives segmental blood supply along its radial border from the radial artery. Posteriorly it receives branches from the posterior interosseus artery and the anterior interosseus via intermuscular branches from the extensor pollicis brevis.^{1, 104} In 25 angiograms this muscle was a type IV.

Extensor Pollicis Brevis:

The extensor pollicis brevis receives its blood by segmental branches proximally from the posterior interosseus artery, and distally from the anterior interosseus artery.^{1, 104} In 25 angiogram this muscle was a type IV muscle.

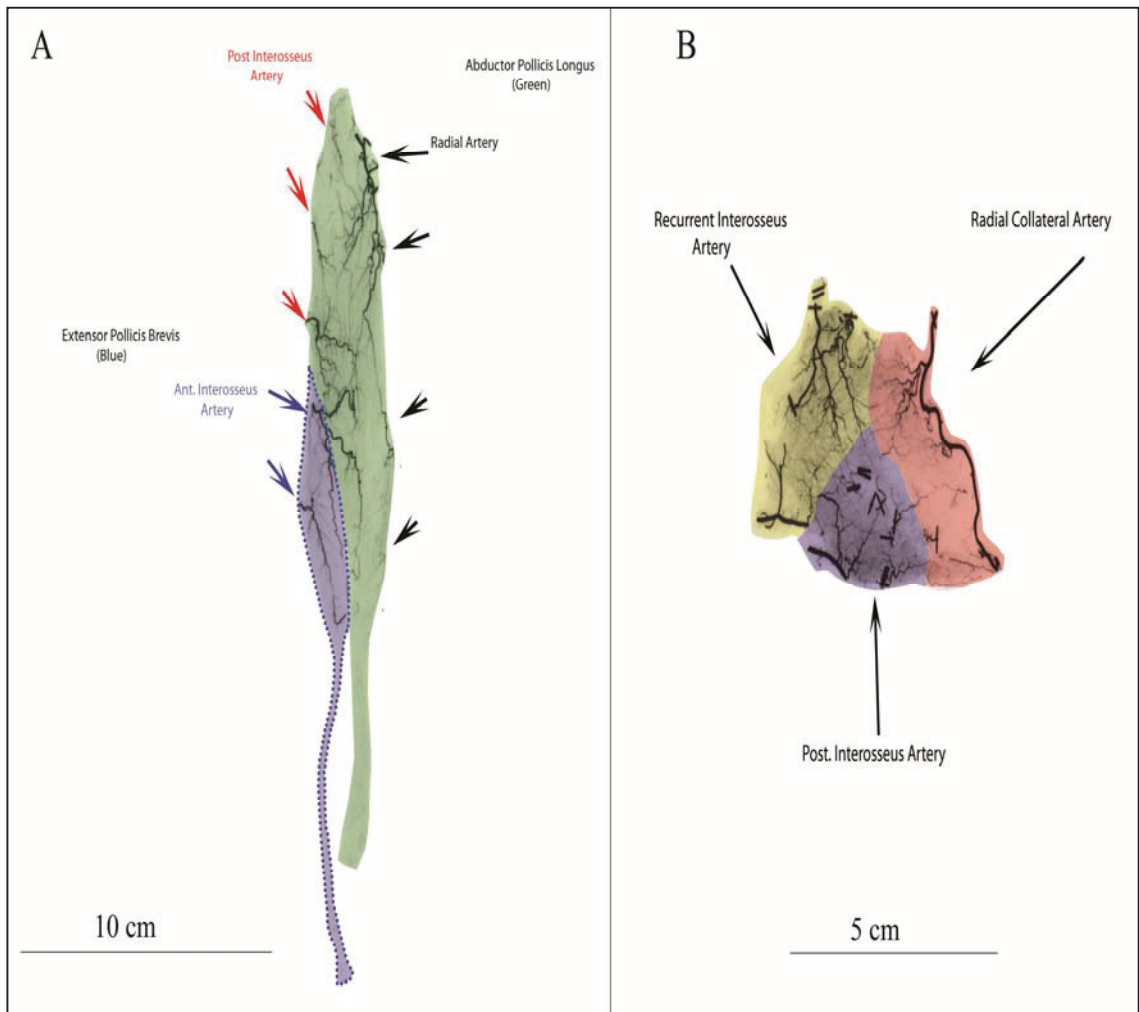


Figure 26: Extensor Pollicis Brevis, Abductor pollicis Longus and Supinator

A. Extensor Pollicis Brevis (blue) receives its blood supply by segmental branches off the anterior interosseus artery. The abductor pollicis longus (green) receives similar segmental blood supply from the radial artery and the posterior and anterior interosseus artery. **B.** Supinator receives its blood supply from the recurrent interosseus artery (yellow), the radial collateral artery (red), and the posterior interosseus artery distally (blue).

Extensor Pollicis Longus:

This muscle receives its blood supply via segmental branches, one from the radial artery proximally, 2-3 from the posterior interosseus artery, and 2 branches from the anterior interosseus artery. This was consistent in 25 angiograms, thus this muscle is a type IV.

Extensor Indicis Proprius:

In 5 angiograms this muscle was type IV. It has minor supply proximally from the posterior interosseus, and the rest of the muscle is supplied by perforating branches from the anterior interosseus artery.

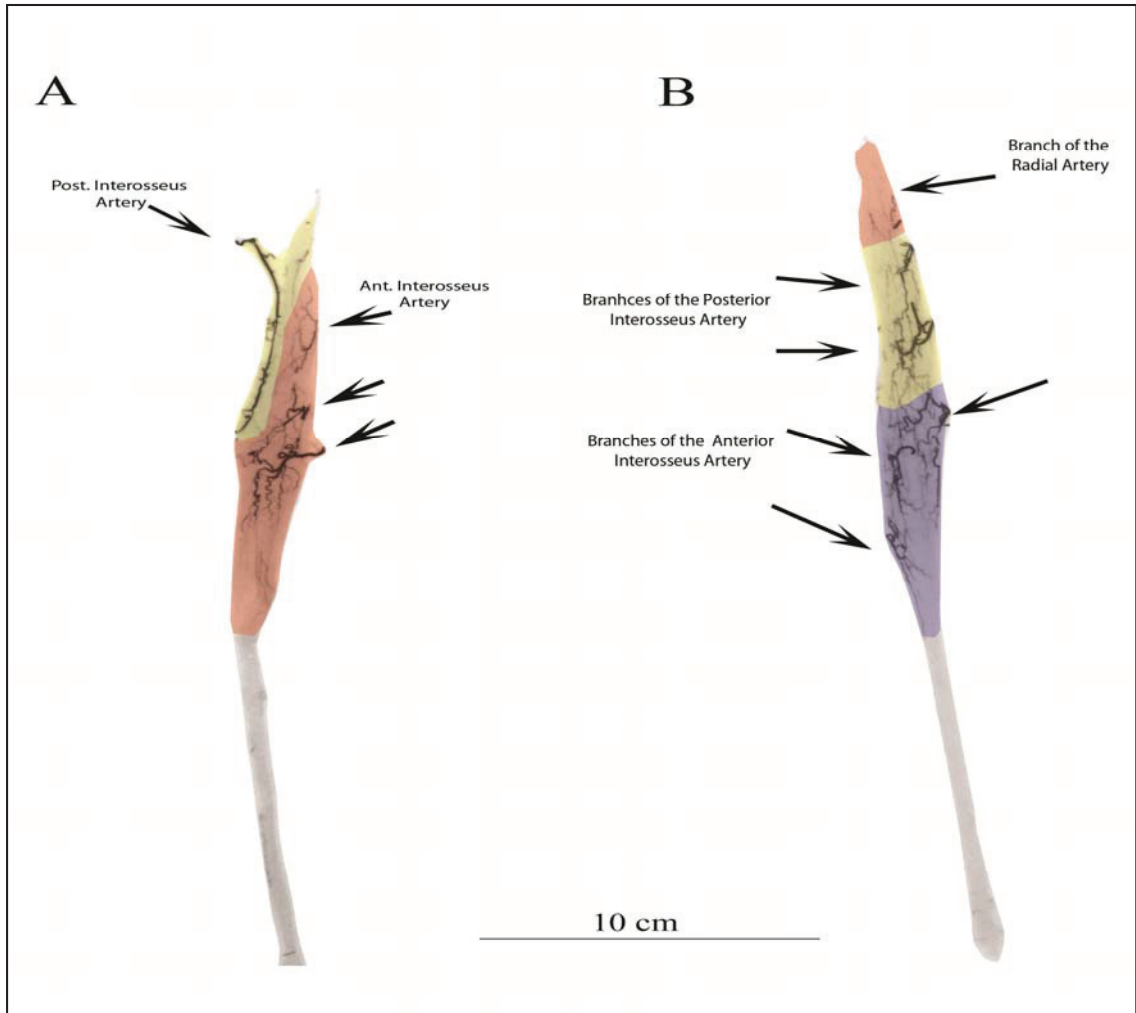


Figure 27: Extensor Indicis and Extensor Pollicis Longus

A. Extensor Indicis is a deep muscle that receives its major blood supply via perforating branches from the anterior interosseus artery (red). The posterior interosseus artery gives off minor branches to the muscle proximally (yellow). **B.** Extensor pollicis longus receives segmental blood supply from the posterior and anterior interosseus artery, as well as the radial artery at its origin.

Table 7: Summary of Angiograms of the Dorsal Antebrachial Muscles

	Type I	Type II	Type III	Type IV	Type V	Total	Current Dominant Type	Muscles Conforming to current classification %	Observed Type	Observed Dominant Type %
The Dorsal Antibrachial Muscles										
Brachioradialis	0	36	0	0	0	36	II	100%	II	100%
Extensor carpi radialis longus	0	38	0	0	0	38	I	0%	II	100%
Extensor carpi radialis brevis	0	0	0	38	0	38	I	0%	IV	100%
Extensor digitorum communis	0	18	0	0	0	18	II	100%	II	100%
Extensor digiti minimi	0	17	0	0	0	17	I	0%	IV	100%
Extensor carpi ulnaris	0	22	0	0	0	22	I	0%	II	100%
Anconeus	0	12	0	0	0	12	I	0%	II	100%
Supinator	0	15	0	0	0	15	III	0%	II	100%
Abductor Pollicis Longus	0	0	0	25	0	25	III	100%	III	100%
Extensor Pollicis Brevis	0	0	0	25	0	25	III	0%	IV	100%
Extensor Pollicis Longus	0	0	0	10	0	10	Not classified	0%	IV	100%
Extensor indicis proprius	0	0	0	5	0	5	Not classified	0%	IV	100%
Total						261				

2.2.3.4 Muscles of the Hand

Hypothenar Muscles

Abductor Digiti Minimi:

This muscle receives its blood supply dominantly by a proximal branch from the deep palmar arch, and a minor branch from the 5th palmar metacarpal artery and dorsal metacarpal. In 8 angiograms, one angiogram conformed to the current type II classification, and 7 angiograms exhibited a type III circulation.¹⁰⁹

Flexor Digiti Minimi brevis:

Flexor digiti minimi brevis receives its blood supply proximally by a dominant branch from the deep palmar arch and minor branches from the 4th palmar metacarpal artery¹⁰⁹. In 8 angiograms 5 were a type II.

Opponens Digiti Minimi:

This muscle receives its blood supply from both superficial and deep palmar arches. This muscle inserts into the 5th metacarpal bone, and it receives segmental blood supply from the dorsal metacarpal artery. The dominant blood supply is from the superficial palmar arch and has a minor supply from the deep palmar arch. Only one angiogram had a type I architecture, and the other 7 angiograms were a type V.

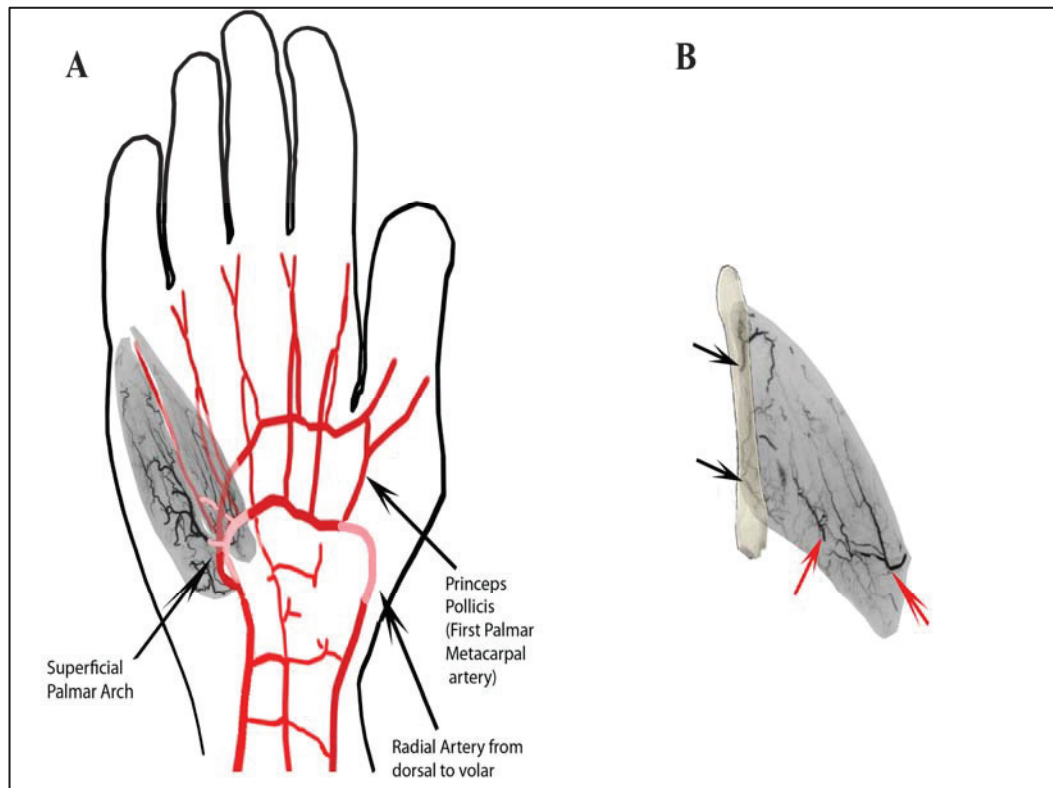


Figure 28: Hypothenar Muscles

The arterial anatomy of the hand in relationship to the hypothenar muscles. **A.** Abductor digiti minimi on the most ulnar aspect of the hand, and radial to it is the flexor digiti minimi brevis; a branch of the deep palmar arch is illustrated in pink entering the two muscles. **B.** The opponens digiti minimi in view with its arterial supply, the muscle receives its main pedicle from the superficial radial artery on the radial aspect, and on the ulnar surface it receives minor segmental branches from the fourth dorsal metacarpal artery.

Thenar Muscles:**Abductor Pollicis Brevis:**

This muscle receives its blood supply from the radial artery. It has 2 major pedicle the first proximal from the princeps pollicis artery, and the second is from dorsal metacarpal artery. This muscle previously classified as type I, however upon review of 8 angiograms it was found to be a type III in 7 angiograms.

Flexor Pollicis Brevis:

This muscle receives its blood supply from the first branch of the radial artery via the superficial palmar artery. In 8 angiograms this was the only significant pedicle to this muscle, yet there is a negligible contribution distally from princeps pollicis artery therefore it was grouped with type I muscle.

Opponens Pollicis:

This muscle is supplied by the radial artery via branches from the superficial palmar artery, princeps pollicis artery, first dorsal metacarpal artery, and the deep palmar arch. The superficial palmar artery here is the dominant blood source and the rest are minor contributors making this muscle a type II.¹¹⁰⁻¹¹⁶ In 8 angiograms this muscle was a type II.

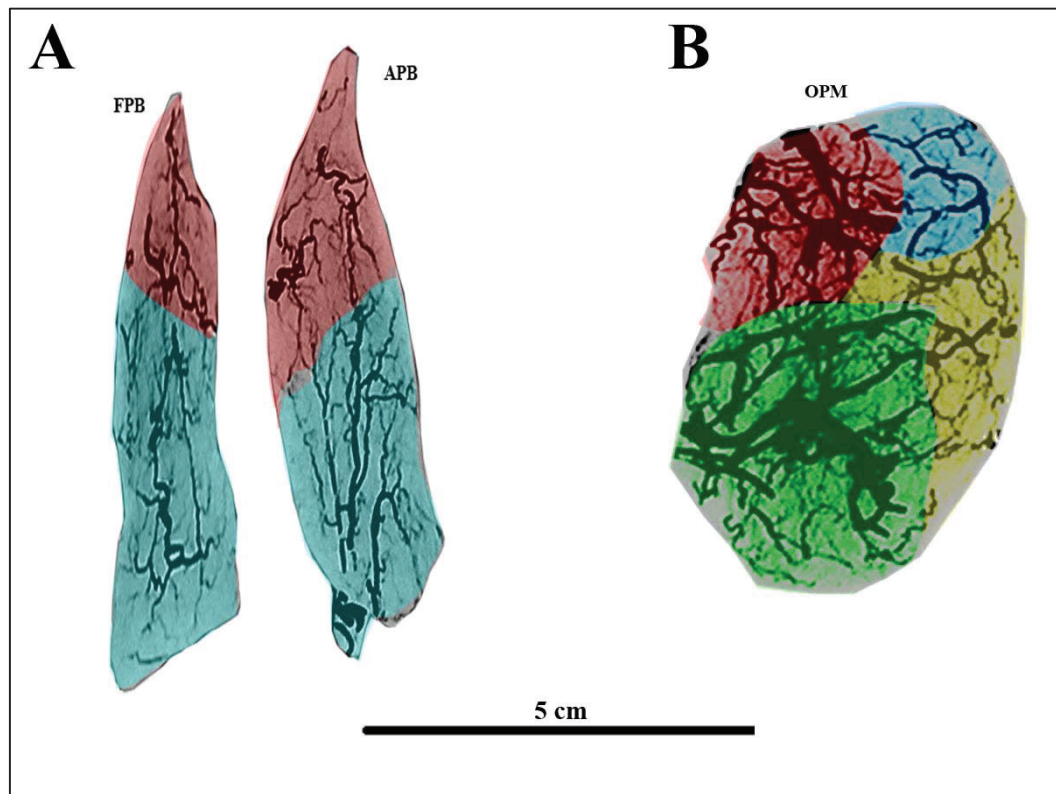


Figure 29: Thenar Muscles

A. Flexor pollicis brevis FPB; in blue the dominant pedicle from the superficial palmar arch, and in red it receives negligible contribution from princeps pollicis artery; Abductor pollicis brevis receives two dominant pedicles proximally from the superficial radial artery (blue) and distally from the princeps pollicis artery. **B.** Opponens pollicis muscle OPM receives its blood supply from the superficial palmar artery (green), and princeps pollicis (blue), and the deep palmar arch (red).

Deep Muscles of the Hand:

Adductor Pollicis:

This muscle has two heads, oblique and transverse both receive their blood supply from the radial artery. The oblique head receives a branch from princeps pollicis artery, and the deep palmar artery. The transverse head receives blood supply from second palmar metacarpal artery. The dominant supply is from the deep palmar arch and the princeps pollicis artery. In 8 angiograms this muscle was type III.

Lumbricals:

Lumbricals receive their dominant blood supply via the superficial palmar arch¹¹⁵. The minor blood supply to the 1st lumbrical is from the radialis indicis and the 4th lumbricals is from its respective dorsal metacarpal artery. The minor blood supply to the 2nd and 3rd lumbricals comes from the palmar metacarpal artery. In 29 out of 32 angiograms this muscle was a type II.

Dorsal Interossei:

In review of 32 dorsal interossei (DIOM 1-4) angiograms, the first dorsal interosseus receives its blood supply mainly from princeps pollicis artery,¹¹⁷ with minor contribution from radialis indicis artery and the first dorsal metacarpal artery,¹¹² making this muscle a type II.

The second dorsal Interosseus muscle receives its blood supply mainly from the second deep palmar artery (deep palmar arch), the second dorsal metacarpal artery. This muscle is a type II.

The third dorsal interosseus muscle receives its blood supply from third dorsal metacarpal artery and third palmar metacarpal artery, this muscles major supply was from the third dorsal metacarpal artery making it a type II muscle.

The fourth dorsal Interosseus muscle receives its blood supply mainly from the fourth palmar metacarpal artery with minor supply from the third dorsal metacarpal artery.¹¹⁰⁻¹¹⁶ This muscle is a type II.

Palmar Interossei:

In review of 24 palmar interossei muscles (PIOM 1-3), the first palmar interosseus was supplied by princeps pollicis with minor contribution from the second dorsal metacarpal artery. This is a type II muscle.

The second palmar interosseus was supplied mainly by the third palmar metacarpal artery with minor contribution from the deep palmar arch. This muscle is a type II.

The third palmar Interosseus was supplied mainly by branches of the fourth palmar metacarpal artery and with minor contribution from the fourth dorsal metacarpal artery. This muscle is type II.¹¹⁰⁻¹¹⁶

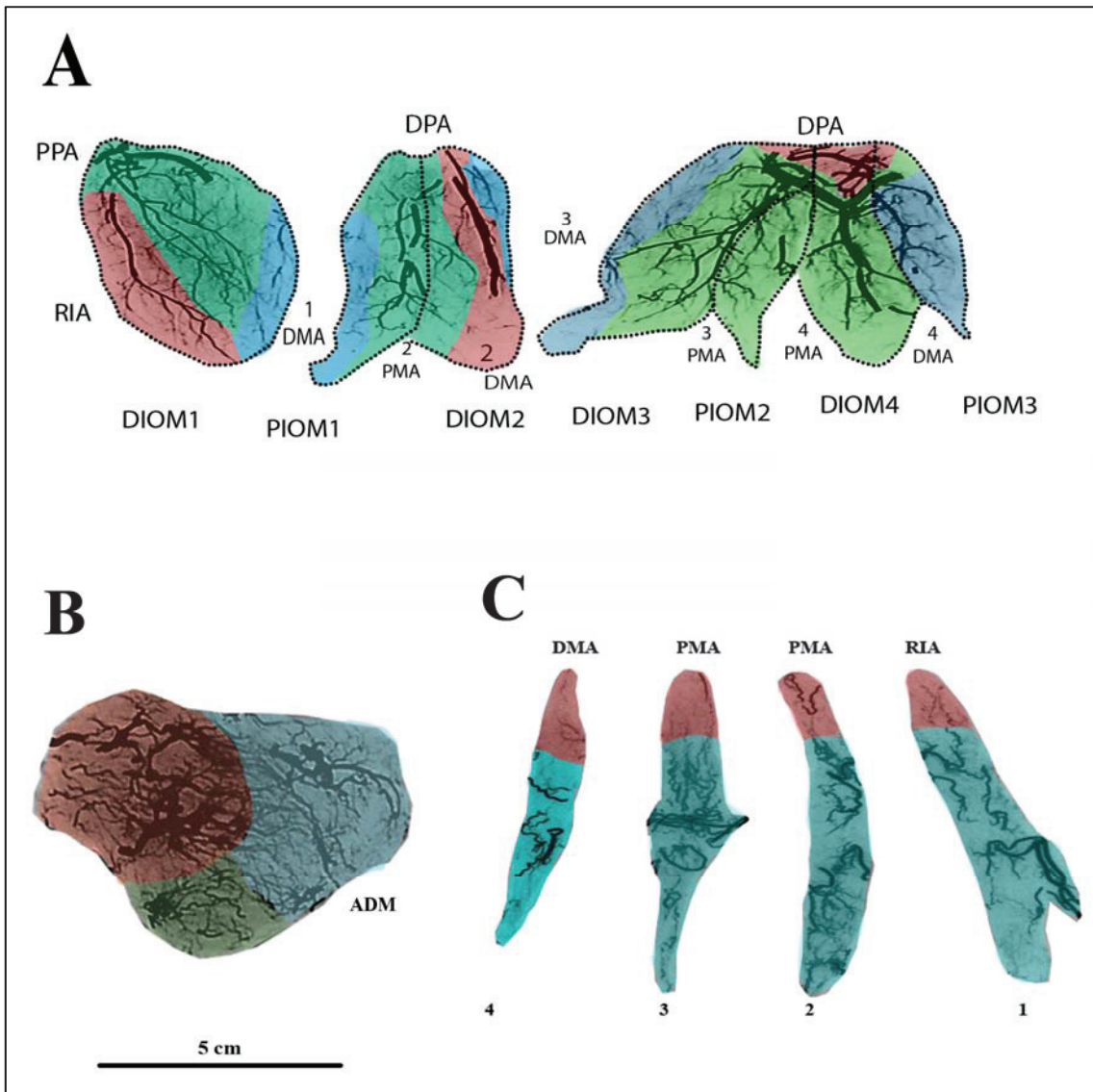


Figure 30: Deep Intrinsic Muscles of the Hand

A. Dorsal interossei muscles DIOM1-4; palmar interossei muscles PIOM 1-3, princeps pollicis PPA; Radialis indicis artery RA; deep palmar arch DPA; palmar metacarpal arteries PMA 1-4, dorsal metacarpal arteries DMA 1-4. **B.** Adductor pollicis muscle APM. **C.** Lumbricals L1-4; corresponding arterial supply is labeled DMCA, RIA, PMA as previously described.

Table 8: Summary of Angiograms of the Hand

Hand	Type I	Type II	Type III	Type IV	Type V	Total	Current Dominant Type	Muscles Conforming to current classification %	Observed Type	Observed Dominant Type %
Thenar muscles										
Abductor pollicis brevis	0	1	7	0	0	8	I	0%	III	88%
Flexor pollicis brevis	8	0	0	0	0	8	Not Classified	Not Classified	II	88%
Opponens pollicis	0	8	0	0	0	8	Not Classified	Not Classified	II	100%
Adductor pollicis	0	0	8	0	0	8	Not Classified	Not Classified	III	100%
Total	8	9	15	0	0	32		0%		
Hypothenar muscles										
Palmaris brevis	0	0	0	0	0	0	Not Classified	Not Classified		
Abductor digiti minimi	3	5	0	0	0	8	I	37%	II	63%
Flexor digiti minimi brevis	2	6	0	0	0	8	II	75%	II	75%
Opponens digiti minimi	0	1	0	0	7	8	Not Classified	Not Classified	V	88%
Total	5	12	0	0	7	24		56%		
Deep muscles										
Dorsal interosseous										
DIOM1	0	8	0	0	0	8	Not Classified	Not classified	II	100%
DIOM2	0	2	6	0	0	8	Not Classified	Not classified	III	75%
DIOM3	0	1	7	0	0	8	Not Classified	Not classified	III	88%
DIOM4	0	8	0	0	0	8	Not Classified	Not classified	II	100%
Total		19	13			32				
Palmar interosseous										
PIOM1	0	8	0	0	0	8	Not Classified	Not Classified	II	100%
PIOM2	3	5	0	0	0	8	Not Classified	Not Classified	II	63%
PIOM3	0	8	0	0	0	8	Not Classified	Not Classified	II	100%
Total	3	21				24				
Lumbricals (1,2,3,4)	0	29	3	0	0	32	Not Classified	Not Classified	II	90%
Total						32				
Total Hand						144				

2.2.4 Lower Extremity

2.2.4.1 Muscles of the Hip

Gluteus Maximus:

This muscle receives two major pedicles, the superior gluteal artery and the inferior gluteal artery. Distally it receives anastomotic branches from the deep branch of the medial circumflex femoral artery.¹¹⁸⁻¹²³ In 28 angiograms this muscle is a type III.

Gluteus Medius:

This muscle receives a major pedicle from the deep branch of the superior gluteal artery. It also receives minor blood supply from the anastomotic branches of the medial and lateral femoral circumflex artery.¹⁰⁴ In 27 angiograms this muscle is a type II.

Gluteus Minimus:

The gluteus medius receives blood supply from its superficial surface by a dominant direct branch from the superior gluteal artery. From its deep surface it receives several segmental branches from the superior gluteal artery and the medial and lateral circumflex femoral arteries.¹⁰⁴ In 31 angiograms this muscle is a type V.

Tensor Fascia Lata:

Tensor fascia lata receives its major pedicle from the ascending lateral femoral circumflex artery. The muscle also receives contribution from the superior gluteal artery.¹⁰⁴ In 18 angiograms this muscle is type II.

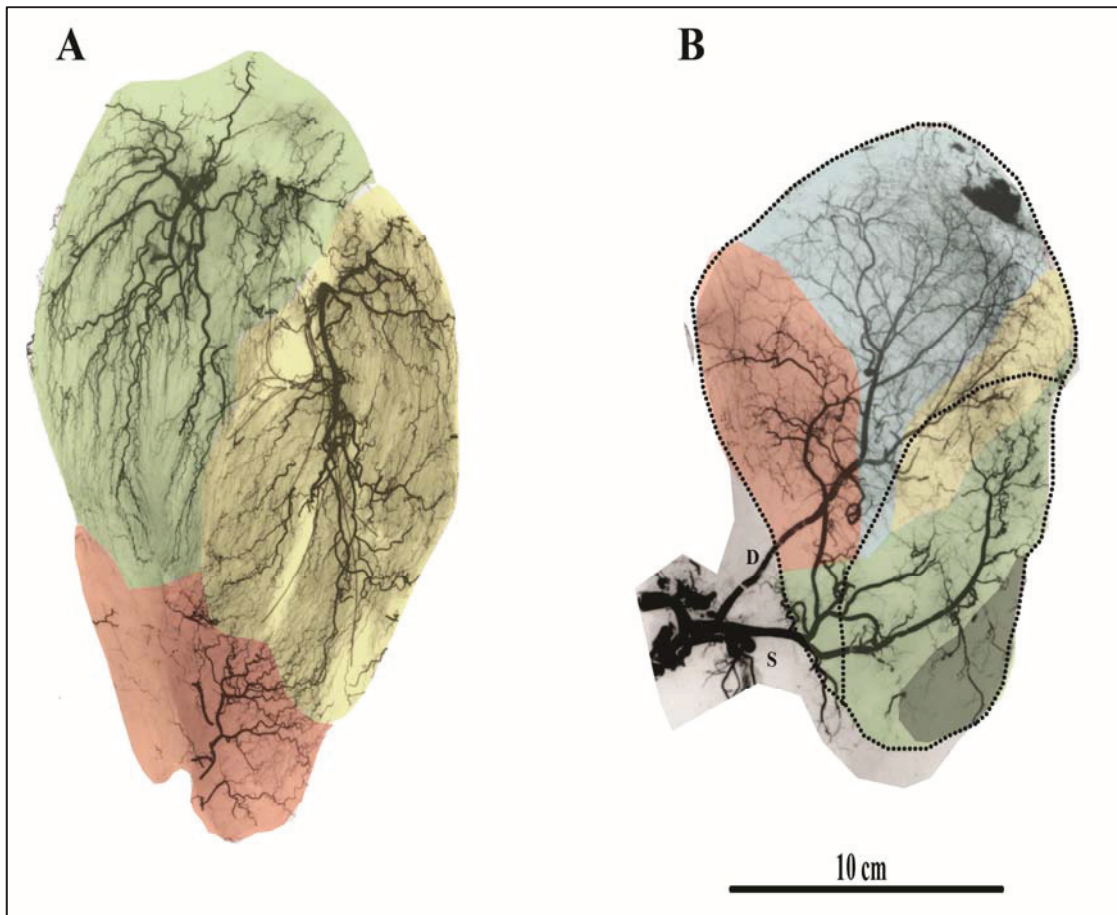


Figure 31: Gluteus Maximus, Medius and Minimus Muscles

A. Gluteus maximus with its two dominant pedicles from both superior gluteal artery (green) and inferior gluteal artery (yellow). The distal part is supplied by the anastomotic deep branch of the medial circumflex femoral artery. **B.** Gluteus medius is the upper part of angiogram B. The red area is the contribution of the superficial branch of the inferior gluteal artery, and the blue area is the major pedicle supplied by the deep branch of the inferior gluteal artery. The lower part of angiogram **B** is the gluteus medius muscle and its blood supply from the superficial branch of the inferior gluteal artery in green, with minor contribution superiorly from the deep branch of the inferior gluteal artery IGA in yellow. The anastomotic branch of the medial circumflex femoral artery provides minor blood supply to the muscle distally.

2.2.4.2 Muscles of the Thigh

Quadriceps Femoris

Rectus Femoris:

This muscle receives a minor pedicle from the ascending branch of the lateral circumflex femoral proximally, and a dominant vascular pedicle from the descending branch of LCFA few centimeters distal to the minor pedicle.^{34, 124} Twenty six out of 30 angiograms showed a type II circulation.

Vastus Lateralis:

Proximally the muscle receives a minor branch from the transverse lateral circumflex femoral artery. Medially it receives intermuscular branches from rectus femoris muscle. The lateral border receives the major arterial supply to the muscle via three perforating branches of the profunda femoris artery. In 30 angiograms this muscle is a type II.

Vastus Medialis:

Proximally vastus medialis receives its dominant blood supply by a branch from the superficial femoral artery. Distally it receives minor branches from the descending genicular artery. In 18 out of 25 angiogram vastus medialis is a type II.

Vastus Intermedius:

Vastus intermedius receives minor segmental blood supply from the superficial femoral artery medially. Laterally it receives a dominant branch from the descending lateral circumflex femoral artery^{104, 125}. In 25 angiograms the blood supply to this muscle is type II.

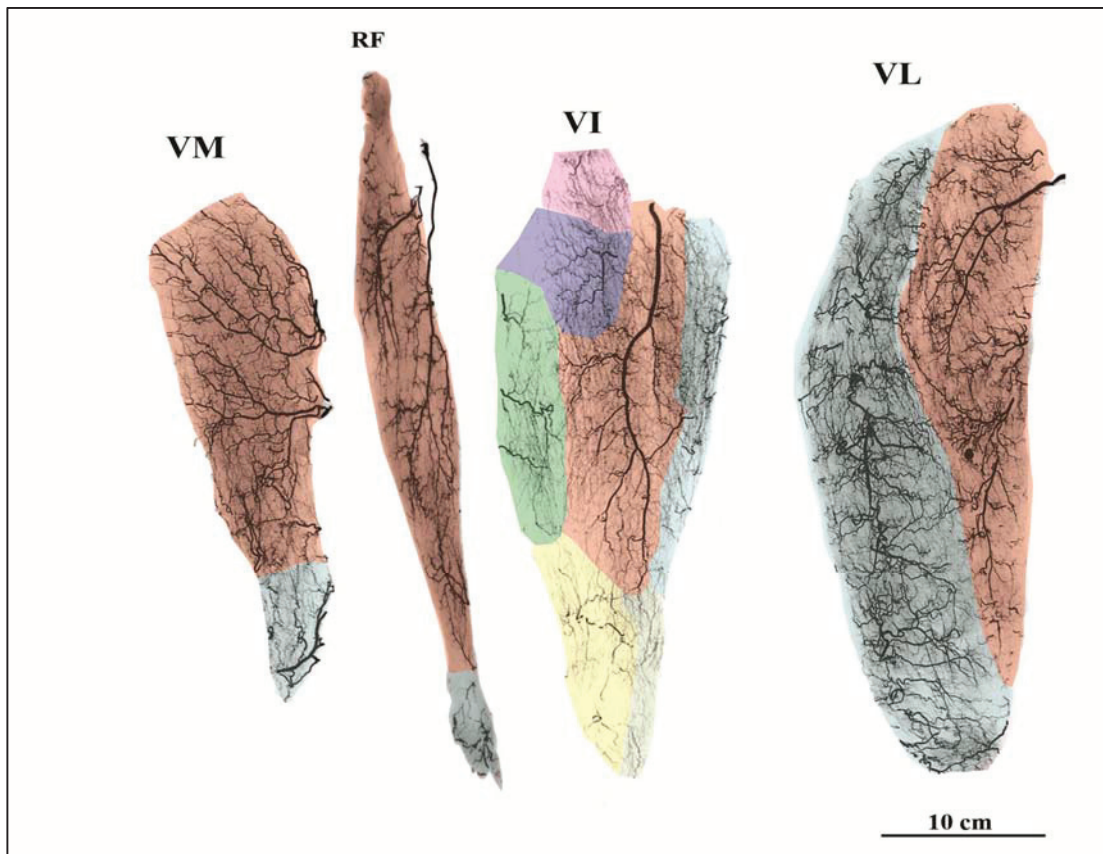


Figure 32: Quadriceps Femoris Muscles

Vastus medialis (VM) to the far left with the major arterial supply from the superficial femoral artery in red, and small contribution distally from the descending genicular artery in blue. **Rectus femoris (RF)** is second from left and it receives a minor pedicle proximally from the ascending branch of the lateral circumflex femoral (LCFA), the major pedicle is the second vessel proximally; distally this muscle receives minor contribution from the descending genicular artery. **Vastus intermedius (VI)** third from the left, this muscle receives minor segmental blood supply from the superficial femoral artery (blue), the descending branch of the lateral circumflex femoral artery provides a dominant branch that supplies the muscle (red). Distally the muscle receives blood supply from both the superior lateral genicular artery and the medial genicular artery (blue and grey). **Vastus lateralis (VL)** is supplied by the descending branch of the LCFA (red) and laterally receives bloods supply from profunda femoris (blue).

Muscles of Medial thigh

Sartorius:

Sartorius receives 6-7 equally distributed branches of the superficial femoral artery. In 52 angiograms this muscle is a type IV.

Gracilis:

The blood supply to the gracilis muscle is by 1 or 2 major pedicles supplied by the medial circumflex femoral artery, and occasionally this vessel arises from the adductor artery. The minor blood supply is via the superficial femoral artery.¹²⁶⁻¹²⁹ In 45 angiograms this muscle is a type II.

Semitendinosus:

Superiorly semitendinosus is supplied by a minor branch from the inferior gluteal artery. The dominant pedicle is from the descending branch of the medial circumflex femoral artery in the proximal third. The first perforating artery of the profunda femoral artery supplies the middle third. Inferiorly near its insertion, semitendinosus is supplied by the medial inferior genicular artery.¹⁰⁴ In 30 angiograms this muscle is a type II.



Figure 33: Muscles of Medial Thigh

A. Semitendinosus receives its blood supply superiorly from the inferior gluteal artery. The dominant pedicle to the muscle is from the ascending branch of the medial circumflex femoral (red). The first perforating branch of profunda femoral provides blood supply to mid substance; the medial genicular artery supplies the distal part. **B.** Gracilis muscle is supplied by the inferior gluteal artery superiorly, and the dominant blood supply is from the descending or adductor branch of the medial circumflex femoral. Distally the medial genicular artery supplies the muscle. **C.** Sartorius receives its blood supply in a segmental fashion from the superficial femoral artery.

Muscles of Posterior thigh:

Biceps Femoris:

The dominant pedicle to biceps femoris long head is the first perforator profunda femoris, and the minor blood supply is via the second and third profunda perforator, superiorly at its origin it receives minor blood supply from the inferior gluteal artery. The dominant blood supply to the short head is from the second and third profunda perforators, and inferiorly it receives minor blood supply from the superior lateral genicular.¹³⁰⁻¹³² In 29 angiograms the long head was a type II and the short head was a type IV.

Semimembranosus:

The dominant arterial blood supply is from first and or the second profunda perforator, the third profunda perforators provides minor contribution. The muscle superiorly receives minor branch from the inferior gluteal artery and distally it receives minor branch from the superficial femoral artery.³⁴ In 30 angiograms this muscle was a type II.

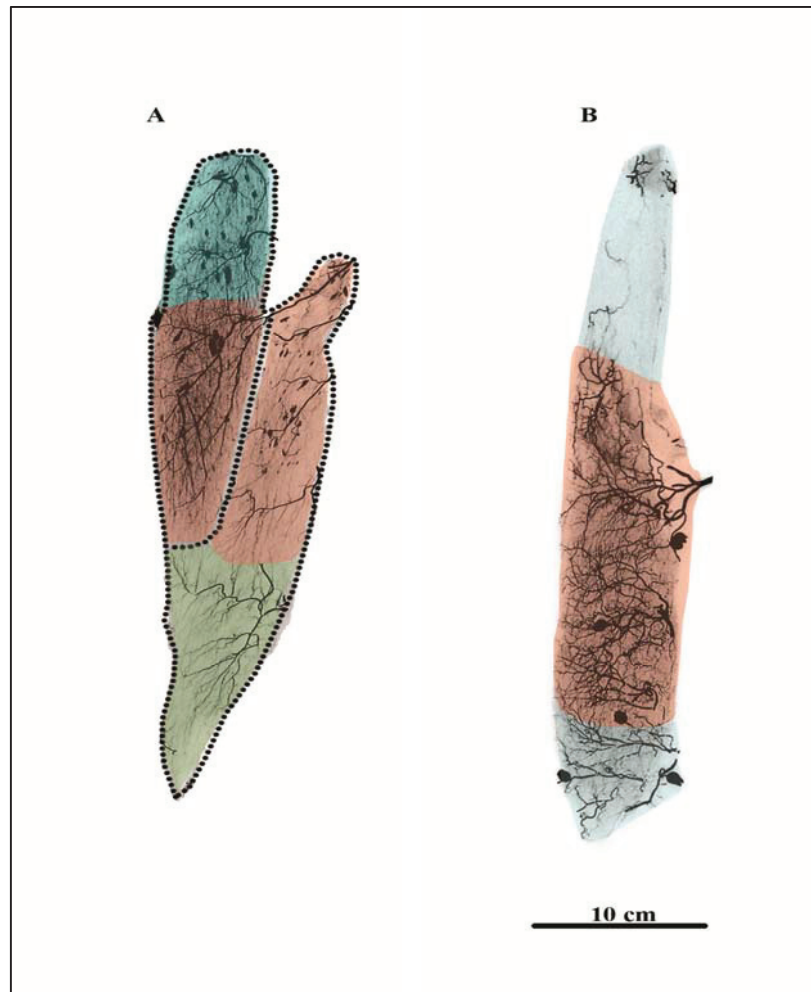


Figure 34: Angiogram of Muscles of the Posterior Thigh

A. Biceps femoris. The long head of biceps femoris, superiorly near its origin receives a branch from the inferior gluteal artery. The dominant blood supply is via the first perforating branch of profunda femoral artery. The short head receives branches from the all three perforators of profunda femoral artery and the distal end receives a branch from the superior lateral genicular artery. **B.** Semimembranosus receives a minor contribution from the inferior gluteal anterior near its origin, and is supplied segmentally via the perforators of profunda femoral artery. Distally the muscle receives minor contribution from the superficial femoral artery.

Table 9: Summary of Angiograms of Muscles of The Hip and Thigh

	Type I	Type II	Type III	Type IV	Type V	Total	Current Dominant Type	Muscles Conforming to current classification %	Observed Type	Observed Dominant Type %
Hip										
Gluteus Maximus	0	0	28	0	0	28	III	100%	III	100%
Gluteus Medius	9	18	0	0	0	27	Not classified	Not classified	II	67%
Gluteus Minimus	0	0	0	0	31	31	Not classified	Not classified	V	100%
Tensor Fasciae Latae	0	18	0	0	0	18	I	0%	II	100%
Total						104				
Thigh										
Quadriceps Femoris										
Rectus Femoris	4	26	0	0	0	30	II	87%	II	87%
Vastus Intermedius	0	18	7	0	0	25	II	72%	II	72%
Vastus Lateralis	0	30	0	0	0	30	II	100%	II	100%
Vastus Medialis	0	30	0	0	0	30	II	100%	II	100%
Total						115				
Sartorius	0	0	0	52	0	52	IV	100%	IV	100%
Gracilis	0	45	0	0	0	45	II	100%	II	100%
Adductor Brevis	0	25	0	0	0	25	II	100%	II	100%
Adductor Longus	0	27	0	0	0	27	II	100%	II	100%
Adductor Magnus	0	28	0	0	0	28	II	100%	II	100%
Biceps Femoris	0	29	0	0	0	29	II	100%	II	100%
Semimembranosus	0	30	0	0	0	30	II	100%	II	100%
Semitendinosus	0	30	0	0	0	30	II	100%	II	100%
Total						266				

2.2.4.3 Muscles of the Leg

Anterior Compartment

Tibialis Anterior:

Proximally it receives a small contribution from the anterior tibial recurrent artery. The anterior tibial artery is the major supply to this muscle and provides its segmental branches that enter the muscle on the lateral border. In 40 angiograms this is a type IV muscle.

Extensor Digitorum Longus:

The proximal part of the muscle receives a branch from the circumflex recurrent artery (from the anterior tibial artery); the rest of the muscle is supplied from its deep and medial surface by segmental branches of the anterior tibial artery. In 39 angiograms this muscle is type IV.

Extensor Hallucis Longus:

This muscle is supplied from its superficial surface by branches from the anterior tibial artery. In 38 angiograms the prevailing pattern was type IV.

Peroneus Tertius:

Peroneus tertius receives segmental blood supply from the anterior tibial artery proximally as well as segmental branches from the fibular artery. In 10 angiograms this muscle was a type IV.

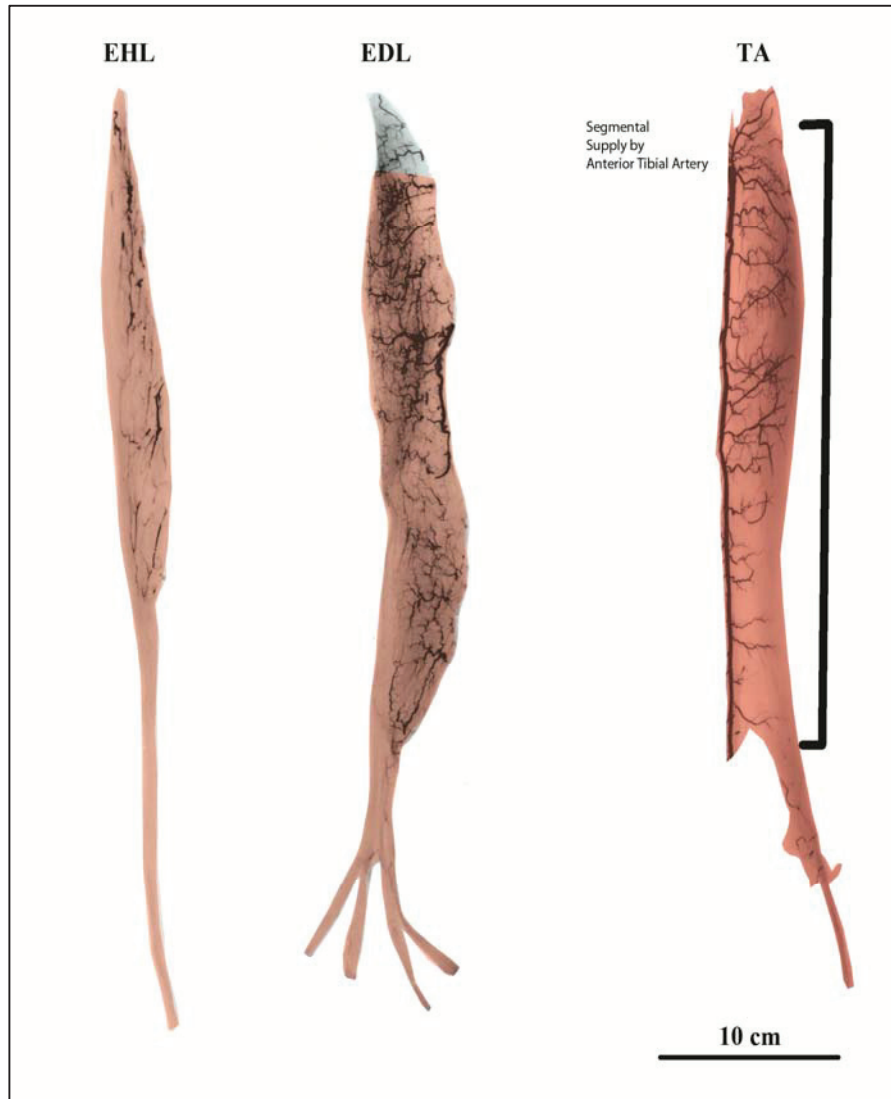


Figure 35: Angiogram of Muscles of Anterior Compartment of the Leg

All angiograms above are supplied by the anterior tibial artery angiosome, and the supply is segmental in nature.

Superficial Posterior Compartment:

Gastrocnemius:

The two heads of Gastrocnemius receive their blood supply independently. The medial sural artery supplies the medial head. The lateral head receives blood supply from the lateral sural artery. The lateral head distally receives minor blood supply from the peroneal artery and the medial head receives minor blood supply from the posterior tibial artery. This muscle is a type II. Previously classified as a type I; in 22 out of 30 angiograms this muscle was a type II.

Soleus:

This muscle receives a dominant pedicle from the popliteal artery, and multiple dominant pedicles proximally from the posterior tibial artery and peroneal artery. Distally the muscle receives multiple minor pedicles from both the posterior tibial and peroneal arteries. This is a type III muscle. In 70 % of the time there is a second dominant pedicle from the peroneal artery making the muscle a type III due to its different arterial source, when all dominant pedicles stem from the posterior tibial artery this muscle is classified as type II this happens only 30% of the time.

Plantaris:

This muscle receives its blood supply from the superficial surface by the lateral sural artery. Proximally it receives minor branches from the popliteal artery. In 66% of angiograms this was a type II muscle.

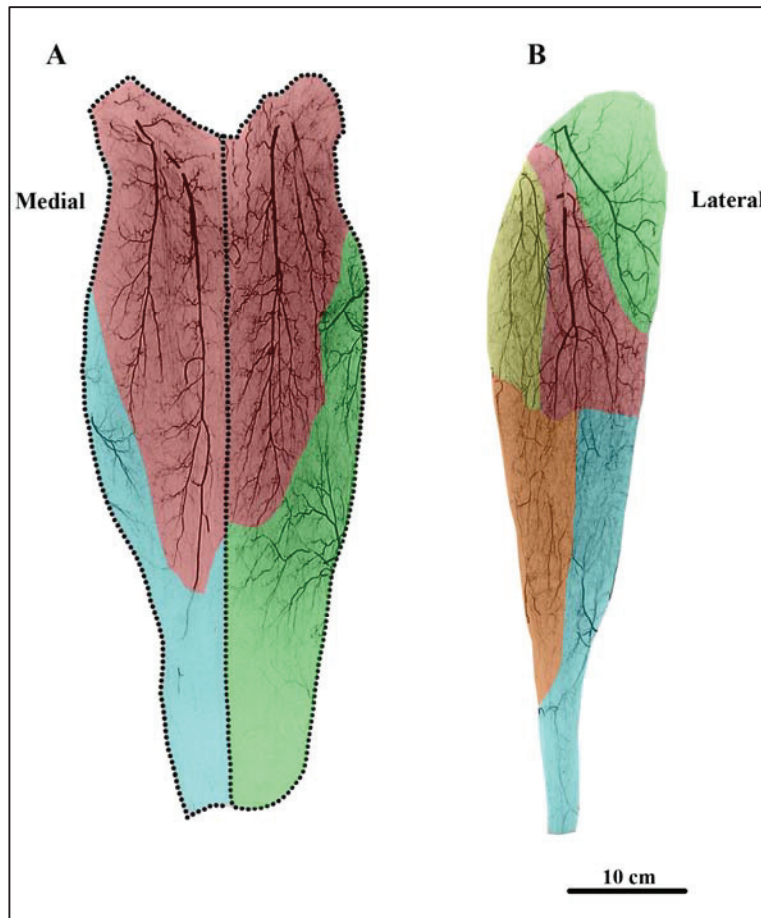


Figure 36: Gastrocnemius and Soleus

A. Gastrocnemius medial and lateral muscles. The medial head is on the left side; the medial head is larger and receives dominant blood supply from the sural arteries (red), and distally from the peroneal artery branches (blue). The lateral sural arteries supply the lateral head, and the posterior tibial arteries supply the lateral head distally with minor branches (green). **B.** The soleus muscles receives a dominant pedicle from the popliteal artery (green) and another dominant pedicels from the peroneal artery (red) and the posterior tibial artery (yellow). Distally the lateral part of the muscle receives minor segmental blood supply from the branches of the peroneal artery (blue), and medially it receives segmental blood supply from the posterior tibial artery (orange).

Deep Posterior compartment:**Popliteus:**

Dominant branches from the medial and lateral inferior genicular arteries supply this muscle, and minor branches from the popliteal artery. In 5 angiograms this muscle was a type III.

Tibialis Posterior:

In 15 angiograms this muscle is always a type IV; it receives its segmental branches from the peroneal artery for most part and distally receives segmental branches from the posterior tibial artery.

Flexor Hallucis Longus:

The peroneal artery provides FHL with its dominant blood supply in an equal and segmental fashion. The posterior tibial artery supplies the distal end of the muscle medially with minor segmental vessels. In 30 angiograms this muscle is a type IV.

Flexor Digitorum Longus:

The posterior tibial artery is the dominant blood supply to this muscle. This muscle receives multiple and equal segmental blood supply. In 32 angiograms this was a type IV muscle.



Figure 37: Muscles of the Deep Compartment of the Posterior Leg

A. Popliteus muscle receives two dominant pedicles; the lateral and medial genicular arteries supply this muscle. **B. Flexor hallucis longus** receives its blood supply in segmental fashion from both the peroneal artery and the posterior tibial artery. **C. Tibialis posterior** is supplied proximally by the peroneal artery (red) and by the posterior tibial artery distally (blue). **D. Flexor digitorum longus** receives its blood supply in a segmental fashion from posterior tibial artery.

Lateral Compartment Muscles:

Peroneus Longus:

The dominant blood supply is the peroneal artery it gives 2-3 branches one of which is usually the largest in caliber. It also receives 2-3 minor branches from the anterior tibial artery. In total of 21 angiograms 18 (80%) had a type II, while 3 (20%) had a type IV vascular architecture.

Peroneus Brevis:

Peroneus brevis receive its major blood supply by 2 dominant pedicles supplied by the peroneal artery, and minor blood supply by 2-3 branches of the anterior tibial artery. In 17 angiograms, 13 (76%) were type II, and 4 (24%) had a type IV architecture.

Table 10: Summary of Angiograms of the Leg

Leg	Type I	Type II	Type III	Type IV	Type V	Total	Current Dominant Type	Muscles Conforming to current classification %	Observed Type
Tibialis Anterior	0	0	0	40	0	40	IV	100%	IV
Extensor Digitorum Longus	0	0	0	39	0	39	IV	100%	IV
Extensor Hallucis Longus	0	0	0	38	0	38	IV	100%	IV
Peroneus tertius	0	0	0	10	0	10	IV	100%	IV
Gastrocnemius	8	22	0	0	0	30	I	27%	II
Plantaris	2	4	0	0	0	6	Not Classified	Not Classified	II
Soleus	0	4	9	0	0	13	II	30%	III
Flexor Digitorum Longus	0	0	0	32	0	32	IV	100%	IV
Flexor Hallucis Longus	0	0	0	30	0	30	IV	100%	IV
Popliteus	0	0	5	0	0	5	Not Classified	Not Classified	III
Tibialis Posterior	0	0	0	15	0	15	IV	100%	III
Peroneal Brevis	0	13	0	4	0	17	II	76%	II
Peroneal Longus	0	18	0	3	0	21	II	80%	II
Total						296			

2.2.4.4 Muscles of the Foot

Dorsum of the Foot

Extensor Digitorum Brevis:

The lateral tarsal artery of the dorsalis pedis supplies this muscle. In some cases it receives dual blood supply from a minor pedicle arising from a second lateral tarsal arteries branching of the dorsalis pedis.¹³³⁻¹³⁵ It is currently a type I muscle and we reviewed 6 muscles with 5 muscles exhibiting type I pattern and only one muscle with a dual blood supply.

Plantar Surface of the Foot

First Layer

Flexor Digitorum Brevis:

The flexor Digitorum brevis typically described as a type II receives its blood supply from both the medial plantar artery (MPA) and the Lateral plantar artery.¹³⁶⁻¹³⁸ The review of 11 muscles did not show any other patterns than previously described. The dominant pedicle is supplied by the LPA and the minor pedicle by the MPA at the muscle's origin.

Abductor Digit Minimi:

This muscle receives its blood supply from the lateral plantar artery (LPA).¹³⁹⁻¹⁴¹ It is currently classified as a type II as it receives one dominant branch proximally and 2 minor muscular branches distally all of which originating from the LPA. This review showed that 5 out of 9 muscles received one dominant source of blood supply and multiple segmental branches from the LPA, while the other four muscles had a type IV configuration in which they all received equal segmental contributions from the LPA and the dorsal fifth metatarsal artery.

Abductor Hallucis:

Abductor hallucis receives its blood supply chiefly from the medial plantar artery (MPA).¹⁴²⁻¹⁴⁸ The pattern of this supply is currently classified as one dominant and 2 to 3 minor branches from the MPA. In review of 9 muscles they all displayed segmental blood supply from the MPA at all levels with equal distribution. Hence this muscle classified as a type IV.

Second Layer:

Quadratus Plantæ (Flexor Accessorius):

This muscle has two heads arising from both sides of the calcaneus, both heads unit to insert on the common tendon of flexor digitorum Longus. Nine muscles were reviewed; the blood supply to this muscle is from the lateral plantar artery.^{149, 150} The LPA courses parallel and lateral to the muscle's belly and provides the muscle with blood

supply in a segmental fashion. This muscle also receives insignificant minor branches from the Medial plantar artery. The dominant classification is type IV.

The Lumbricals:

There are four lumbricals in the foot; they all arise from the tendons of flexor digitorum longus.¹⁴⁹ In 5 angiograms it was noted that the blood supply to these muscles was mostly via intermuscular supply from the quadratus plantae muscle. The pattern of blood supply to the lumbricals was grouped with type IV because of the observed intermuscular segmental pattern.

Third Layer

Flexor Hallucis Brevis:

This muscle has a lateral and a medial head. The blood supply to both heads is from the medial plantar artery.¹³⁷ The medial head receives one major branch from the superficial MPA, as well as a distal minor branch from the first dorsal metatarsal artery. The lateral head receives a branch from deep MPA, and a minor branch from first plantar metatarsal artery. This muscle is a type II.

Flexor Digitorum Minimi Brevis:

This muscle is mainly supplied by the lateral plantar artery.^{109, 139, 149} It also receives 3-4 minor branches from the plantar and dorsal metatarsal arteries. The overall pattern of its arterial supply is type II.

Adductor Hallucis:

This muscle has two heads, a slender transverse head with no bony origin and an oblique head originating from the long plantar ligament. The blood supply to this muscle is from the dominant branch of the deep plantar arch to the oblique head and segmentally from the plantar metatarsal arteries to the transverse head, and therefore is a type V muscle.

Fourth Layer

Dorsal Interosseus Muscles:

The dorsal Interosseus muscles have a bipennate structure and are four in number.^{149, 151} The blood supply is from dorsalis pedis via the arcuate artery proximally and the dorsal metatarsal artery distally. The pattern of blood supply to this muscle is type II.

Plantar Interosseus Muscles:

The plantar Interosseus muscles have a unipennate structure and are 3 in number they receive their blood supply from the lateral plantar artery, and are considered a type II.^{152, 153} Proximally the interosseus muscle receives a direct branch from the deep plantar arch, and distally close to its insertion it receives minor branches from the plantar metatarsal artery.

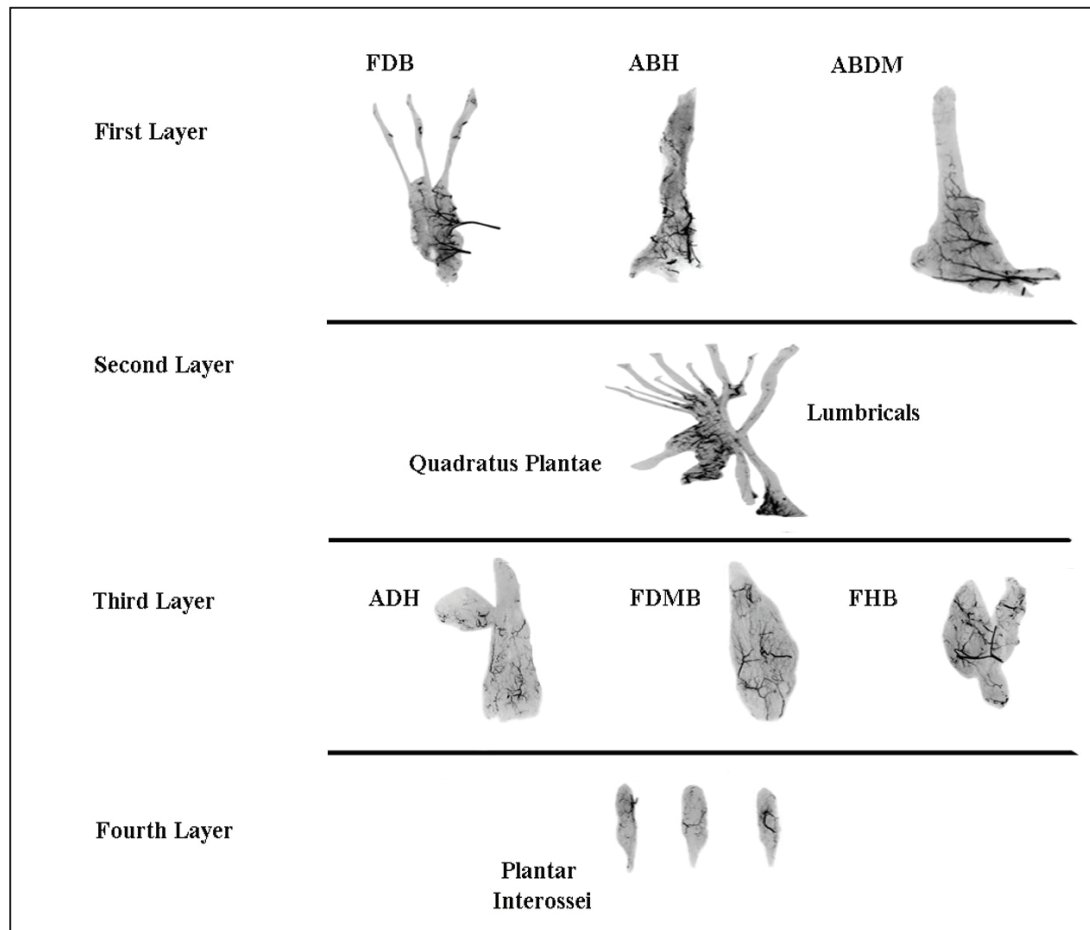


Figure 38: Intrinsic Muscles of the Foot

Angiograms of intrinsic muscles of the feet are organized by their anatomical layers.

Table 11: Summary of Angiograms of the Foot

Foot	Type I	Type II	Type III	Type IV	Type V	Total	Current Dominant Type	Muscles Conforming to current classification%	Observed Type	Observed Dominant Type %
Abductor hallucis	0	0	0	14	0	14	II	0%	IV	100%
Flexor digitorum brevis	0	10	0	0	0	10	II	100%	II	100%
Abductor digiti minimus	0	0	0	4	5	9	II	0%	IV & V	Type V in 55%
Quadratus plantae	0	0	0	11	0	11	Not Classified	Not classified	IV	100%
Lumbricals	0	0	0	20	0	20	Not Classified	Not classified	IV	100%
Adductor hallucis	0	0	0	0	6	6	Not Classified	Not classified	V	100%
Flexor digiti minimii brevis	0	7	0	0	0	7	Not Classified	Not classified	II	100%
Flexor hallucis Brevis	0	7	0	0	0	7	Not Classified	Not classified	II	100%
Dorsal interossei	0	32	0	0	0	32	Not Classified	Not classified	II	100%
Plantar interossei	0	24	0	0	0	24	Not Classified	Not classified	II	100%
Extensor digitorum brevis	5	1	0	0	0	6	I	83%	I	83%
Total						146				

2.2.5 Discussion

Skeletal muscles have a wide range of utility in reconstructive surgery, since they provide definitive tissue coverage, and robust vascular supply. The Blood supply to skeletal muscles is mainly via Axial, Intramuscular and intermuscular vessels. Mathes and Nahai's classification describes patterns related to extramuscular and intramuscular component of the vascular supply⁴⁴⁴. 4, 6, 34

The angiosome concept is an important concept in understanding the composite anatomic vascular territories of skin and underlying muscles. The pattern of blood supply to each muscle is also a crucial concept when considering a muscle for local or distant transfer.

In type I, muscles have a single vascular pedicle and are grouped together. This is helpful when grouping muscles together, but the true nature of vascular supply is usually redundant, and many muscles exhibit peripheral contribution from adjacent muscles and bones. Type I is the least common type among muscles, with the head and neck area having the highest percentage of this type (Table 12).

Type II muscles were the most prevalent type in the body. The vast majority of muscles could be classified as type II. The best way in our opinion is to classify these muscles according to their angiosome source, as it will limit classification of this type as type I or III when there is vascular disease or technical issues with the angiogram. The description of segmental blood supply in the Mathes and Nahai's classification is based on pattern of supply but not dominance of supply. The size of different segments are more important and usually the size correlates better with the angiosome source, for example; if the angiosome source is the dominant supplier to a muscle the vascular segments from that angiosome are usually the largest of all segments supplying any given muscle.

Type III muscles were most prevalent in the head and neck, torso and upper extremity. Type III muscles are an excellent example of a muscle that receives two major pedicles from different arterial sources.

In Mathes and Nahai's classification major pedicles from opposite sides are necessary to classify a muscle as type III. A better description would be based on the dominance of the angiosome supplying the muscle; therefore a type III muscle is a muscle with 2 major pedicles from 2 dominant angiosomes. Type IV muscles are most common in the lower extremity, and type V are mostly found in the torso.

In this review we introduce a modification to the Mathes and Nahai's muscle classification to incorporate the angiosome principle to its context^{1, 15, 154, 155} this modification will include muscles that might not fall into any of the five types, and distinguish muscles with segmental blood supply stemming from adjacent muscles or bones from muscles with segmental blood supply from a well defined vascular pedicle. Knowledge of the angiosome pattern of vascular supply to muscle will allow a better understanding of vascular supply to skeletal muscles and facilitate their harvest.

Table 12: Range of Vascular Variation per Body Region

Region	Number of Angiograms	Number of Muscles	Variation Range
Head and Neck	118	17	0-25%
Torso	404	18	10-34%
Upper Extremity	890	48	12-37%
Lower Extremity	927	40	17-45%

Table 13: Vascular Patterns per Body Region

	Type I	Type II	Type III	Type IV	Type V
Head & Neck	10%	54%	26%	0%	9%
Torso	0%	25%	22%	21%	32%
Upper Extremity	2%	44%	10%	30%	14%
Lower Extremity	5%	51%	2%	37%	5%

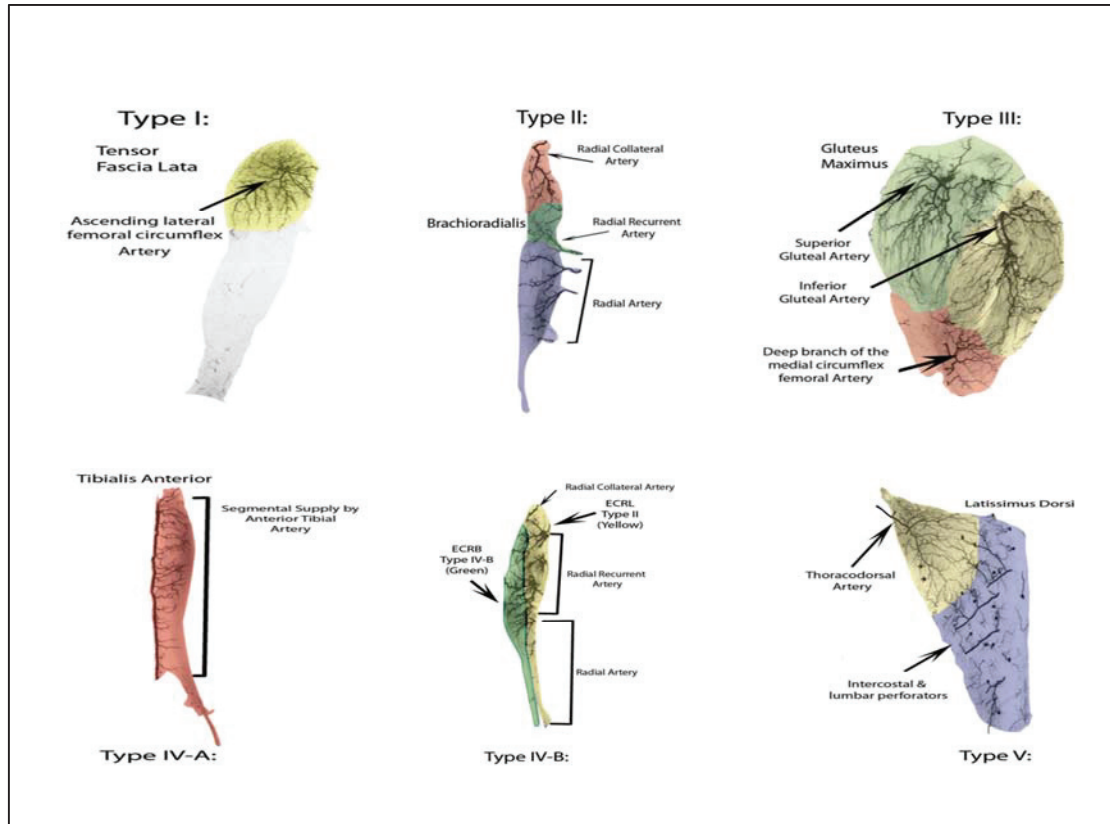


Figure 39: The Modified Mathes and Nahai's classification

The Modified Mathes and Nahai's classification is based on the Angiosome concept.^{1, 15, 155} All pedicles were described in addition to their angiosome source.

Type I: Single Angiosome provides the muscle with a single dominant pedicle.

Type II: Single Angiosome supplying the muscle with dominant pedicle(s).

Minor pedicle(s) if present are either from the same or additional Angiosomes.

Type III: Two or more Angiosomes supplying the muscle with dominant pedicles. Minor pedicles if present could belong to the same or additional Angiosomes.

Type IV: Segmental blood supply with the distinction made between muscles that receives their supply from adjacent vessels (**Type IV-A**) and muscles that are entirely dependent on their bony or muscular attachment to receive segmental blood supply (**Type IV-B**)

Type V: Two or more Angiosomes supplying the muscle with dominant pedicle(s) and segmental blood supply. Minor pedicles if present are either from the same or additional Angiosomes.

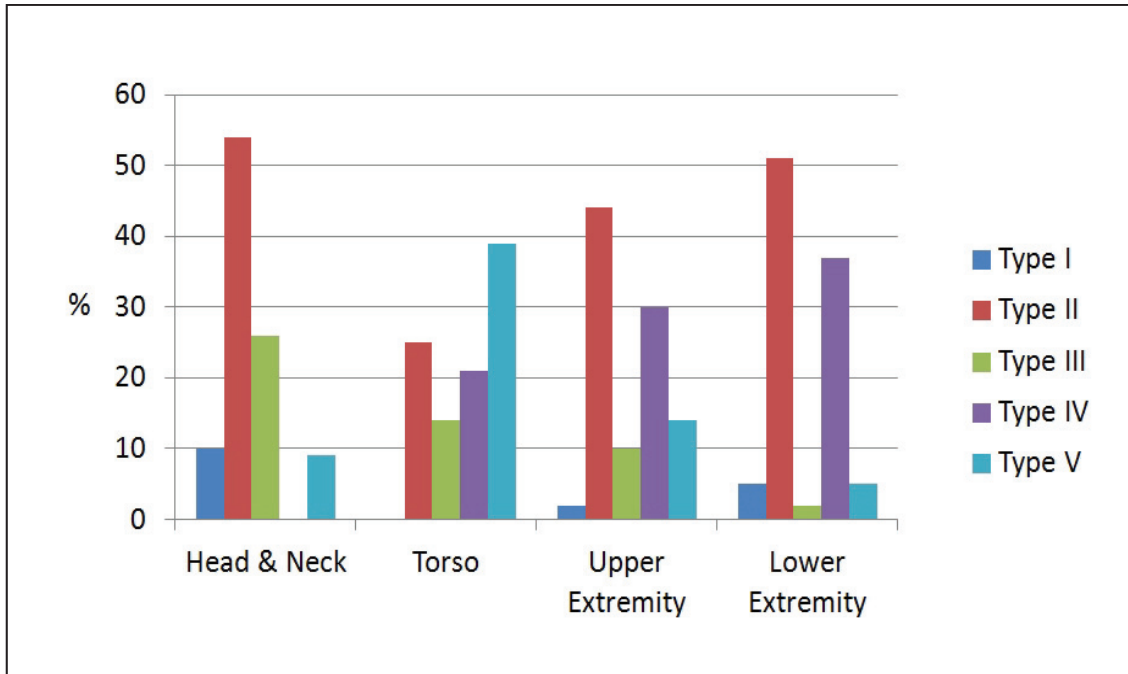


Figure 40: Vascular Pattern Distribution

The most prevalent type of arterial supply is II, except in the torso where type V is more prevalent. Type IV is second in prevalence after type II in the all extremities.

2.2.6 Conclusion of Phase I

Mathes and Naha's classification focuses on the pattern of blood supply to each muscle and the angiosome concept focuses on the origin of the branches that supply various tissues, Taylor et al describes this concept best as tracing the arterial supply from the major vessel to its minor branches similar to that of tracing the trunk of a tree to its leaves, hence the term "trunk to leaves".¹⁵⁴ Therefore, it is important to underline the distinction between muscles that have one or more angiosomes and muscles that have one or multiple branches supplying them.

We suggest a modified classification that combines both concepts to limit the differences in describing arterial supply to muscles, and to facilitate a better understanding of muscles that have higher probability to survive surgical manipulation and distant transfer.

Chapter 3.0 Three Dimensional Analysis of the Vascular Anatomy (Phase II)

3.1 Introduction

Three-dimensional modeling in the form of stereolithography models (STL) provides accurate and useful information about various structures of the body. Current three dimensional imagery techniques are promising for a brighter future for the fields of anatomy and surgery. The ability to reconstruct and visualize bone, muscle and intricate vascular structures in a layer-by-layer fashion provides a great planning tool for reconstructive surgeons and an accurate educational instrument for surgical residents.

3.1.1 History of Three Dimensional Imaging

In reconstructive surgery knowledge of the three dimensional anatomy is crucial for optimizing surgical outcomes. The advent of three-dimensional imaging techniques adds a valuable tool for better surgical planning.

Volume rendering is achieved by collecting a series of cross sections from a computed tomography (CT) or magnetic resonance (MR) scanners and creating three dimensional volume using software that employs complex algorithmic calculations in the process of developing these images, this concept was first introduced in 1988 by Drebin et al.¹⁵⁶

The utility of the volume rendering technique became apparent with the introduction of commercially available software. There are several methods of performing volume rendering on CT stacked images. The most accurate method is considered to be the volume ray casting it is an image based volume rendering technique, in which the emanates is computed directly from the output image, and not the input volume data as in the case of object based technologies. This fundamental fact allows for

accurate measurements to be obtained from the generated images with precision and accuracy that is reproducible and reliable.¹⁵⁷

The use of volume rendering technique was popularized in many areas of biomedical sciences. Surgical specialties such as neurosurgery, vascular surgery and general surgery were fast to explore and apply this new technology to their clinical and research practice. The field of plastic and reconstructive surgery remains in the early stages in applying this technology in preoperative planning and research areas.

This review outlines the importance of three-dimensional imaging in surgical planning, and also reviews injection techniques with potential utility in three-dimensional imaging.

3.1.2 Importance of Three Dimensional Imaging in Surgical Planning

Knowledge of the three dimensional nature of vascular anatomy is crucial, and in many instances failure or success of surgical flaps depends on the surgeon's knowledge of the vascular anatomy as well as how thin his flap should be. Traditional two-dimensional angiograms do not have the same advantage as three-dimensional techniques where the flap is designed with knowledge of the anastomoses between arterial systems in a layer-by-layer fashion.¹⁵⁸⁻¹⁶⁰

To exemplify the usefulness of this technology we reviewed the work of several authors who employed this technology to answer questions relevant to their daily practice. For instance, the use of 3 dimensional imaging in planning ALT flaps was recently described by Schaverien et al. to explain the difference in outcome of thinned ALT flaps between Caucasian and Asian populations.³⁰

Tregaskiss et al studied the anatomy of the anterior abdominal wall and described the unique vascular anatomy of the deep inferior epigastric artery (DIEA) to explain the ischemia-related morbidity observed with DIEA-based perforator flaps. They also concluded that preservation of superficial epigastric perforators adjacent to the costal margin during abdominoplasty will likely improve abdominal wall perfusion and reduce donor-site morbidity.¹⁶¹ Garbher et al. outlined the need for future studies to look at the optimal injection mixture for 3D computed tomography.³³

Three dimensional STL models allows visualization of anatomical structures, and depending on the quality of computed tomography data and the relative thickness of each computed tomography slice the structures visualized in the STL model will have accurate morphometric details of many different anatomical structures.¹⁶²⁻¹⁶⁵ The ability to render each structure or part of it transparent, and hide and show these structures on demand allows unprecedented access to these anatomical structures; this feature is of great value in preoperative planning. However, there are many difficulties and technical challenges that we will need to overcome to achieve the best anatomical models that can provide accurate and detailed morphometric data. In our angiographic studies, the most challenging single factor was to find a suitable contrast media that generates the least amount of artifacts, and captures the detailed vasculature in all structures; especially bone.

3.2 Review of Current Popular Contrast Mixtures

3.2.1 Lead Oxide Gelatin Mixtures

The lead oxide gelatin mixture is currently the gold standard for angiographic studies. It has been extensively described and is well known to produce optimal 2 dimensional angiograms of organs, muscles and skin.^{20, 22, 166}

This technique was used by several authors including our laboratory.^{20, 22, 166} ^{20, 22, 166} ^{20, 22, 166} ^{20, 22, 166} The success or failure of this technique depends on lead oxide's concentration, viscosity of mixture and CT scanner settings.

3.2.2 Iodine Based Mixtures

In clinical settings, iodine is the solution of choice. Many studies have utilized iodine in generating 2 dimensional images in living subjects.¹⁶⁷⁻¹⁷⁰ No studies have described mixing iodine with gelatin to view the vasculature in cadavers.

3.2.3 Barium Based Mixtures

Barium sulfate is the solution of choice for most studies in North America due to its safety and cost effectiveness, was first described by Hinman et al in 1923.¹⁷¹ Mathes and Nahai and many other researchers have used barium sulfate.^{6, 20, 91, 92, 105, 126, 172-175}

Barium sulfate was not used to generate any images in 3D studies of the vasculature.

3.2.4 Gadolinium Based Mixtures

Typically gadolinium mixtures are used in clinical practice for large vessel imaging and mostly for enhancement when utilizing MRI machines. No experiments have been reported that mixed gadolinium with gelatin or attempted its use in cadaveric

angiographic research.¹⁷⁶⁻¹⁷⁸ Its main advantage in clinical work is its lower toxicity in patients with renal dysfunction.

3.2.5 Discussion

Three-dimensional imaging delivers better visualization of the microvasculature. However, the ability of 3D techniques to produce high quality images and models is dependent on several factors, factors including scanner resolution, software calculation methods and the graphics processing abilities. Images are not static anymore, with the advent of three-dimensional modeling data can be viewed from many angles and more useful information can be obtained with valuable teaching models to be created.

The injection technique is crucial to the process producing high quality models. The production of optimal images depends on using elements that have precise concentrations; elements such as lead oxide, barium, or iodine are typically used in these mixtures. These elements if used in higher concentrations will generate unwanted artifacts that will contribute to lower quality images; also lower concentrations will diminish the ability of the scanner to detect smaller size vessels. The use of a higher resolution CT scanner or more sophisticated software will not compensate for any of these deficiencies.

In our review we found that most injection mixtures utilized in the production of three-dimensional images are based on mixtures that were previously used in 2 dimensional x-ray generated angiograms. This is problematic for two reasons; the first is that angiograms are obtained using single planner X-ray machines that are known to hide the detailed three-dimensional nature of the vasculature by producing 2 dimensional images. The second reason is that these mixtures were optimized for single planner

imaging in which artifacts are not a major issue due to their lower sensitivity and single planner technology; hence the use of a highly sensitive rotating multiplanar three dimensional CT will definitely produce major artifacts if the mixture was not optimized and properly selected for this technique.

3.2.6 Conclusion

The literature does not provide enough information about which contrast mixture is considered optimal for computed tomography when three dimensional angiography techniques. There is a need to assess the best injection technique suitable for CT scanning of cadavers that will generate the optimal images of vascular architecture smaller than 5 mm in diameter.

3.3 Part (A) Animal Injection Study

Abstract A: A Novel Three Dimensional Technique for Imaging Vessels in Animals

Three-dimensional reconstruction from CT scanned images is a valuable technology that allows visualization of vascular anatomy and the collection of detailed measurements with minimal dissection. In this study, we compare 4 injection techniques utilizing 4 animals to establish the optimal method for CT scanning of human cadaveric specimens.

Four New Zealand white rabbits were euthanized in accordance with the University ethical guidelines. Each animal was injected with one of four angiographic mixtures (Group A: modified lead oxide with gelatin; Group B: modified iodine with gelatin; Group C: barium sulphate with gelatin; and Group D: gadolinium with gelatin). CT scans were obtained, and the images were processed using MIMICS software. Angiographic images of endosteal, subcutaneous and intermuscular arteries were scored by radiodensity values in Hounsfield units (hu), measurements of the 3D volumes, and values of the smallest vessel diameter detected by each technique was documented.

The arterial radiodensity mean values were: Group A, endosteal 2475; subcutaneous 1475; and intramuscular 1250 (hu); Group B for the endosteal 1776, subcutaneous 976, and intramuscular 853 (hu); Group C, only visceral circulation 576(hu); Group D: no radiodensities detected. The smallest vessel diameter detected was: Group A, 0.2 mm; Group B, 0.5 mm, Group C, 0.5 mm; Group D, no vessels detected. The mean 3D volumes were: Group A, 18.67 cm³; Group B, 22.3 cm³; Group C, 6.7 cm³; Group D, 0 cm³.

In conclusion, under filling is a major issue with barium and iodine injections. Contrast spilling and leaks are equal in both lead and barium mixtures, and gadolinium injection was determined to be unsuitable for this CT scanning experiment. A reduced mixture of lead oxide generated the best vascular filling for 3D imaging.

3.3.1 Objectives

The objectives of the animal study was to define the best injection protocol for 3D evaluation of the vascular anatomy, and to reduce artifacts and noise by defining the appropriate CT Scanner Settings, and to determine the smallest vessel caliber traceable with this technique.

3.3.2 Materials and Methods

Four New Zealand white rabbits were euthanized in accordance with the University ethical guidelines. Each animal was injected with one of four angiographic mixtures (Group A: modified lead oxide with gelatin; Group B: modified iodine with gelatin; Group C: barium sulphate with gelatin; and Group D: gadolinium with gelatin). CT scans were obtained, and the images were processed using MIMICS software. Angiographic images of endosteal, subcutaneous and intermuscular arteries were scored by radiodensity values in Hounsfield units (hu), measurements of the 3D volumes, and values of the smallest vessel diameter detected by each technique was documented.

3.3.2.1 Animal Injection Protocol

Step One: Euthanasia with 1.5 ml of phenobarbital injection to rabbit ear vein.

Step Two: Exposure of carotid art and internal jugular vein.

Step Three: Insertion of catheters in both vein and artery for injection

Step Four: Preparation for injection 200 ml/kg of 9 % potassium chloride (KCL) (9 g in 100 ml) warmed to 50 °C.

Step five: Float rabbit in a plastic container in warm water and inject the contrast solution mixture.

3.3.2.2 Group A: Modified Lead Oxide with Gelatin

Step One: Flush specimen with 200ml/kg of specimen 50 °C warmed of 0.9% KCl solution.

Step Two: Mix 52g of 300-bloom gel in 100 ml of water.

Step Three: Add 60g Pb₂O₃/100 ml water to gel solution.

Step Four: Formalin (10%) 40-50 ml/kg of specimen an hour afterwards.

Step Five: store animal at 4 °C for 24 hours.

3.3.2.3 Group B: Modified Iodine with Gelatin

Step One: Flush specimen with 200mL/kg of specimen 50 °C warmed of 0.9% KCl solution.

Step Two: Mix 5g of 300-bloom gel in 100ml of water.

Step Three: Add 30 ml (10g iopamidol) of Isovue 370 to gel solution.

Step Four: Formalin (10%) 40-50ml/kg of specimen an hour afterwards.

Step five: Store animal at 4 °C for 24 hours.

3.3.2.4 Group C: Barium Sulphate with Gelatin

Step One: Flush specimen with 200mL/kg of specimen 50 °C of 0.9% KCl solution.

Step Two: Mix 5g of 300-bloom gel in 100ml of water.

Step Three: Add 0.4 ml/Kg to the mixture solution. (Living subjects receive 0.2ml/kg)

Step Four: Formalin (10%) 40-50ml/kg of specimen an hour afterwards.

Step five: Store animal at 4 °C for 24 hours.

3.3.2.5 Group D: Gadolinium with Gelatin

Step One: Flush specimen with 200mL/kg of specimen 50 °C of 0.9% KCl solution.

Step Two: Mix 2g of 300-bloom gel in 100 mL of water.

Step Three: 400 g / 100 ml of mixture solution

Step Four: Formalin (10%) 40-50ml/kg of specimen an hour afterwards.

Step Five: Store animal at 4 °C for 24 hours.

3.3.2.6 Computed Tomography Scanner Settings

A multi row detector CT scanner (Siemens sensation 64) was used to scan the animals. There were many variables in computed tomography setting that can help produce better quality images. The voltage applied through an x-ray tube when it reaches its maximal voltage is termed peak (kilovoltage kVp), the difference between black, white and shades of gray is determined by this parameter. The penetration of different tissues in the body requires different kVp. The milliamperere mAs plays an important role in x-ray

penetration in the presence of different densities. Although less critical the increase in mAs when slice thickness was at 0.5 mm. produced slightly better images (less artifacts from contrast agent). Only when the slice thickness exceeded 2 mm that the value of mAs made a difference in the image quality.

Slice increment was as important as slice thickness. Smaller slice increment at 0.5 mm produced optimal images (range 0.5-2 mm). Slice with more pixels produced less artifact than slice with fewer pixels; pixel range (378-512pxl). These settings were established based on review of multiple textbook and papers in the radiology literature as well as multiple attempts when scanning of each animal.¹⁷⁹⁻¹⁸¹

A voxel is 3D unit composed of pixel generated from axial, coronal and sagittal formats (Figure 41). The voxel is viewed in 3D by applying a volume ray casting techniques as previously mentioned in chapter three.

The optimal CT scan settings are listed in Table 14.

Table 14: Optimal CT Scanner Setting for All Groups

KVp	Pixel width	Pixel height	Pixel size	Slice increment	Slice thickness	mAs
120-140	512 pxl	512 pxl	0.4 mm	0.5 mm	0.5 mm	74

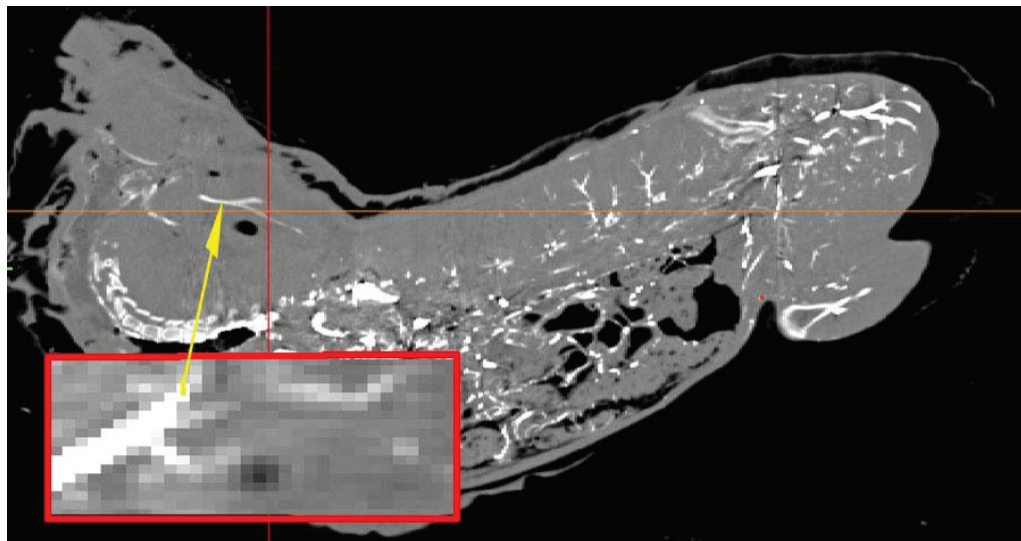


Figure 41: CT sagittal view of a rabbit with a magnified pixel

3.3.2.7 Computer Aided Design and Data Analysis

In review of the three-dimensional imaging literature and analyzing data with several three-dimensional imaging software, it was determined that MIMICS by Materialise had the best supportive literature,^{158-160, 182} and the user interface is most user friendly.

MIMICS allows its user to import raw data in form of DCM series, and allows the user to verify the integrity of this data prior to creating projects. The software manufacturer also responded to our request to help with minimizing artifacts generated by lead oxide via adding a median type filter to help with artifact reduction.

The STL model generated for the vascular tree is then fitted with central lines to measure the diameter of the vessel. This is set at 1 mm interval along the course of the vessel. MIMICS is also capable of tracing the surface distance of the STL model to provide an accurate estimate of the pedicles length. In addition mimics generates volume and surface area measurements for each STL model created, this helps with estimating the volume of blood supply received from each vessel and its branches inside the muscles' STL model.

The steps needed to generate a Steriolithographic 3D model were as follow:

First step: Import raw data in the form of DCM images, and verify integrity and sequence of images.

Second step: Crop project to anatomical areas and save the mimics (mcs) file.

Third step: Identify anatomical structures to be studied and in the cropped project and apply a general segmentation to the voxels of interest.

Fourth step: The generated model of voxels can then be assessed to see if matches the anatomical areas on each corresponding CT layers (axial, coronal and sagittal).

Fifth step: MIMICS has many tools to specifically target difficult areas to segment.

Thresholding using multislice editors and livewire tool and so on where very helpful in producing the final models.

3.3.3 Results

The optimal settings were established and can be found in Table 14. The data was analyzed using MIMICS and 3D models were generated. The Hounsfield (hu) units for each structure and contrast material are outlined in Figure 46. Lead oxide hu scale ranged between 1450-3071 hu depending on density of voxels in each CT slice. Barium hu scale ranged between 1300-2600 hu depending on density of voxels in each CT slice (Figures 43, 47B).

Iodine had a density range between 1200 and 2080. Gadolinium density was indistinguishable from other soft tissue densities when complexed with gelatin (Figure 44). The reduced lead oxide gelatin mixture produced the best models. Iodine had a lower filling value than lead oxide and barium. In comparison to barium sulfate, Lead oxide gelatin complex produced a higher viscosity solution and had minimal leakage around water shed areas (Figures 42, 47C,D).

The lead oxide injected rabbit was dissected to compare the length and diameter of the aorta to the length and diameter recorded from the STL model. The STL model produced a 30.8 cm long vessel with an arterial diameter of 3.4 mm. Dissection of the aorta revealed a 30.6 cm with a diameter measuring 3.2 mm.

Table 15: Vascular Radiodensities in Select Tissues

Mean arterial radiodensity within tissues (hu)	Endosteal	Subcutaneous	Intramuscular/Visceral	Smallest diameter measured (mm)
Lead Oxide	2475	1475	1250	0.2 mm
Barium Sulfate	1776	976	853	0.5 mm
Iodine	0	0	576	0.5 mm
Gadolinium	0	0	0	0

Modified lead oxide Gelatin Mixture

Dimensions (mm)	Minimum (mm)	Maximum (mm)	Delta (mm)
X	47.70	218.24	170.55
Y	15.87	132.78	116.90
Z	-1194	-809.39	384.61

Volumetric and Surface Areas	
Volume	316.17 cm ³
Surface	738.3 cm ²
# Triangles	243884
# Points	125604



Figure 42: Morphometric Data of Lead oxide injection group

Modified Barium Gelatin Mixture

Dimensions (mm)	Minimum (mm)	Maximum (mm)	Delta (mm)
X	47.70	218.24	170.55
Y	15.87	132.78	116.90
Z	-1194	-809.39	384.61

Volumetric and Surface Areas	
Volume	305.67 cm ³
Surface	728.4 cm ²
# Triangles	243884
# Points	125604

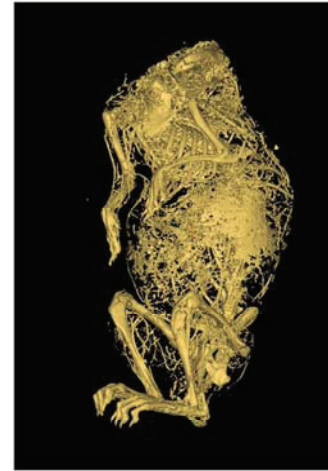


Figure 43: Morphometric Data of Barium Gelatin injection group

Modified Iodine Gelatin Mixture

Dimensions (mm)	Minimum (mm)	Maximum (mm)	Delta (mm)
X	47.70	218.24	170.55
Y	15.87	132.78	116.90
Z	-1194	-809.39	384.61

Volumetric and Surface Areas	
Volume	302.68 cm ³
Surface	719.7 cm ²
# Triangles	243884
# Points	125604

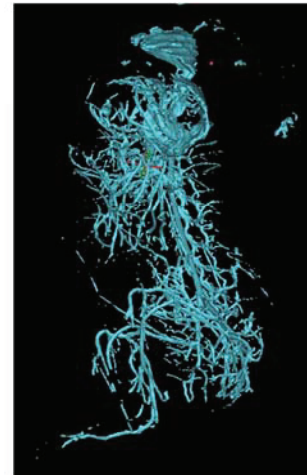


Figure 44: Morphometric Data of Iodine Gelatin injection group

Modified Gadolinium Gelatin Mixture

Dimensions (mm)	Minimum (mm)	Maximum (mm)	Delta (mm)
X	47.70	218.24	170.55
Y	15.87	132.78	116.90
Z	-1194	-809.39	384.61

Volumetric and Surface Areas	
Volume	279.67 cm ³
Surface	714.2 cm ²
# Triangles	243884
# Points	125604



Figure 45: Morphometric Data of Gadolinium Gelatin injection group

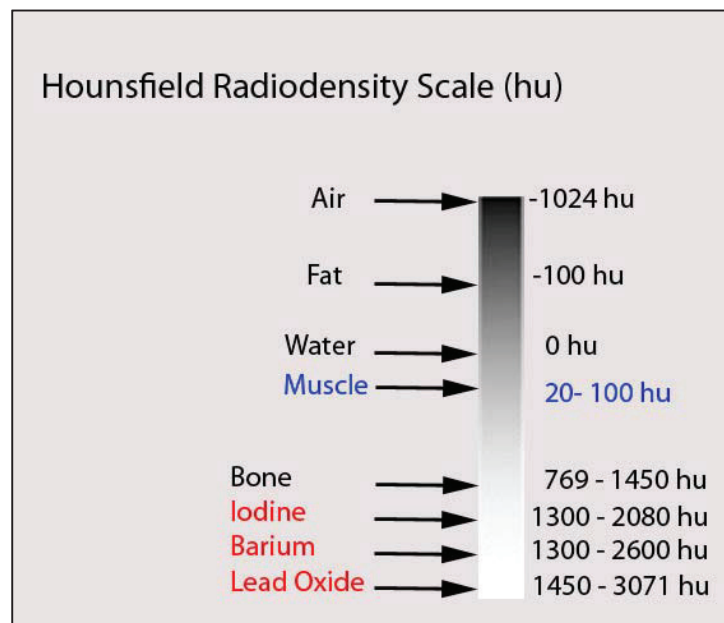


Figure 46: Hounsfield Radiodensity Scale

The mean range of Hounsfield unit for all mixtures were identified and presented in this figure.

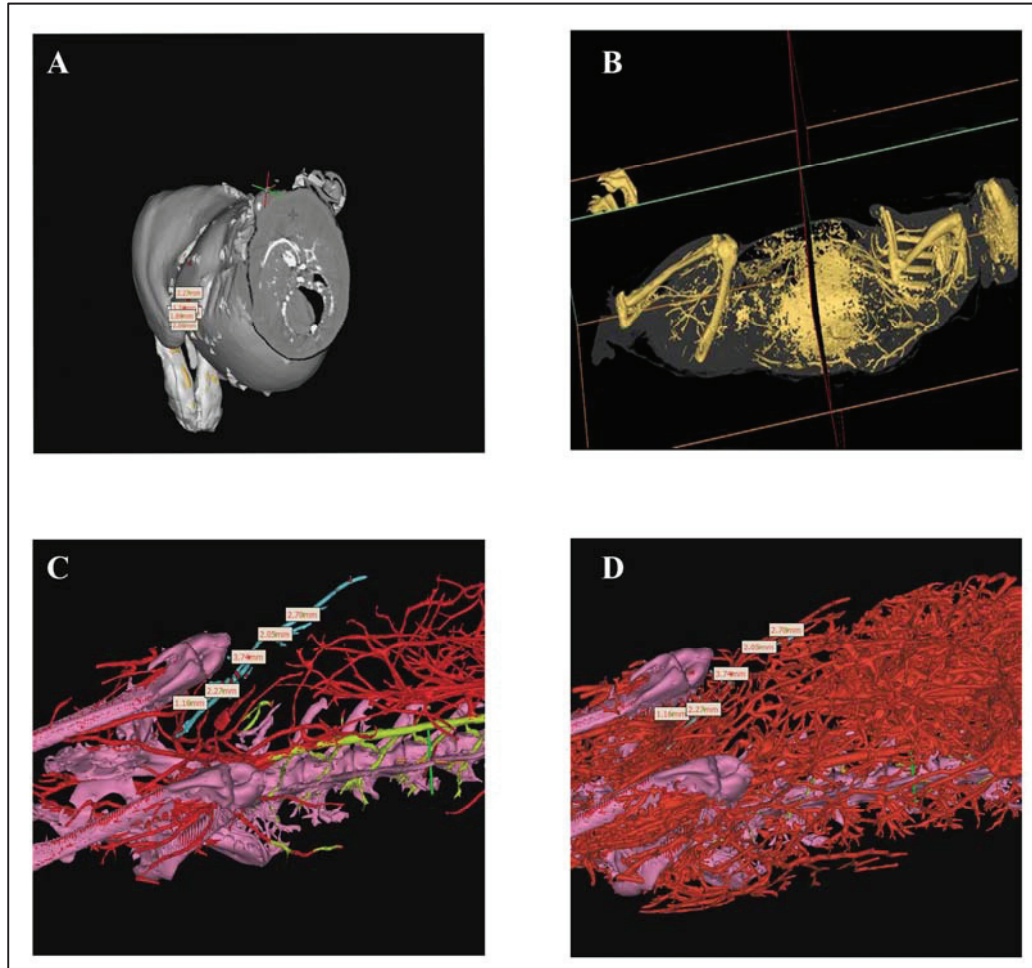


Figure 47: Rabbit Injection study

A) STL model of a lead oxide injected rabbit with dicom image demonstrating the absence of artifacts in an axial slice. **B)** STL model of a Barium sulfate injected rabbit with evidence of injection spillage in the flank area around the choke zones between the intercostal arteries and the deep and superficial circumflex iliac arteries of the abdomen and flank. **C)** Image of the Aorta of the lead oxide injected rabbit with the superficial system hidden in the model to demonstrate the ability to measure the length and diameter of the aorta. **D)** The lead oxide injected rabbit with the superficial arterial system in view; note the complexity and detailed arterial anatomy.

3.3.4 Discussion

In 2002, Tang et al described a modified lead oxide with gelatin technique for plain x-ray angiograms, which was different than what Rees, and Taylor described in 1986.^{21, 22} Tang et al. described a 100 g per 100 ml of 5 % gelatin. In this pilot study, the objective was to assess whether this change would help obtain better images on CT scanners. Dr. Tang recommended a reduced mixture of 60 g per 100 ml of 5 % gelatin; this slight modification proved crucial in the rabbit study to obtain optimized CT images, this in addition to factors related to CT scanner settings see Table 14. Also worth noting, that the quality of the final images were related to factors such as concentration and viscosity of the injected solution, too viscous or too dilute created lower quality images, a pulsatile injection at 120 mmHg produced better filling of the vascular tree. The injection was easier when the temperature of the injectate was set at $\geq 40^{\circ}\text{C}$.

3.3.5 Conclusion

In conclusion, under filling is a major issue with barium and iodine injection. Gadolinium injection was not suitable for CT when mixed with gelatin, contrast spilling and leaks are slightly higher in barium than the lead oxide mixture. A reduced mixture of lead oxide generated the best vascular filling and 3D images.

Chapter 4.0 Cadaver Injection Study, Phase II Part (B)

Abstract B: Three Dimensional Analysis of Human Skeletal Muscles

The transfer of muscles as a functional unit in an effort to restore function is a complex procedure that requires a donor muscle with reliable and suitable anatomy, and appropriate dynamic structure to meet the functional needs of the recipient site. The goal of functional muscle transfer is to restore active motion and satisfy a patient's particular functional need. The success of such procedures is dependent on the ability of the surgeon to select the most appropriate muscle. The muscle selected must be well vascularized. The main focus of this project was on potential donor muscles for functional muscle transfer.

We hypothesized that muscle is supplied by a consistent number of predictable vascular pedicle that originated from defined number of source arteries (angiosomes) and that muscle transfer in whole or segmental transfer is possible based on knowledge of the multitude of vascular pedicles with major contribution to each muscle, hence increasing the options available for harvesting muscle flaps.

Seven fresh human cadavers were injected utilizing a modified lead oxide injection technique, which was optimized in an animal injection study. Each vascular pedicle with diameter greater than 0.5 mm was recorded, and compared to 3D virtual Stereolithography models (STL) generated from Computed tomography images. A selected group of 20 skeletal muscles representing surgically accessible muscles in areas of the head and neck, trunk, upper and lower extremity underwent 3D STL modeling to provide information regarding average surface area and volume of muscle supplied by each pedicle. Information related to average pedicle length, diameter, and course was documented.

In conclusion, our hypothesis that skeletal muscles have consistent and predictable blood supply in 280 skeletal muscles held true. The information generated in 3D format, helped produce valuable qualitative and quantitative data to assist surgeons in finding options for donor muscles.

4.1 Materials and Methods

Seven fresh human cadavers were injected utilizing a modified lead oxide injection technique, which was optimized in an animal injection study. Three fresh cadavers were also radiographed and then dissected. Each vascular pedicle with diameter greater than 0.5 mm was recorded, and compared to 3D virtual stereolithography models (STL) generated from computed tomography images. A selected group of 20 skeletal muscles representing surgically accessible muscles in areas of the head and neck, trunk, upper and lower extremity underwent 3D STL modeling to provide information regarding average surface area and volume of muscle supplied by each pedicle. Information related to average pedicle length, diameter, and course was documented.

4.2 Results and Discussion

4.2.1 Head and Neck

Temporalis:

The temporalis muscle as surgical flap was first described by Yalovine in 1898.

¹⁸³ The Temporalis muscle is frequently harvested as a muscle or myofascial flap, and occasionally as a myo-osseous flap. The myo-osseous flap is useful in craniofacial reconstruction; the myo-osseous blood supply is poorly understood.

Temporalis muscle origin is from the temporal fossa, and inserts into the coronoid process of the mandible. The temporalis is innervated by the deep temporal branches of the anterior division of the mandibular branch of the trigeminal nerve.

The blood supply of the temporalis was demonstrated in first chapter of this thesis, upon studying the muscle in 3D we found an interosseous communicating branch with the middle meningeal vessel; this communicating branch was not previously outlined. Figure 48 is a video that shows this relationship in real time 3D, and Figure 49 shows a dissection image next to a 3D static image.

A communication with a mean diameter 0.6 ± 0.13 mm between the middle temporal artery (MTA) and middle meningeal artery (MM) was found in 13/14 muscles. Figure 51 depicts this arterial interosseous relationship.

The muscles mean volumes and arterial blood supply from the morphometric analysis is shown in Table 16. Figure 50 represents the percentage in volume supplied by each vascular pedicle.

The Temporalis & its Myosseous Territory in 3D

Figure 48: Temporalis 3D Angiogram

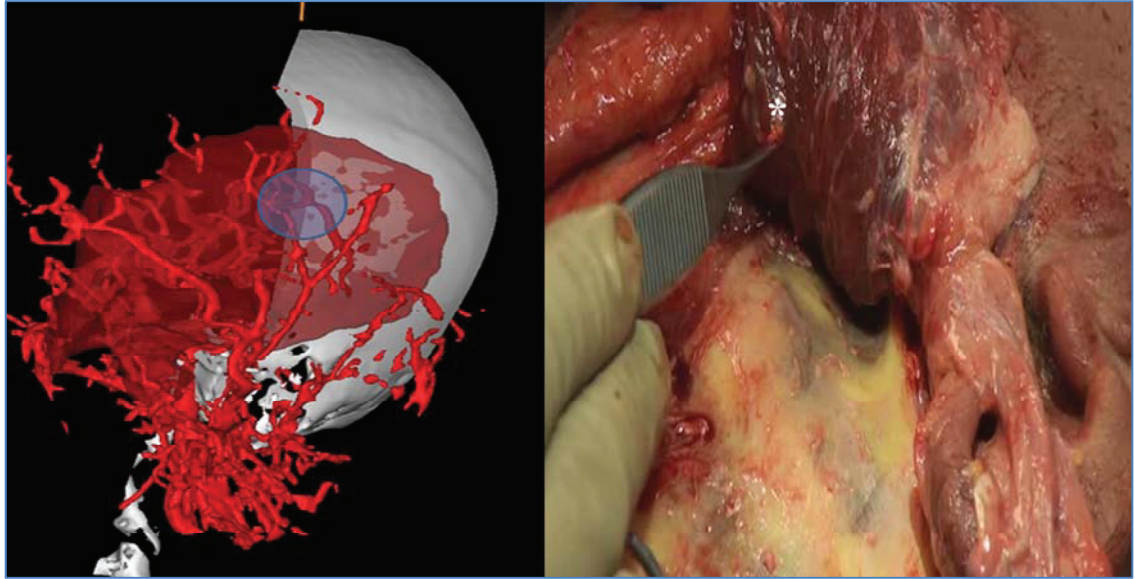


Figure 49: Temporalis 3D-Capture and Dissection

Blue circle to the left outlines the interosseous communication, the vascular pedicle found on dissection (*) to the right. Communication with a mean diameter 0.6 ± 0.13 mm between the middle temporal artery (MTA) and the middle meningeal artery (MM) was found in 13/14 muscles.

Table 16: Three Dimensional Analysis of Temporalis

	Anterior Deep Temporal Artery	Posterior Deep Temporal Artery	Middle Temporal Artery
Mean Muscle volume (cm ³)	16.3 ± 3.1	25.3 ± 2.4	13.6 ± 1.4
Mean Length of Pedicle (cm)	4.5 ± 1.2	4.3 ± 0.9	2.6 ± 0.7
Mean Diameter (mm)	1.2 ± 0.18	1.3 ± 0.21	0.7 ± 0.13

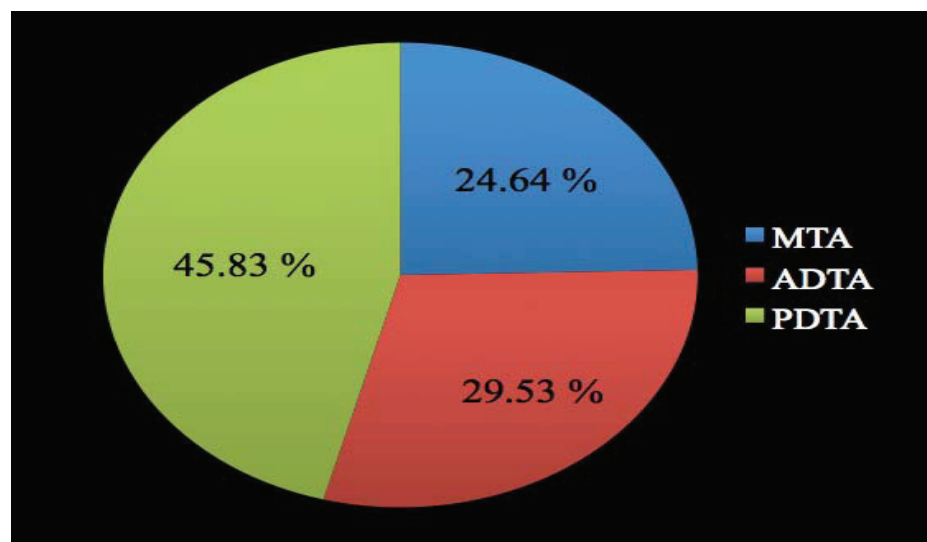


Figure 50: Mean Contribution of each Vessel to Temporalis Volume in Percentage

MTA = Middle temporal artery; ADTA = Anterior deep temporal artery; PDTA = Posterior deep temporal artery.

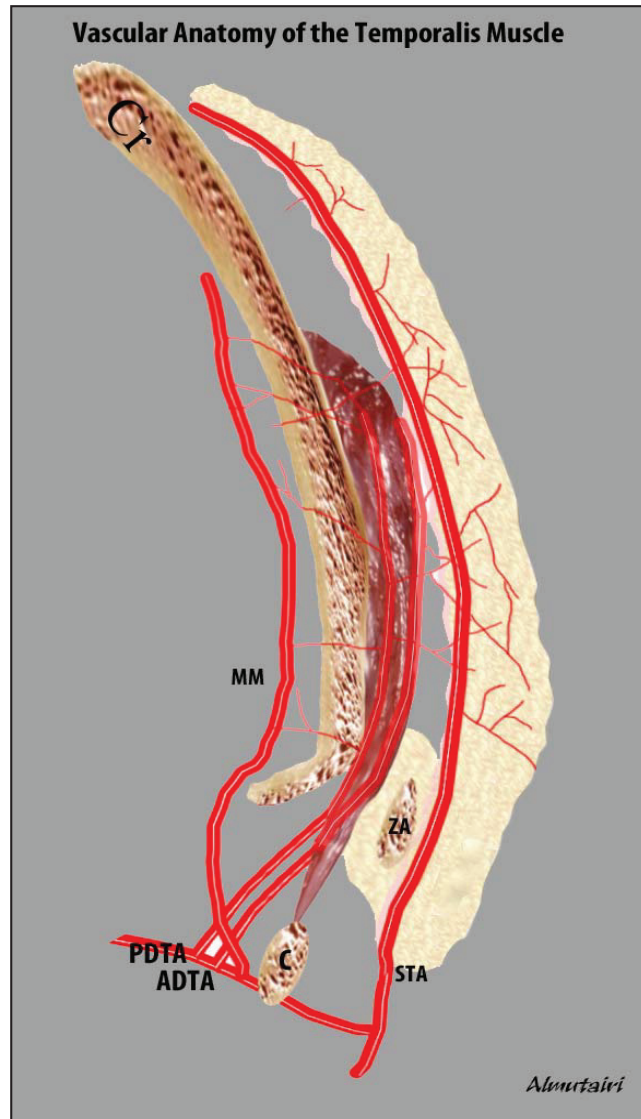


Figure 51: Schematic Illustration of the Vascularity of Temporalis

Middle meningeal (MM); Anterior deep temporal artery (ADTA); Posterior deep temporal artery (PDTA); Superficial temporal (STA). Coronoid Process (C); Cranium (Cr); Zygomatic Arch (A).

Masseter:

The masseter muscle can be transferred as a local flap in the head and neck particularly for facial reanimation, however the vascular anatomy is not well documented.^{39, 184} The masseter originates from the zygoma and maxilla, and inserts on the ramus and angle of the mandible. The masseteric nerve of the mandibular branch of the trigeminal nerve innervates the masseter. This innervation is important clinically as it could serve as a donor site for patients with facial paralysis. The masseter is supplied by the deep masseteric artery via the internal maxillary artery, as well segmental blood supply by the facial artery via the inferior and superior masseteric arteries.

The masseter arterial anatomy is illustrated in Figures 52 and 53. The mean volume of this muscle was $22.7 \text{ cm}^3 \pm 0.8$. The deep masseteric artery (DMA) is found deep to the temporalis insertion on the mandible (Figure 53B). This vessel supplies a mean of $43\% \pm 5$ of the masseter volume with a mean diameter $1.4 \text{ mm} \pm 0.3$. The other half of the masseter was supplied by the facial artery via its superior masseteric artery (SMA) a branch of the transverse facial artery, the mean volume of masseter supplied by this vessel was $32\% \pm 4$, the mean diameter of the SMA was $0.9 \text{ mm} \pm 0.4$. The inferior masseteric artery supplies a mean volume $24\% \pm 5$; the mean diameter of the inferior masseteric artery is $0.6 \text{ mm} \pm 0.2$. A summary of morphometric data can be found in Table 17.

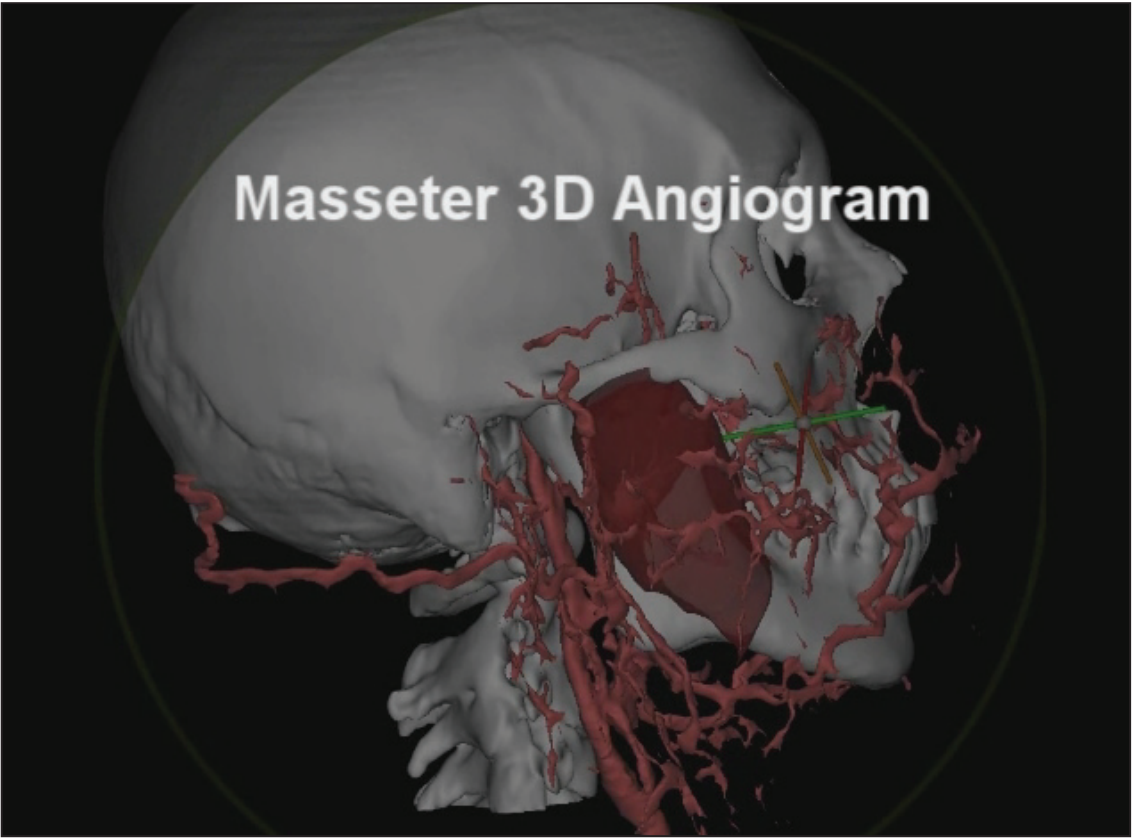


Figure 52: Masseter 3D Angiogram

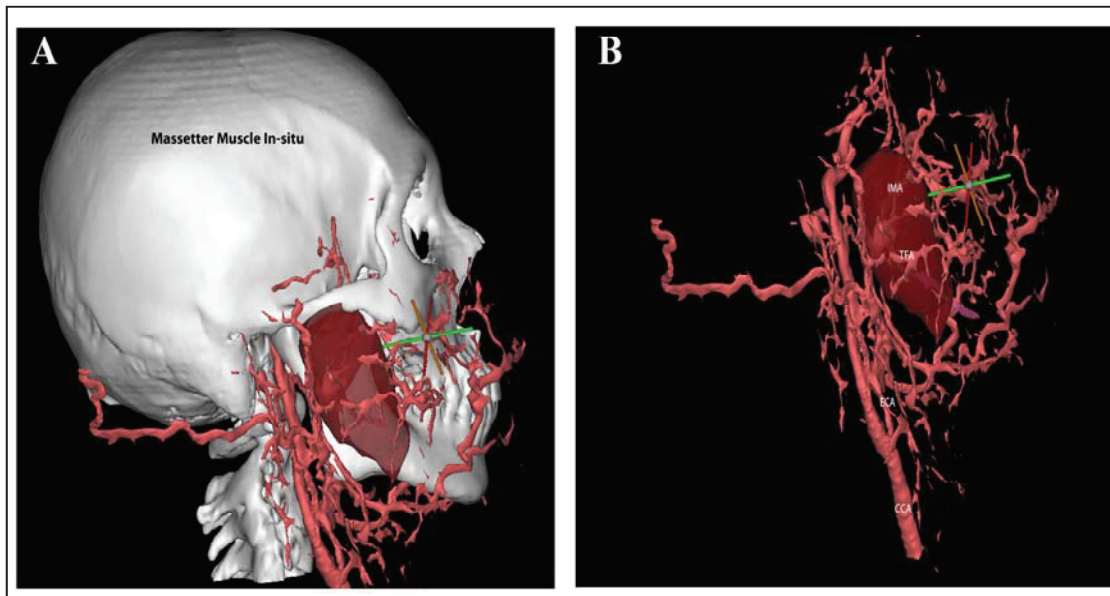


Figure 53: Masseter in 3D

The arterial anatomy of the masseter is shown with the deep and superficial blood supply to the muscle.

Table 17: Three Dimensional Analysis of Masseter

	Deep Masseteric Artery	Superior Masseteric Artery	Inferior Masseteric Artery
Mean Muscle volume (cm³)	9.7 ± 1.1	7.2 ± 0.9	5.4 ± 1.1
Mean Length of Pedicle (cm)	2.7 ± 0.6	3.1 ± 0.5	2.1 ± 0.3
Mean Diameter (mm)	1.4 ± 0.3	0.9 ± 0.4	0.6 ± 0.2

4.2.2 Trunk

Trapezius

Trapezius is a diamond shaped muscle that has cervical, scapular and thoracic parts. This muscle lies superficial to all musculature of the back, and has unique anatomy and relevant surgical applications. Baek et al in 1980,¹⁸⁵ was the first to describe the trapizeus as a surgical flap. Trapezius is mainly utilized as a pedicled flap, but has the portential to be partially transferred as free flap.

The muscles is supplied by the occipital artery (OA), deep cervical artery, transverse cervical artery (TCA), deep and superficial branches, superficial branch of the dorsal scapular artery (DSA), vertebral radicular perforators and the posterior intercostal arteries (PICA).

The smallest zone of perfusion is near the muscle's occipital origin and is supplied by branches of the occipital artery, and deep cervical artery. The part around the root of the neck and the posterior shoulder is the largest zone of perfusion, and is supplied mostly by the deep branch of the transverse cervical artery, but with contribution form the superficial branch of TCA especially to the overlying skin medial to the posterior shoulder. The suprascapular artery supplies a small are laterally near the acromion. The 3D study confirms that the transverse cervical artery is the dominant arterial supply.

The mean diameter for the transverse cervical artery is $2.3 \text{ mm} \pm 0.2$; the mean pedicle length is $7.4 \text{ cm} \pm 3$. The deep branch mean diameter is $2.1 \text{ mm} \pm 0.4$, and the mean pedicle length for the deep branch of the transverses cervical artery is $5.3 \text{ cm} \pm 0.9$,

the superficial branch mean diameter is 1.8 ± 0.3 , and with an mean pedicle length of $3.2 \text{ cm} \pm 0.3$.

The mean volume of trapezius muscle is $145.4 \text{ cm}^3 \pm 5$, the transverse cervical vessel contributes to $45\% \pm 3$ of the volume and the deep branch contributes to $36\% \pm 2$ of muscle volume, the superficial branch contributes to $9\% \pm 1.6$ of the muscle's volume. The occipital artery contributed to $8\% \pm 2$ of the muscle's volume. The suprascapular artery supplied $5\% \pm 2$ of the muscle's volume.

The dorsal scapular artery descends along the medial border of the scapula and sends a superficial perforating branch that supplies the middle third of the muscle on its deep surface. The dorsal scapular artery is the dominant blood supply to the lower trapezius $17\% \pm 3$. The lower part of the muscle is much smaller in volume, and the dorsal scapular shares the supply to the inferior aspect of the muscle with the vertebral radicular perforators and the posterior intercostal arteries. The diameter of the DSA is $2.1 \text{ mm} \pm 0.3$ and the mean length was $4.2 \text{ cm} \pm 1$. Table 18 contains summary of the 3D morphometric data.

The dominance of the dorsal scapular artery in the lower trapezius is of great surgical significance, since it allows segmenting the muscle for transfer without compromising its function. Figures 54 and 55 illustrate the anatomy of this muscle.

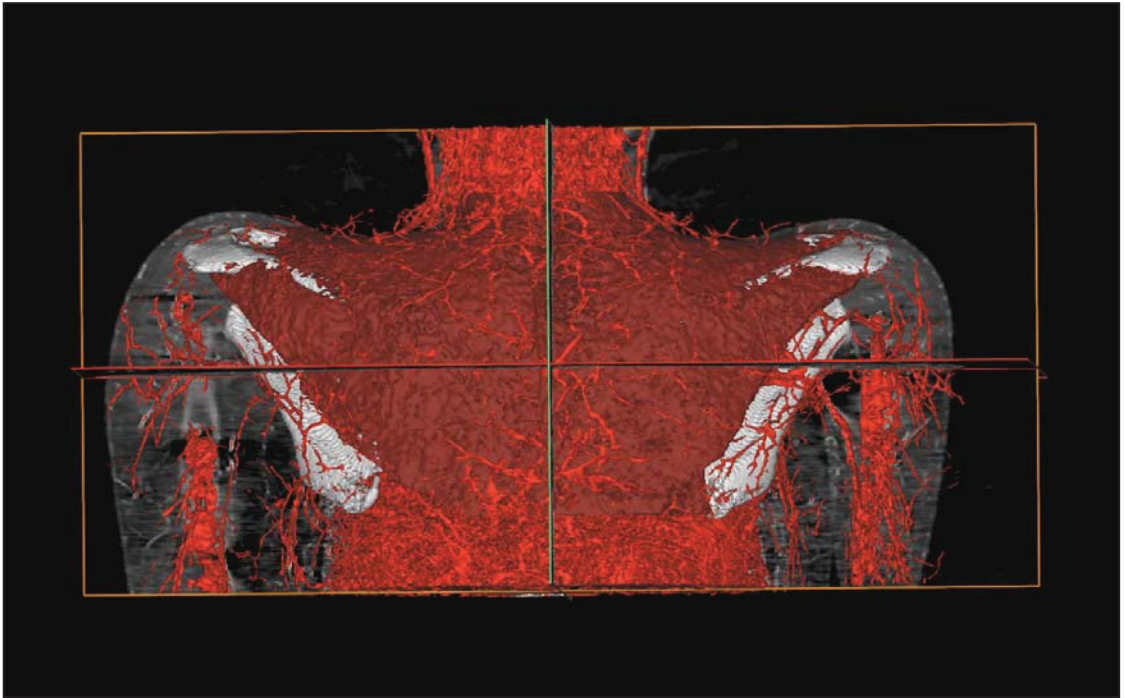


Figure 54: Trapezius 3D Angiogram

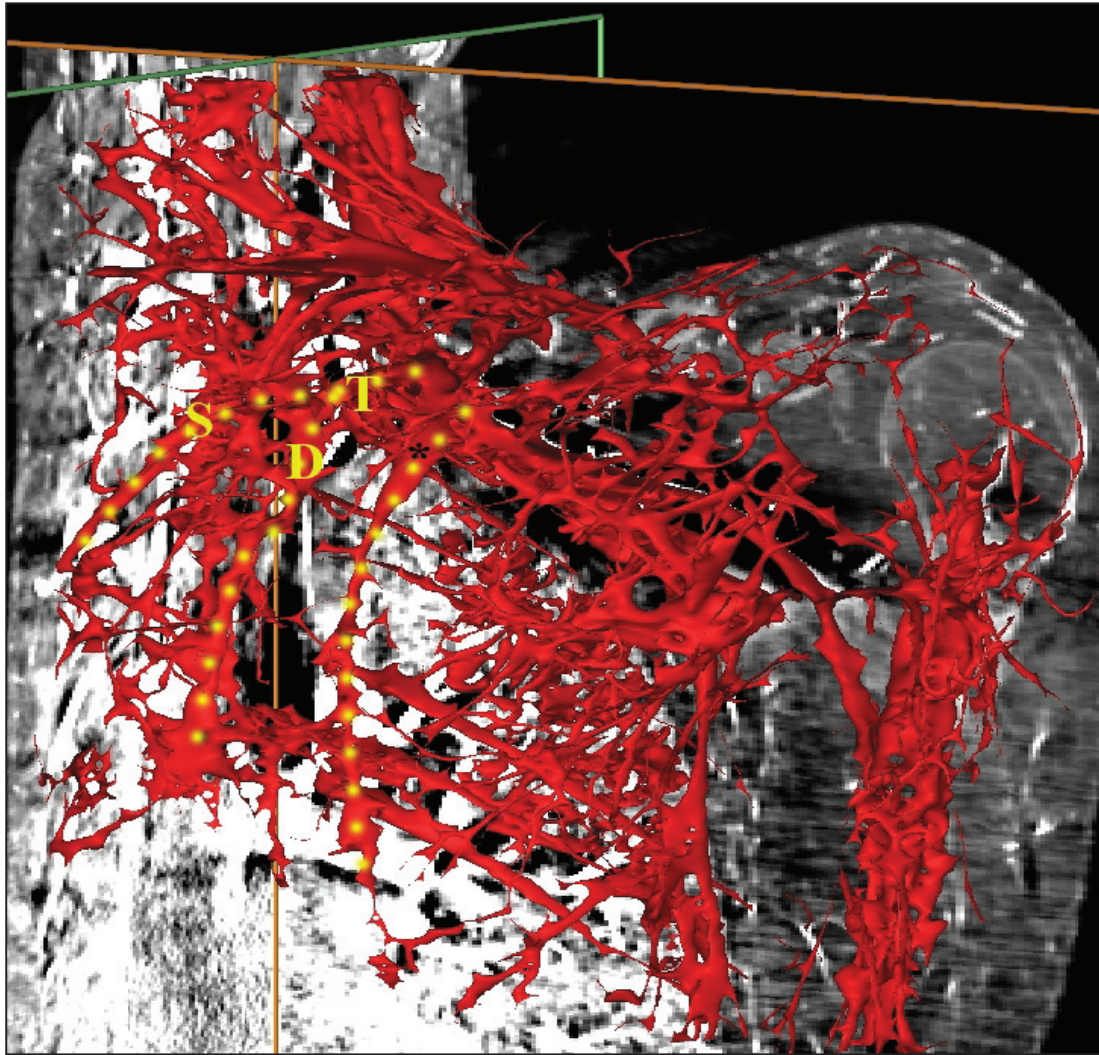


Figure 55: Dorsal Scapular Artery

The dorsal scapular artery (*) sends a perforating branch from the deep surface of the muscle to supply the inferior part the trapezius muscle. This muscular perforator is an independent branch separate from the deep or descending branch of the transverse cervical artery (D). Medially note the other significant branch of the transverse cervical artery; the superficial cervical artery (S).

Table 18: Three Dimensional Analysis of Trapezius

	Transverse Cervical Artery	Deep Transverse Cervical Artery	Superficial Transverse Cervical Artery	Dorsal Scapular Artery
Mean Muscle volume (cm³)	65.4 ± 7.3	52.3 ± 2.9	4.8 ± 2.3	24.7± 0.74
Mean Length of Pedicle (cm)	7.4 ± 3	5.3 ± 0.9	3.2 ± 0.3	4.2 ± 1
Mean Diameter (mm)	2.3 ± 0.2	2.1 ± 0.4	1.8 ± 0.3	2.1 ± 0.3

Latissimus Dorsi

In reconstructive surgery the latissimus dorsi is considered the workhorse flap with the most reliable blood supply. The latissimus dorsi flap was described almost a hundred years ago by Tansini. This muscle has three vascular territories. The mean volume of latissimus dorsi was $442 \text{ cm}^3 \pm 34$. The thoracodorsal artery is the dominant arterial supply and enters the proximal part of the muscle $8 \text{ cm} \pm 4$ distal to its insertion, supplying $42 \% \pm 4$ the proximal part of the muscle. The lower and posterior parts are supplied by 6 ± 2 posterior intercostal arteries and 5 ± 2 thoracolumbar perforators (TLP). The total volume of muscle supplied by PICA perforators is $36 \% \pm 2$. The thoracolumbar perforators supply $22 \% \pm 3$. The thoracodorsal artery anastomoses with intercostal, thoracolumbar perforators and the arcade formed by the dorsal scapular and descending branch of the circumflex artery at the inferior angle of the scapula within the muscle in all samples (Figures 56,57). The mean diameter of the thoracodorsal artery (TDA) is $3.1 \text{ cm} \pm 0.5$, the mean volume of muscle supplied by the TDA $185.6 \text{ cm}^3 \pm 17.6$. For detailed summary of the morphometric data see Table 19.

Table 19: Three Dimensional Analysis of Latissimus Dorsi

	Thoracodorsal artery	Posterior Intercostal Arteries	Thoracolumbar Perforators
Mean Muscle volume (cm³)	185.6 ± 17.6	159.1 ± 8.8	97.2 ± 13.3
Mean Length of Pedicle (cm)	10.8 ± 2 cm	3.6 ± 0.7	3.1 ± 0.5
Mean Diameter (mm)	3.1 ± 0.5	0.8 ± 0.2	0.6 ± 0.2

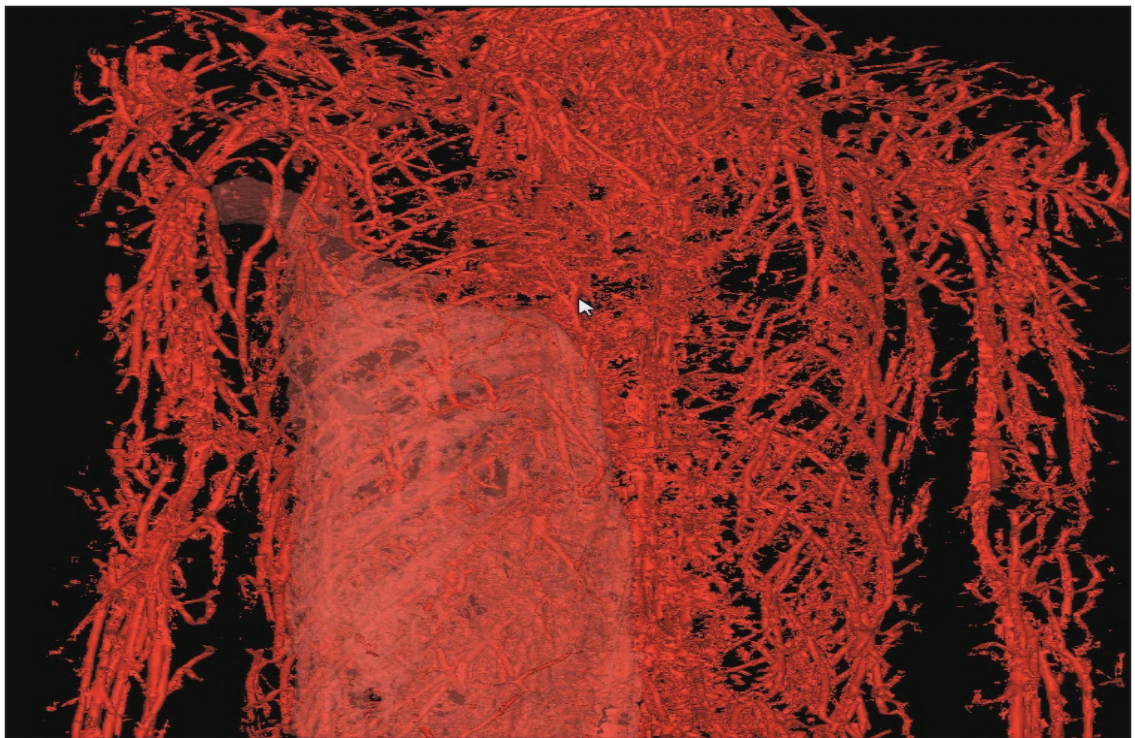


Figure 56: Latissimus Dorsi 3D Angiogram

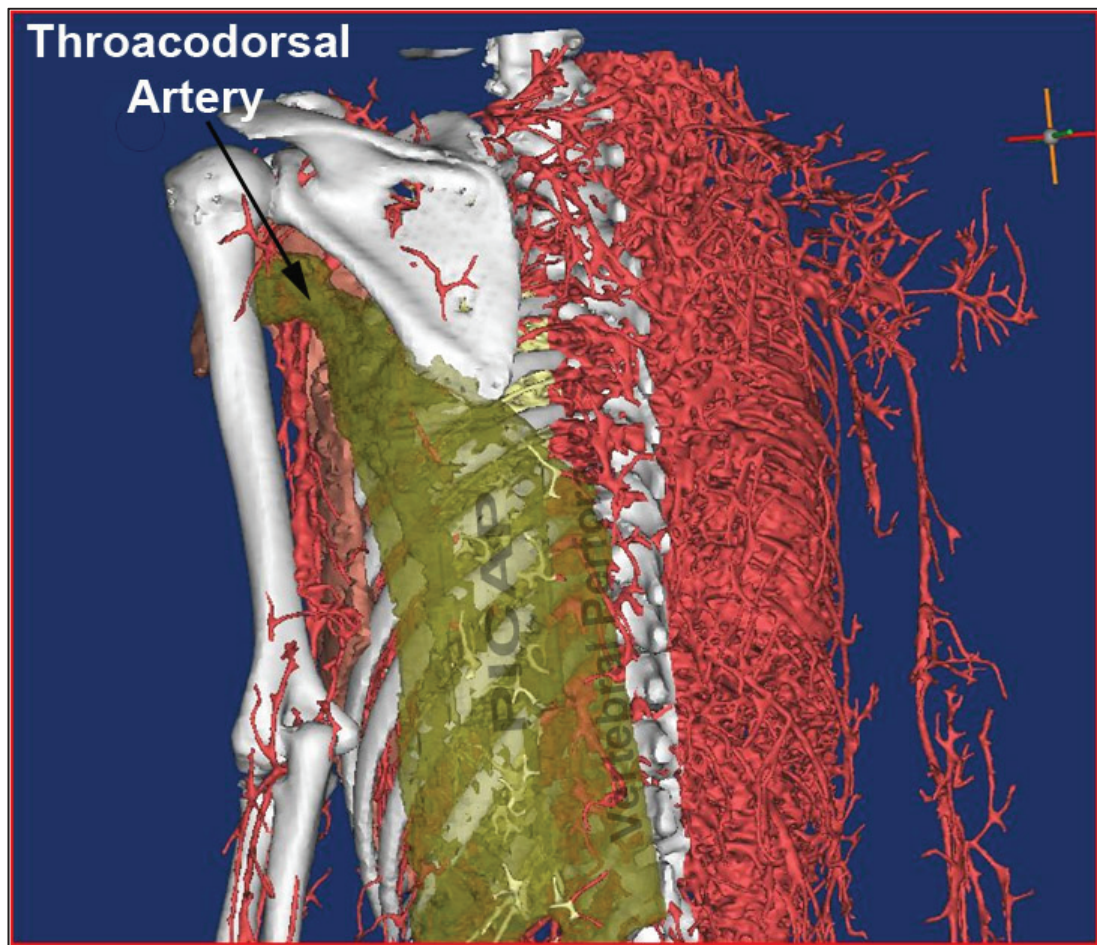


Figure 57: Latissimus Dorsi Vascular territories

The three vascular territories of the latissimus dorsi muscle outlined in this 3D capture.
From a dynamic STL also see Figure 56.

4.2.3 Upper Extremity

Coracobrachialis

Parry et al described coracobrachialis as a muscle with a dominant single pedicle that can be used as surgical flap.¹⁰⁵ Hober et al later described its use as a transposition flap for coverage of the axillary artery based on its dominant proximal blood supply.¹⁸⁶

Coracobrachialis takes origin from the coracoid process and inserts on the proximal and medial surface of the humerus. The muscle is innervated by 2 branches from the musculocutaneous nerve. The blood supply to this muscle is from a direct branch of the axillary artery proximally, and is the dominant pedicle its length is $2.6 \text{ cm} \pm 0.3$, the diameter of this vessel $1.2 \text{ mm} \pm 0.3$, and it supplies $55 \% \pm 4$ of the muscle's volume. The remaining blood supply was from the brachial artery in a segmental fashion constituting the $43 \% \pm 3$. The average diameter of this pedicle Table 21 contains summary of the data. Figure 58 demonstrates the arterial anatomy.

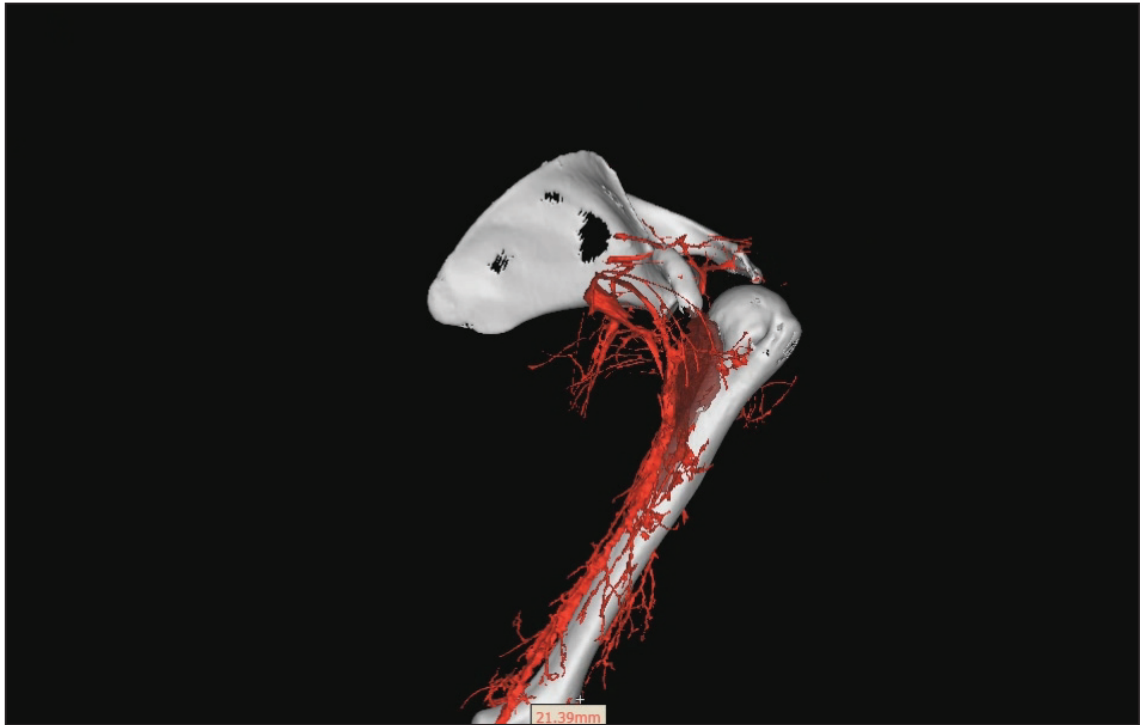


Figure 58: Coracobrachialis Three Dimensional Angiogram

Table 20: Three Dimensional Analysis Data Coracobrachialis

	Coracobrachialis artery	Profunda Brachii
Mean Muscle volume (cm³)	6.5 ± 0.4	5.1 ± 0.35
Mean Length of Pedicle (cm)	2.6 ± 0.3	0.6 ± 0.2
Mean Diameter (mm)	1.2 ± 0.3	0.6 ± 0.1

Biceps Brachii

The biceps brachii muscle has a unique vascular anatomy, and an important essential motor function, despite that its vascular anatomy allows partial splitting of the muscle to be used on its own as free segmental muscle transfer or to be included with myocutaneous lateral or medial forearm flap (Figure 59).

The major supply to this muscle is via two large branches from the brachial artery in the middle mass of the muscle. The biceps vessels have a longer intermuscular than their extramuscular course. The mean length of the branches of the brachial artery supplying the muscle is $4.2 \text{ cm} \pm 0.8 \text{ cm}$; the length of the extramuscular course of the brachial artery branches had a mean of $2 \text{ cm} \pm 0.3$. The mean diameter of the branches from the brachial artery is $1.6 \text{ mm} \pm 0.2$. The mean volume of the muscle is $101.9 \text{ cm}^3 \pm 4$. The muscle receives small contribution from profunda brachii from its lateral surface (Table 21).

Table 21: Three Dimensional Analysis of Biceps Brachii

	Brachial Artery Branches	Profunda Brachii
Mean Muscle volume (cm³)	98.6 ± 2.4	0.52 ± 0.11
Mean Length of Pedicle (cm)	2 ± 0.3	1.2 ± 0.3
Mean Diameter (mm)	1.6 ± 0.2	0.6 ± 0.12



Figure 59: Biceps Brachii 3D Angiogram

Brachialis

The brachialis muscle also has a unique anatomy related to its innervations, blood supply. Surgically the muscle is accessible via both medial and lateral incisions. The lateral incision is favorable should segmental transfer be considered. The muscle can be split from the lateral aspect due to the dual innervations it receives, the musculocutaneous nerve always innervates this muscle but in 83 % of the case this muscle receives lateral contribution from a descending branch of the radial nerve.¹⁸⁷ The vascular anatomy is dominant to the brachial artery but there is a minor contribution from the profunda brachii on its lateral surface as seen in the 3D model in Figure 60. This unique characteristic of brachialis permits segmenting of the lateral aspect of the muscle based on the profunda branch it receives and the radial innervation to the lateral aspect of the muscle.

The brachialis muscle receives its blood supply from the brachial artery and the ulnar recurrent artery, as well as the profunda brachii muscle. There are 4 ± 1 vascular pedicles entering the Brachialis muscle. The mean diameter from the brachial artery is the largest measuring $1.7 \text{ mm} \pm 0.3$. The mean length of each the branches of the Brachialis is $2 \text{ cm} \pm 0.5$. Profunda brachii sends branches to the lateral aspect of the muscle, the branches of profunda 3 ± 1 ; the diameter is $1.4 \text{ mm} \pm 0.2$, and mean length $2.2 \text{ cm} \pm 0.6$. The ulnar recurrent artery supplies this muscle on its distal end with constant 2 branches, mean length $1.9 \text{ cm} \pm 0.4$. With a $1.6 \text{ mm} \pm 0.2$. The muscle's mean volume is $24.2 \text{ cm}^3 \pm 2$. The profunda brachii supplies $80 \% \pm 4$ of its volume, ulnar recurrent supplies $15 \pm 3 \%$ and the profunda brachii supplies $5 \% \pm 1$. Figure 60 shows the relevant vascular anatomy to this muscle, and Table 22 summaries the above-mentioned data.

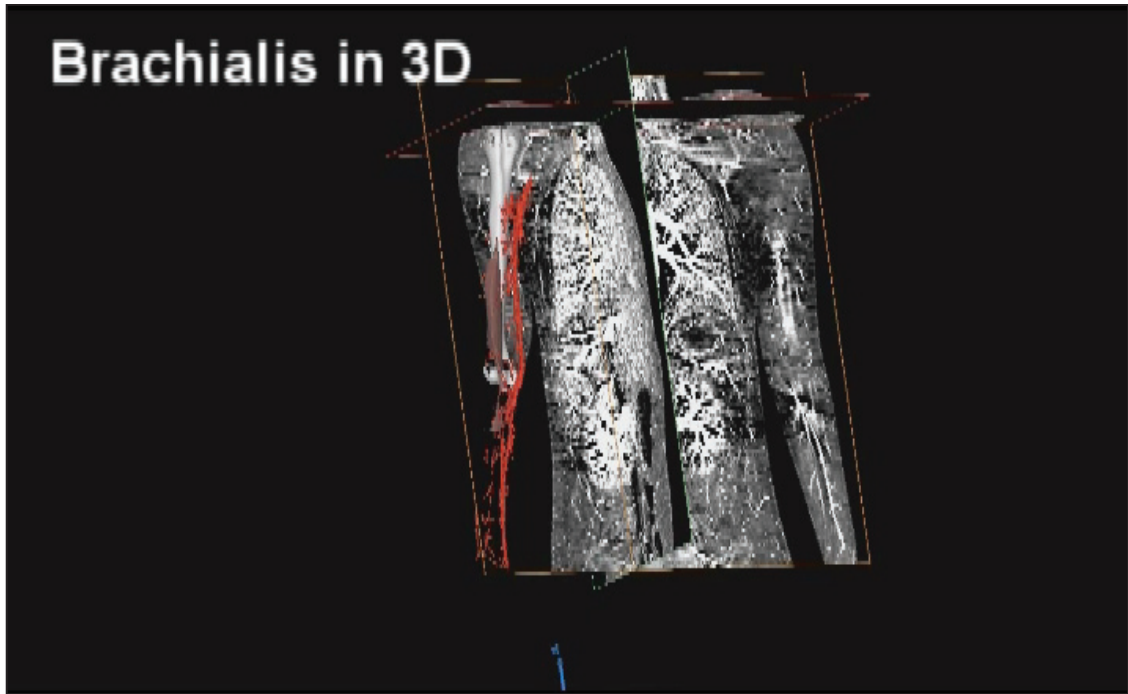


Figure 60: Brachialis 3D Angiograms

Table 22: Three Dimensional Analysis of Brachialis

	Brachial Artery Branches	Ulnar recurrent Branches	Profunda Brachii Branches
Mean Muscle volume (cm³)	19.4± 0.96	3.6 ± 0.7	1.2 ± 0.2
Mean Length of Pedicle (cm)	2 ±0.5	1.9 ± 0.4	2.2 ± 0.6
Mean Diameter (mm)	1.7 ± 0.3	1.6 ± 0.2	1.4 ± 0.2

Thenar Muscles:

The thenar muscles of the hand are among the smallest muscles of the body, the thenar muscle are commonly used in hand reconstruction, and typically the process of pollicization and toe to thumb transfer require thorough knowledge of their anatomy and blood supply.

Abductor Pollicis brevis

The abductor pollicis brevis is a small muscle flap that has been utilized clinically to reconstruct thumbs or cover adjacent and very small hand defects.^{90, 188-190} The APB is the most radial muscle of the thenar group it originates from the tubercle of the scaphoid and the transverse carpal ligament, and it inserts on the radial side of the base of the proximal phalanx of the thumb.

Its arterial blood supply is mainly from the superficial radial artery; there are 3 ± 1 branches that enter the muscle at its origin, midway and distally. The mean diameter for the superficial branches $0.6 \text{ mm} \pm 0.2$. The superficial branches supply 100 % of the muscle's volume with the proximal branch being the dominant supply constituting 40 % of the muscle's volume (Figure 61). Table 22 contains summary of the thenar muscles data.



Figure 61: Abductor Pollicis Brevis

The branches of Abductor pollicis brevis numbered from 1-4. Note that the superficial radial artery has a radial (**a**) and a palmar (**b**) division, and the radial division (**a**) supplies the APB.

Flexor Pollicis Brevis

Flexor pollicis brevis muscle receives its blood supply from the superficial palmar artery as well as the deep palmar arch for its deep head. The dominant blood supply to the superficial head was from the branches of the superficial radial artery, particular the radial division. The deep head also received segmental blood supply from both deep and superficial radial systems with the deep system being dominant (Figure 62).

The number of branches from the superficial system was 6 ± 2 , and the deep system 4 ± 1 . The superficial system supplied $70 \% \pm 4$ of the superficial head and the deep system supplied $60 \% \pm 5$ of the deep head.



Figure 62: Flexor Pollicis Brevis

The flexor pollicis brevis with the superficial head on the radial aspect (**s**), and the deep head on the ulnar aspect (**d**)

Opponens Pollicis

The deepest of the thenar muscles, and is supplied completely by the radial division of the superficial radial artery. It receives 6 ± 2 very small segmental branches, the details of all thenar muscles data is summarized in Table 22. Figure 63 demonstrates the 3D anatomy of the thenar muscles

Table 23: Summary of Three Dimensional Analysis of Thenar Muscles

	Abductor Pollicis Brevis	Flexor Pollicis Brevis	Opponens Pollicis
Mean Muscle volume (cm³) *	7 ± 1.5	16.3 ± 3	3.5 ± 0.7
Branches from Superficial radial	3 ± 1	6 ± 2	6 ± 2
Branches from deep palmar arch	0	4 ± 1	0
Largest diameter vessel (mm)	0.8	0.7	0.6

* Previous Tables indicated mean muscles volume supplied by a vascular pedicle; this Table only states the actual mean volume of each muscle instead

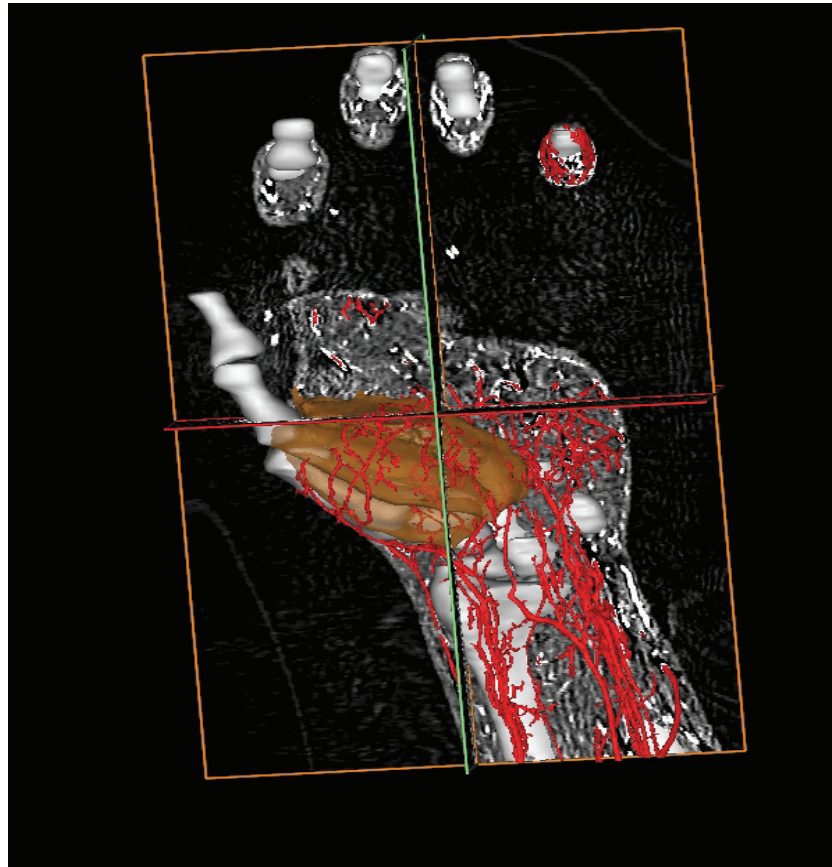


Figure 63: Thenar Muscles 3D Angioram

4.2.4 Lower Extremity

Tensor Fascia lata

The tensor fascia lata TFL musculocutaneous flap was described in 1978 by Nahai et al.¹⁹¹ The muscle and its overlying skin enjoy robust blood supply. Safe harvesting of myocutaneous, fasciocutaneous or perforator skin flaps from this area is only possible with detailed knowledge of the course and distribution of the ascending branch of the lateral circumflex femoral artery (LCFA).

The ascending branch of the LCFA was always the dominant pedicle to TFL. The mean diameter to TFL is $2.2 \text{ mm} \pm 0.6$; the mean volume for the TFL muscle is $54.9 \text{ cm}^3 \pm 3.7$. The TFL also receives minor contribution from the deep branch of the superior gluteal artery; the mean volume supplied by the deep branch of the superior gluteal artery is $5 \text{ cm}^3 \pm 0.7$. Table 24 outlines the mean lengths of vascular tree. Figure 64,65 shows details of the vascular anatomy of this muscle.

Table 24: Mean lengths of Lateral Circumflex Femoral Vascular tree

Ascending branches to TFL	Length (mm)
1- Ascending Pedicle	34.92
2- Superior intramuscular branch prior to branching	8.40
3- Inferior intramuscular prior to branching	8.18
4-Superior terminal branch of the superior branch of the ascending LCFA	23.78
5-Inferior terminal branch of the superior branch of the ascending LCFA	14.60
6-Superior terminal branch of the middle branch of the ascending LCFA	23.04
7-Middle terminal branch of the middle branch of the ascending LCFA	37.77
8-Inferior terminal branch of the middle branch of the ascending LCFA	20.50
9-Branch of the descending LCFA supplying the <u>illiotibial</u> tract	15.73

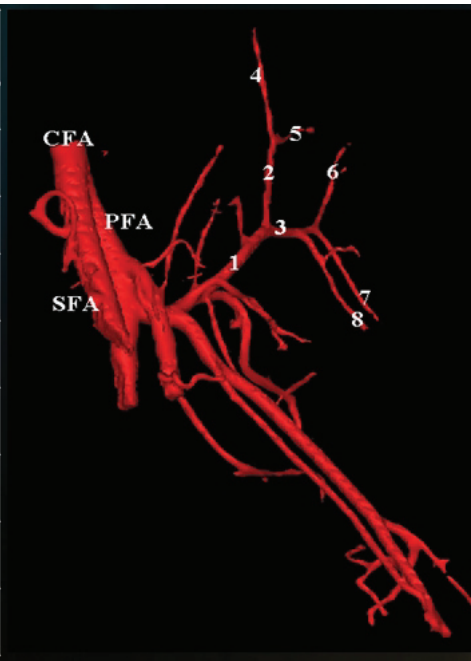



Figure 64: Tensor Fascia Lata 3D Angiogram

**Vascular supply to
the Tensor Fascia lata
and overlying skin**

Figure 65: TFL Perforator Flap in 3D

Sartorius

Sartorius is a muscle that has many potential applications in reconstructive surgery. So far, its application has been limited to transposition to cover small defects in the groin,¹⁹² this muscle has segmental blood supply and segmental innervation lending itself well to the concept of segmental transfer.¹⁹³

The superficial femoral artery is the major blood supply to sartorius. There is a small contribution from the common femoral at its proximal origin.

The mean volume of the muscle is $87.5 \text{ cm}^3 \pm 11.9$. The mean number of pedicles to this muscle is 6.8 ± 1.236 . The mean diameter of pedicles to this muscle is $1.5 \text{ mm} \pm 0.27$, the descending genicular artery supplied the muscle with the largest pedicle, the pedicles diameter is 2 mm in diameter and with a mean length of $4.3 \text{ cm} \pm 1.2$, and is typically found at the distal third of the muscle. Table 25 summarizes the morphometric findings of the Sartorius muscle. Figure 66 shows the anatomical details of Sartorius in 3D.

Table 25: Three Dimensional Analysis of Sartorius

	Mean Total Volume	Common Femoral Artery	Superficial Femoral Artery	Descending Genicular Artery
Mean Muscle volume (cm ³)	87.5 ± 11.9	3.3 ± 1.4	65.8 ± 5.2	18.4 ± 8
Mean diameter of pedicles (mm)	1.5 ± 0.27	1.6 ± 0.15	1.3 ± 0.23	1.8 ± 0.13
Mean number of Pedicles	6.8 ± 1.23	1.3 ± 0.5	3.8 ± 0.78	1.66 ± 0.7
Mean length of pedicles (cm)	2.7 ± 0.69	3.1 ± 0.7	2.4 ± 0.4	4.3 ± 1.2



Figure 66: Sartorius 3D Angiogram

Gracilis

Gracilis is currently a workhorse flap for functional muscle transfer. Its unique anatomy and ease of harvest made it the go to flap in functioning muscle transfer. Hari et al. was first to demonstrate the functional transfer of the gracilis for facial paralysis in 1976.¹⁷

The main vascular pedicle to gracilis is supplied by the medial circumflex femoral artery.

The detailed branching system of the medial circumflex femoral artery is not well illustrated in many anatomical atlases and textbooks.¹⁹⁴⁻¹⁹⁷ The literature also has few studies describing the different branches of this vessel.¹⁹⁸⁻²⁰⁰

The most common branching system observed is illustrated in Figure 67.

The Gracilis takes origin from ischiopubic ramus and inserts into the pes anserinus. In some reconstructive surgery textbooks the gracilis main pedicle is described to be from an ascending branch of the medial circumflex femoral artery, and in others it is described as a separate branch of profunda known as the adductor artery. Despite the well known variation in the take off of the medial circumflex femoral artery, our findings were compatible with the Federative Committee on Anatomical Terminology (FCAT); we consistently found the MCFA to have deep and superficial branches, as well as an ascending branch. The ascending branch supplied the proximal origin to the muscle but was not found to be the dominant pedicle to the muscle as some authors have described. The dominant pedicle was from an ascending ramus of the deep branch of the MCFA. This relationship is illustrated in Figure 64. The gracilis muscle also receives minor segmental blood supply from the superficial femoral artery. Figure 68 is a 3D angiogram of gracilis. The mean volume of the gracilis muscle was $69.4 \text{ cm}^3 \pm 5.5$. The mean volume supplied by the medial circumflex femoral artery $42.4 \text{ cm}^3 \pm 3.7$. The mean

volume supplied by the ascending branch of the MCFA was $3.39 \text{ cm}^3 \pm 0.2$. The mean volume supplied by the branches of the superficial femoral artery is 24.8 ± 1.7 . Table 26 contains summary of the morphometric data.

Table 26 Three Dimensional Analysis of Gracilis

	Total	Deep branch of MCFA	Superficial Femoral Artery	Ascending branch of MCFA
Mean Muscle volume (cm ³)	69.4 ± 5.5	42.4 ± 3.7	24.8 ± 1.7	3.39 ± 0.2
Mean diameter of pedicles (mm)	1.04 ± 0.49	1.7 ± 0.2	0.7 ± 0.13	0.67 ± 0.1
Mean number of Pedicles	4.1 ± 0.73	1 ± 0	2.07 ± 0.73	1 ± 0
Mean length of pedicles (cm)	3.7 ± 1.9	6.5 ± 0.4	2.34 ± 0.4	2.5 ± 0.35

MCFA = Medial circumflex femoral artery

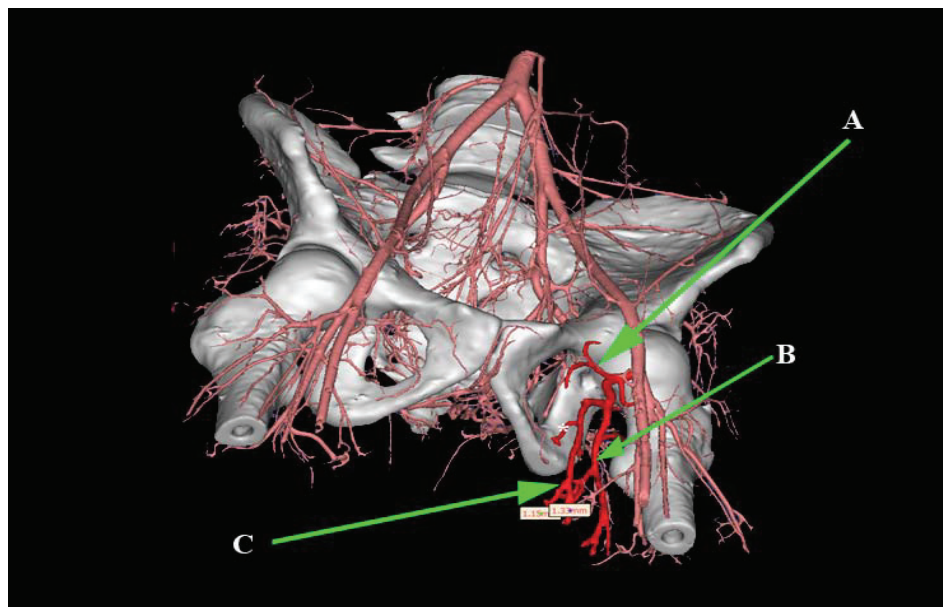


Figure 67: Medical Circumflex Femoral Artery (MCFA)

A) Ascending branch of the MCFA. B) Superficial branch of MCFA. C) Deep branch of MCFA.

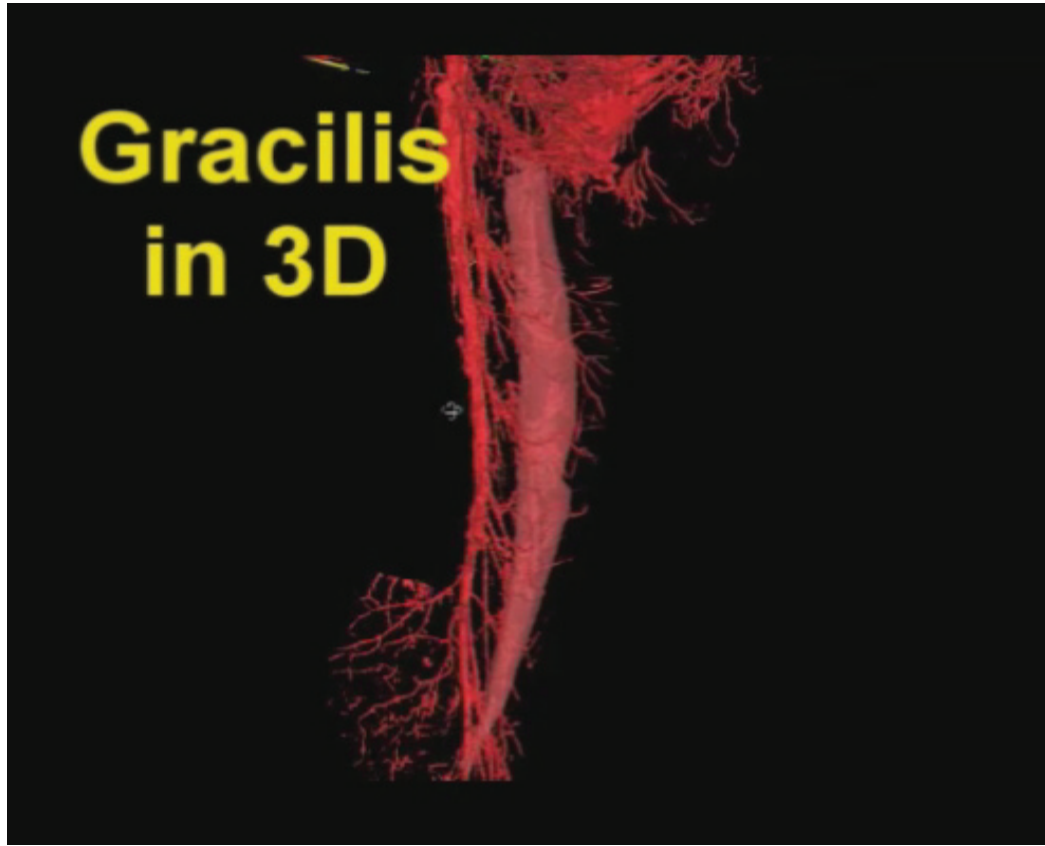


Figure 68: Gracilis 3D Angiogram

Gluteus Maximus

The gluteus maximus muscle is commonly used as a regional flap especially in the reconstruction of pressure sores. The dual dominant arterial supply by both the superior and inferior gluteal arteries makes this muscle a great donor for segmental transfer (Figures 69,70). The medial circumflex femoral MCFA also supplies this muscle distally near its insertion. The gluteus maximus is not typically used as free flap due to its indispensable function.

The mean volume of gluteus maximus was $694 \text{ cm}^3 \pm 44$, the mean volume of the muscle supplied by the superior gluteal artery is $306 \text{ cm}^3 \pm 6$, and the mean volume of the muscle supplied by the inferior gluteal artery is $368 \text{ cm}^3 \pm 9$. Please refer to Table 27 for detailed morphometric analysis.

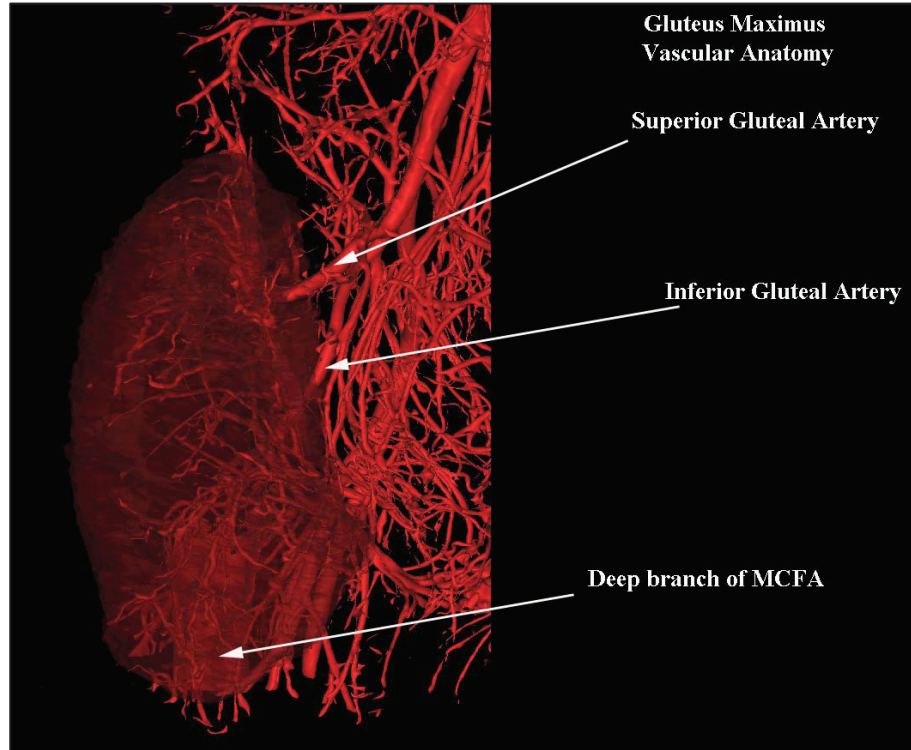


Figure 69: The Arterial Architecture of Gluteus Maximus

MCFA= Medial circumflex femoral artery

Table 27: Three Dimensional Analysis of Gluteus Maximus

	Total	Inferior Gluteal Artery	Superior Gluteal Artery	Deep branch of MCFA
Mean Muscle volume (cm³)	694 3± 44	368 ± 9	306 ± 5.6	19.1 ± 0.8
Mean diameter of pedicles (mm)	2.5 ± 0.9	2.95 ± 0.6	3.15 ± 0.42	1.3 ± 0.2
Mean length of pedicles (cm)	4.4 ± 1.13	4.86 ± 0.9	3.14 ± 0.5	5.3 ± 0.54

Gluteus Maximus and Medius in 3D

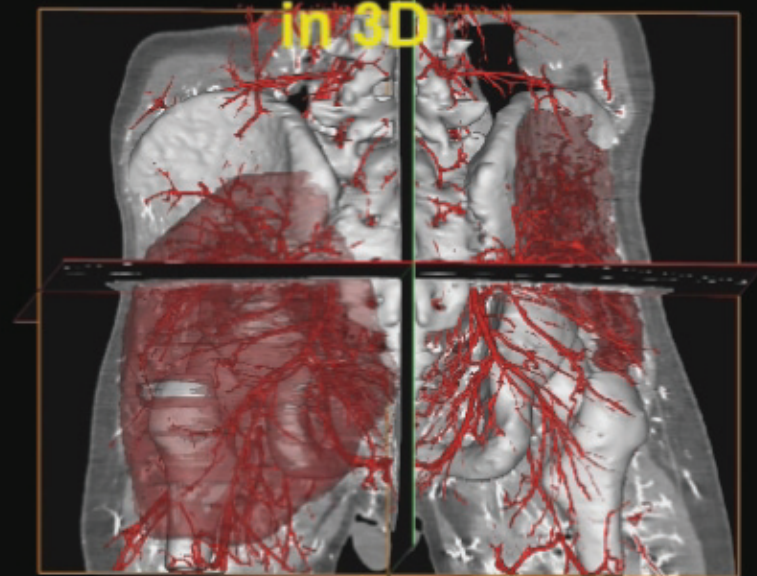


Figure 70: Gluteus Maximus and Medius 3D Angiogram

Gastrocnemius

Gastrocnemius has A reliable blood supply and is well known for its application in coverage of proximal third defects of the leg. The muscle has not been studied or used clinically as free flap or for functioning muscle transfer. The medial head is the larger of the two heads. The blood supply is from the medial and lateral sural arteries, as well as the peroneal artery distally for the lateral head and the posterior tibial artery distally for the medial head (Figures 71,72).

The mean muscle volume was $498 \text{ cm}^3 \pm 44.5$, the mean number of pedicles entering the lateral head proximally was 2.6 ± 0.48 , and the mean diameter of all pedicles to the lateral head was $1.09 \text{ mm} \pm 0.54$.

The mean number of pedicles entering the medial head proximally was 2.23 ± 0.48 ; the mean diameter of all pedicles to the medial head was $1.2 \text{ mm} \pm 0.68$.

The mean volume of the muscle that supplied by the lateral sural arteries was $103.4 \text{ cm}^3 \pm 21$, and the mean volume of muscle supplied by the medial sural artery was $245 \text{ cm}^3 \pm 18$. Please see table 28 for detailed morphometric data.

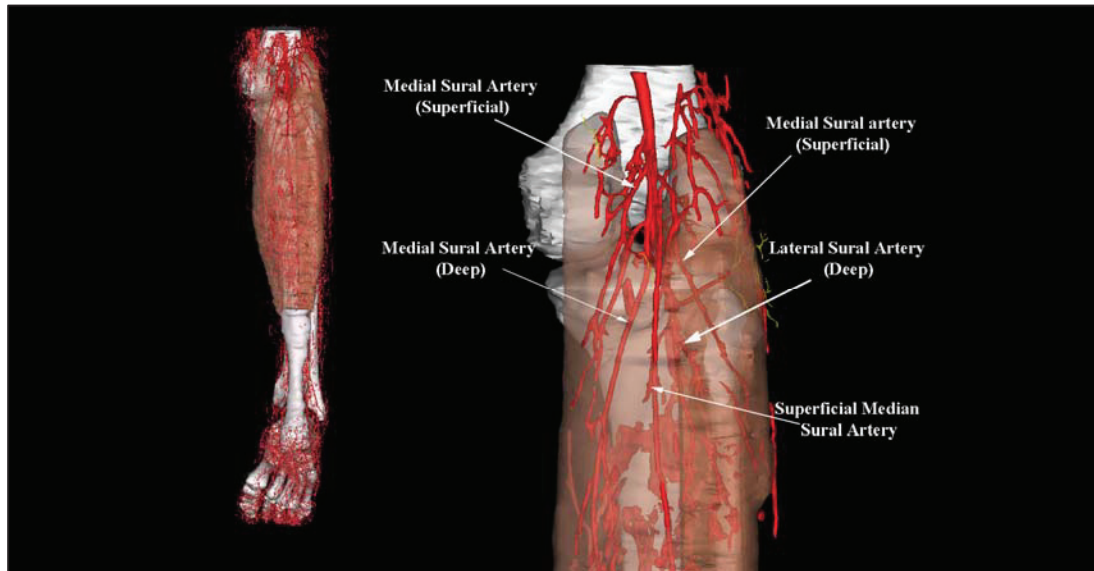


Figure 71: Arterial anatomy of Gastrocnemius

Table 28: Three Dimensional Analysis of Gastrocnemius

	Muscle Volume (cm ³)	Mean Number of branches	Mean diameter (mm)
Total	498 ± 44.5	2.8 ± 0.73	1.15 ± 0.6
Medial Head	349.7 ± 20	2.6 ± 0.48	1.2 ± 0.68
Lateral Head	148.3 ± 31	3 ± 0.9	1.09 ± 0.54
Medial Sural Artery	245 ± 18	2.53 ± 0.51	1.9 ± 0.37
Lateral Sural Artery	103.4 ± 21	2.23 ± 0.48	1.67 ± 0.36
Peroneal artery	44 ± 10.8	3.76 ± 0.44	0.7 ± 0.17
Posterior tibial artery	104.7 ± 8.7	2.76 ± 0.43	0.66 ± 0.13

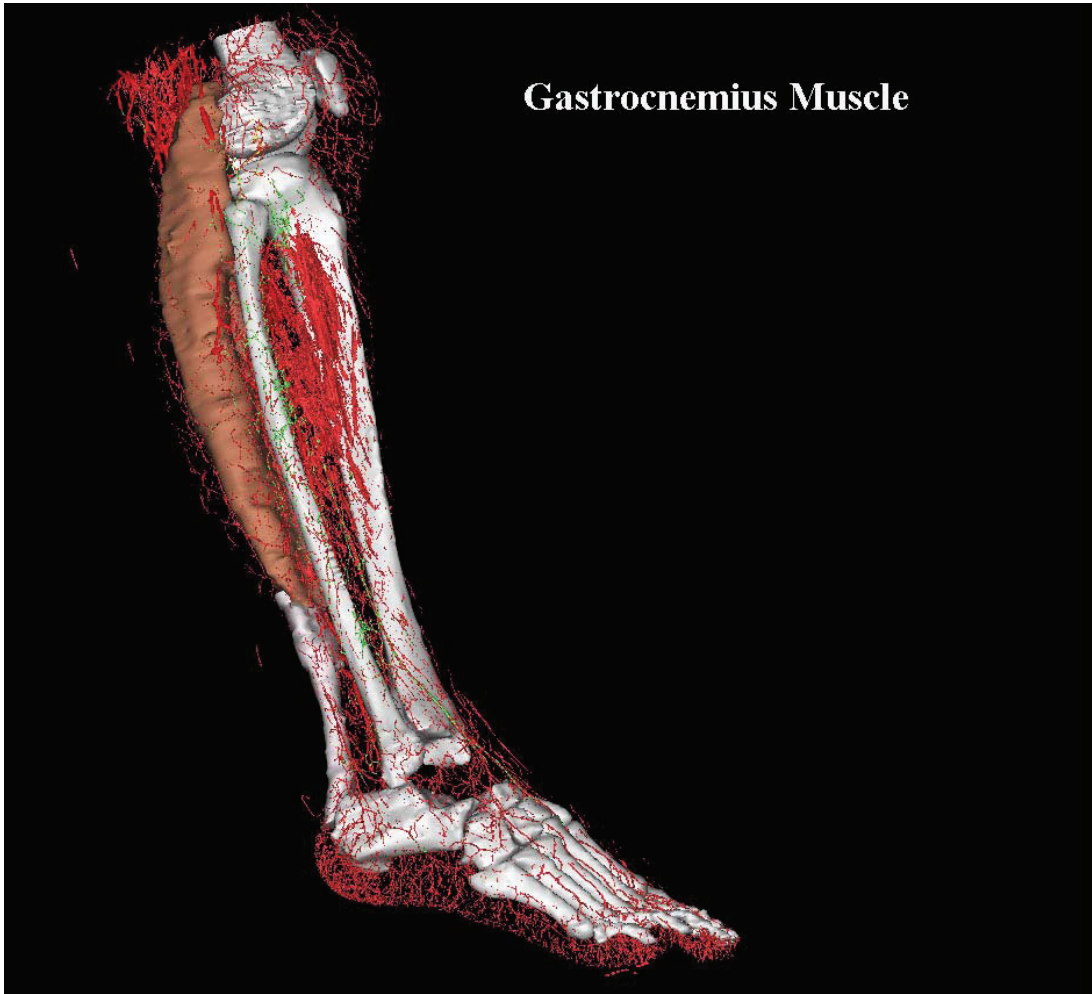


Figure 72: Gastrocnemius in 3D

Soleus

The soleus muscle originates from the soleal line on the proximal third of the tibia and from the proximal and mid part of the fibula. At the middle third of the muscle, a midline fibrous band splits the muscle into lateral and medial belly. Soleus is described as a regional flap for the coverage of middle third defects of the leg. Tobin et al. described a hemi soleus flap based on reverse flow from either the peroneal or the posterior tibial arteries distal branches.²⁰¹ The main blood supply is derived from the popliteal, peroneal and posterior tibial arteries (Figure 73). The muscle's average volume is $186 \text{ cm}^3 \pm 9$. The average volume supplied by the soleal branch of the popliteal artery is $55.8 \text{ cm}^3 \pm 2.65$, the average volume supplied by the proximal branch of the peroneal artery is $46.5 \text{ cm}^3 \pm 2.2$, and the average volume supplied by the proximal branch of the posterior tibial artery is $27.9 \text{ cm}^3 \pm 1.3$. The average volume of muscle supplied by the posterior tibial artery distally is $19.55 \text{ cm}^3 \pm 0.92$, and the average volume supplied by the peroneal artery is $36.3 \text{ cm}^3 \pm 1.72$ (Table 28).

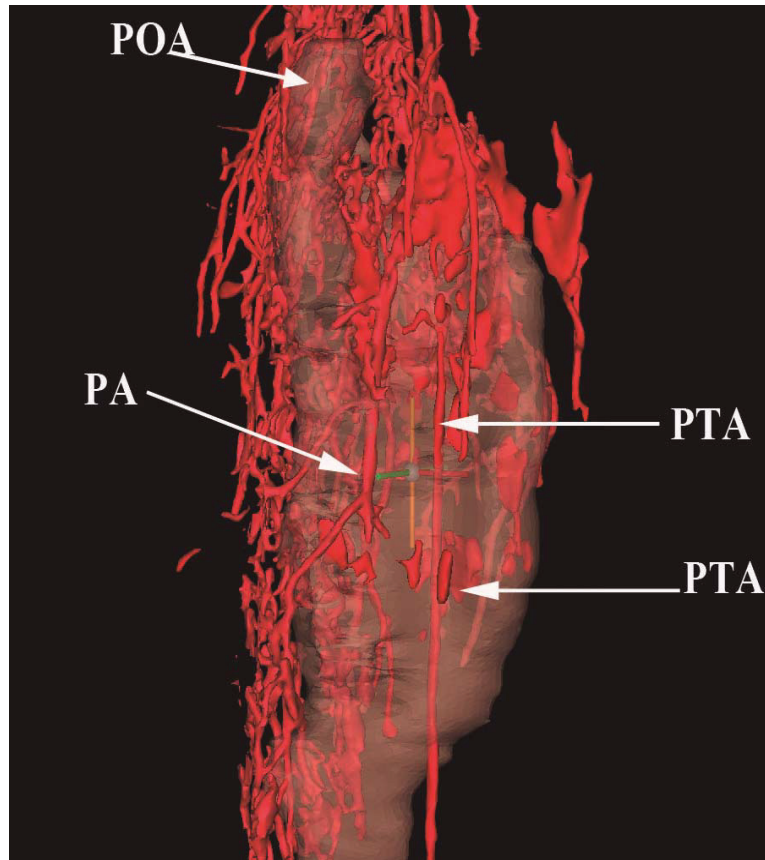


Figure 73: Posterior surface of Soleus

POA= Popliteal artery, PA= Peroneal artery, PTA= Posterior tibial artery.

Table 29: Three Dimensional Analysis of Soleus

	Total	Popliteal Artery	Proximal Peroneal Arty	Proximal Posterior Tibial Artery	Distal Peroneal Artery	Distal Posterior Tibial Artery
Soleus Volume (cm³)	186 ± 9	55.86 ± 2.6	46.5 ± 2.2	28 ± 1.3	36 ± 1.7	19.5 ± 0.9
Mean Diameter (mm)	1.2 ± 0.4	1.24 ± 0.25	1.6 ± 0.3	1.58 ± 0.3	1 ± 0.18	1 ± 0.17
Mean Pedicle length (cm)	3.4 ± 0.7	3.3 ± 0.3	3.8 ± 0.81	4.26 ± 0.52	2.99 ± 0.15	3 ± 0.3
Mean Number of Pedicles	3.5 ± 1.2	2.07 ± 0.73	3.07 ± 1	4 ± 0.67	4.3 ± 0.89	4.35 ± 0.84

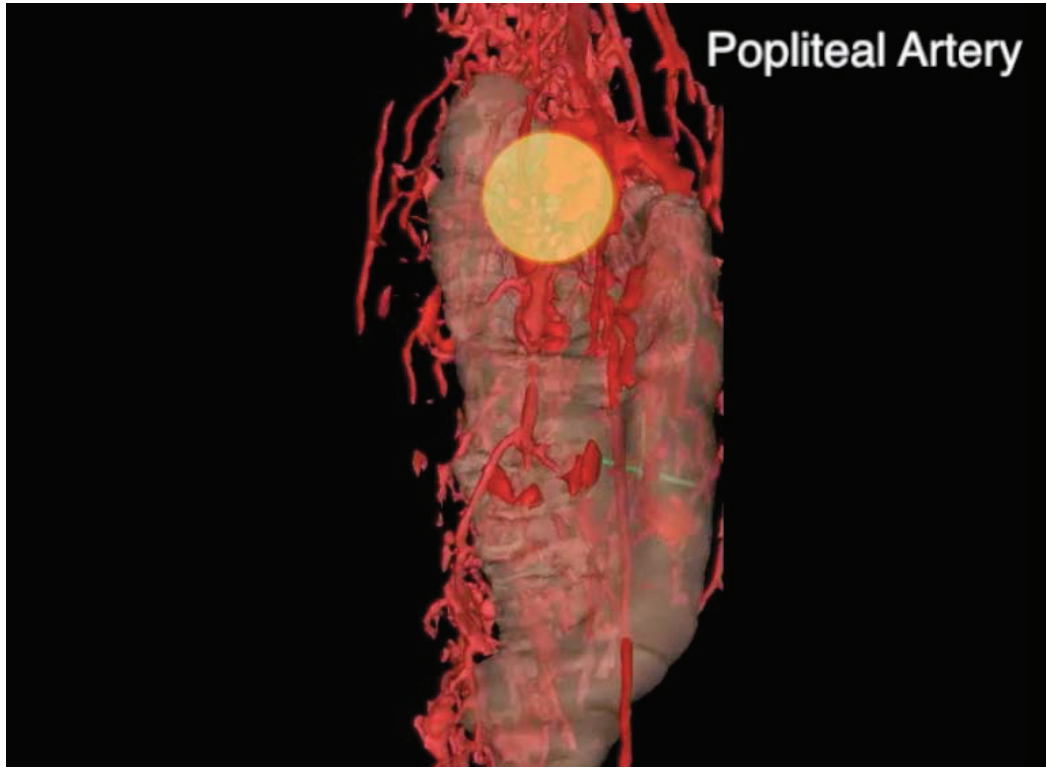


Figure 74: Soleus in 3D

Foot Muscle:

The small muscles of the foot are described as local flaps for coverage of pressure ulcers and small defects of the foot. The arterial anatomy of the foot was first described by Dubreuil-Chambardel.²⁰² Thorough knowledge of pedicles length and diameters of muscles of the feet will increase the potential application of these small muscles by allowing free transfer for both coverage and function.

Extensor Digitorum Brevis:

This muscle is supplied by proximal and distal branches of lateral tarsal artery (LTA); a direct branch of the dorsalis pedis (Figures 75, 76). The mean volume of EDB supplied by the proximal branch was $3.5 \text{ cm}^3 \pm 0.4$, and the mean volume supplied by the distal branch was $1.88 \text{ cm}^3 \pm 0.26$. The mean diameter of the proximal branch was $0.7 \text{ mm} \pm 0.3$, and the diameter of the distal branch was $0.4 \text{ mm} \pm 0.1$. The mean pedicle length of the proximal branch was $4.5 \text{ cm} \pm 0.8$, and the mean pedicle length of the distal branch was $2.2 \text{ cm} \pm 0.2$ (Table 30).

Flexor digitorum Brevis:

The flexor digitorum brevis (FDB) receives its blood supply from the Lateral plantar artery (LPA) proximally, the medial plantar artery (MPA) and fifth dorsal metatarsal artery distally (Figure 76). The mean volume of FDB supplied by the major branch of the lateral plantar artery was $4 \text{ cm}^3 \pm 0.9$, and the mean volume supplied by the minor branch of lateral plantar artery was $2 \text{ cm}^3 \pm 0.4$. The mean volume supplied by the distal branches of the medial plantar artery was $0.6 \text{ cm}^3 \pm 0.2$. The mean diameter of the major

branch of the lateral plantar artery was $0.8 \text{ mm} \pm 0.2$, and the mean diameter of the minor branch of the lateral plantar artery was $0.7 \text{ mm} \pm 0.1$. The mean diameter of the minor branches of the medial plantar artery was $0.5 \text{ mm} \pm 0.2$ (Table 30)

Abductor Digit Minimi:

Abductor digiti minimi (ABDM) muscle receives its blood supply by a major branch from the lateral plantar artery (LPA), and multiple minor segmental branches of the lateral plantar artery distally (Figure 76). The mean volume of ABDM supplied by the major branch of LPA was $5.8 \text{ cm}^3 \pm 0.9$, and the mean volume of ABDM supplied by the minor branches from LPA was $3.8 \text{ cm}^3 \pm 0.6$. The mean diameter of the major branch of LPA was $0.4 \text{ mm} \pm 0.1$, and the mean diameter of the minor branches of LPA was $0.3 \text{ mm} \pm 0.08$ (Table 30).

Abductor Hallucis:

Abductor hallucis (ABH) receive its blood supply chiefly from the medial plantar artery (MPA). The proximal branch is the major blood supply and the distal branches provide the minor blood supply to the ABH (Figure 76). The mean volume of ABH supplied by the major branch of MPA was $10.1 \text{ cm}^3 \pm 2.4$, and the mean volume of ABH supplied by the minor branches of MPA was $4.3 \text{ cm}^3 \pm 1$. The mean diameter of the major branch of MPA was $0.8 \text{ mm} \pm 0.2$, and the mean diameter of the minor branches of MPA was $0.4 \text{ mm} \pm 0.05$ (Table 30).

Table 30: Three Dimensional Analysis of the Foot Muscles

Name	Name Of Pedicle	Mean Diameter (mm)	Mean Pedicle Length (cm)	Mean Muscle Volume (cm³)
Extensor Digitorum Brevis	Proximal lateral tarsal artery	0.7 ± 0.3	4.5 ± 0.8	3.5 ± 0.4
	Distal lateral tarsal artery	0.4 ± 0.1	2.2 ± 0.2	1.88 ± 0.26
	Lateral Plantar artery (major)	0.8 ± 0.2	0.9 ± 0.2	4 ± 0.9
Flexor Digitorum Brevis	Lateral Plantar artery (minor)	0.7 ± 0.1	0.7 ± 0.1	2 ± 0.4
	Distal medial plantar artery (minor)	0.5 ± 0.2	0.4 ± 0.06	0.6 ± 0.2
	Fifth dorsal metatarsal artery	0.3 ± 0.05	0.6 ± 0.04	3.7 ± 0.66
Abductor Digiti Minimi	Lateral planter artery (major)	0.4 ± 0.1	0.7 ± 0.1	5.8 ± 0.9
	Lateral planter artery (segmental)	0.3 ± 0.08	0.4 ± 0.1	3.8 ± 0.6
Abductor Hallucis	Medial plantar artery (major)	0.8 ± 0.2	1.3 ± 0.2	10.1 ± 2.4
	Distal medial plantar artery (minor)	0.4 ± 0.05	0.8 ± 0.1	4.3 ± 1

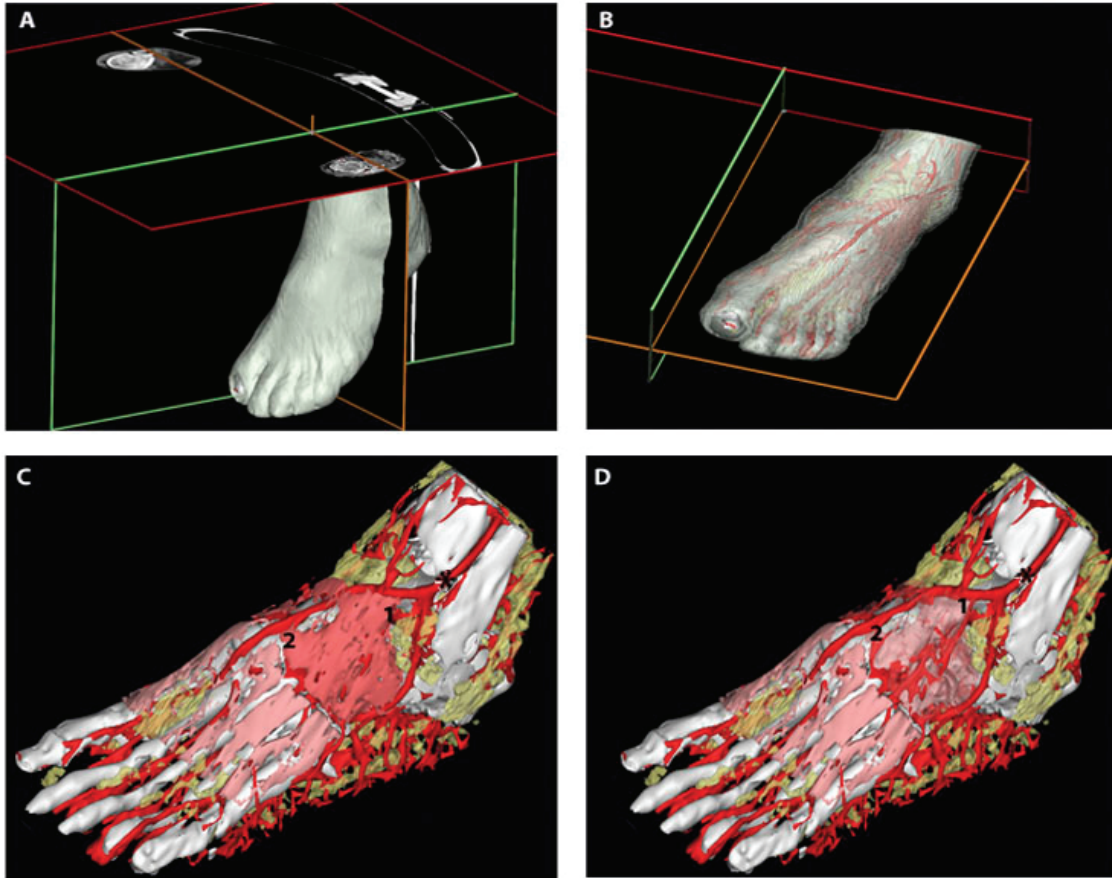


Figure 75: Extensor Digitorum Brevis

A. Three-dimensional rendering of the foot. **B.** Skin of the dorsum of the foot rendered transparent and the dorsalis pedis outlined in red. **C.** Extensor digitorum brevis (EDB) with its vascular pedicles, * is the take off point of dorsalis pedis artery, 1 and 2 are the proximal and distal branches of lateral tarsal artery to EDB. **D.** The muscle rendered transparent to view the intramuscular course of the vascular pedicles.

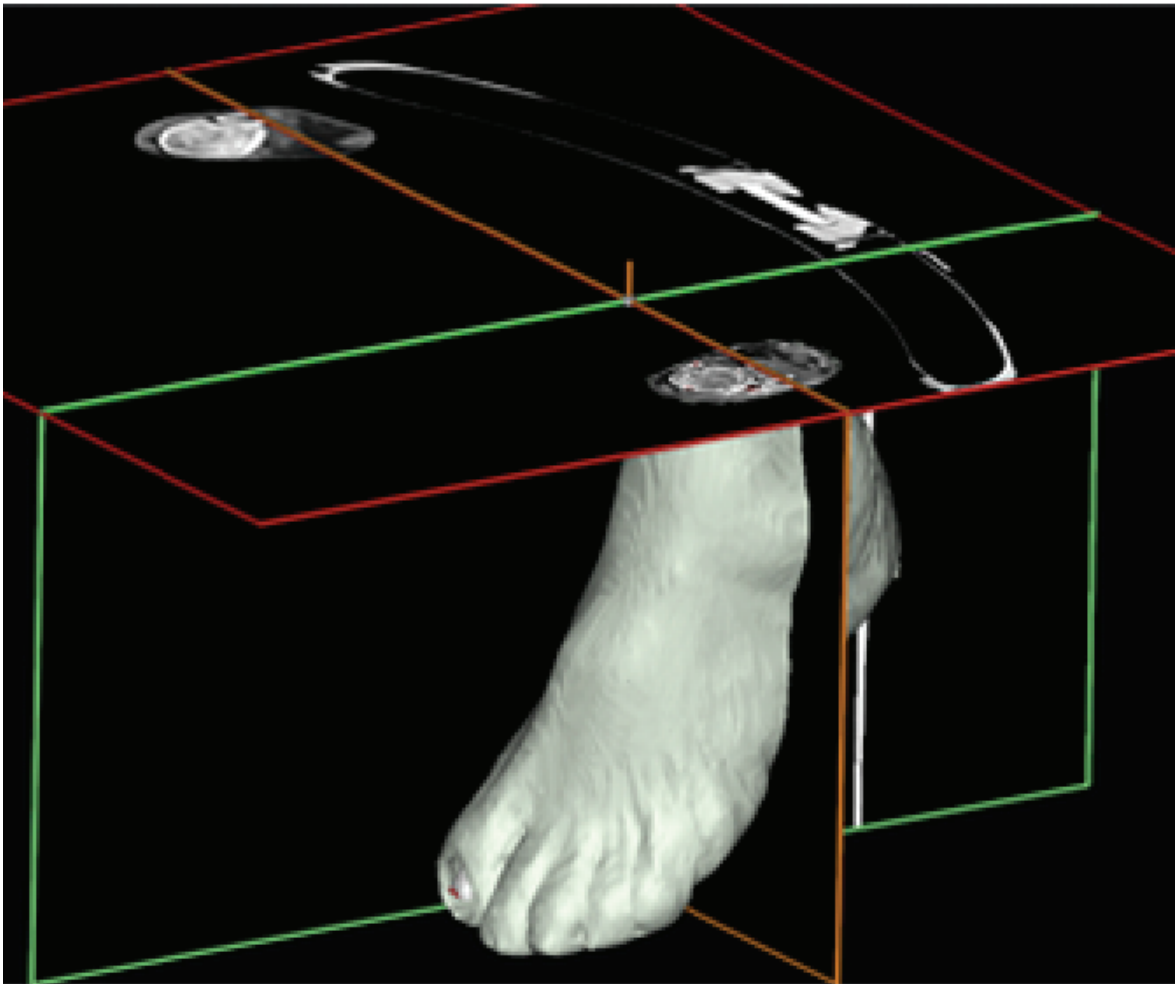


Figure 76: Foot 3D Angiogram

Chapter 5.0 Conclusion

Skeletal muscles are transferred with the intention of soft tissue coverage, as well as providing volume to obliterate dead space, and to provide motor function at the recipient site. The suitability of 20 skeletal muscles for distant free transfer was studied using a novel 3D technique.

In functional transfer knowledge of muscle volume is crucial. For example the use of a free functioning muscle for facial reanimation requires a muscle with a small volume and long neurovascular pedicle. Segmenting muscles for functional transfer has not gained momentum due to shortage of anatomical information regarding muscle volume, lengths and diameters. The application of segmental muscle transfer serves the purpose of preserving donor muscle function, as well as to provide adequate and custom tailored muscle that suits needs of the recipient site.

The total number of pedicles studied using this technique was 2017; the longest pedicle measured was the thoracodorsal artery measuring 12.8 cm as well as the largest diameter at 3.6 mm. The technique provided important details with regards to smaller muscles and vessels, the smallest vascular pedicle in diameter was of the fifth dorsal metatarsal artery at 0.25 mm, and shortest pedicle was from the medial plantar artery distally to the flexor digitorum brevis and measured 3.4 millimeters.

The strengths of our study stems from its educational value, clinical relevance and potential role for refining surgical procedures. In education it is said that a picture is worth a thousand words, we believe that our 3D models bring additional value to the learning process. The fact the anatomical planes can be explored and viewed from virtually any angle, allows for

precise viewing of complex anatomical relationships and fast access to knowledge which in the past could only be learned from anatomical atlases. The difficulty with learning from anatomical atlases is that many diagrams are hand drawn and sometimes fail to reflect the real nature of the anatomy, on the contrast our 3D models are 100% reflection of anatomical findings in cadavers. Our experience with the models created in this project has been very rewarding with the division of plastic surgery at Dalhousie University. During our grand rounds, seminars and research meetings the value of these models was demonstrated to educate residents and medical students in areas of surgical anatomy of flaps, craniofacial, hand and lower extremity procedures. In Figure 77 we show a free bone flap elevated in three dimensions to explain to our residents and students the anatomical basis of such procedure.

The detailed anatomy offered by this technique can also provide explanation to certain adverse outcomes in surgery. For example; in craniofacial surgery and specifically craniosynostosis the separation of the temporalis muscle from the periosteum of the cranium is part of the surgical approach. Craniofacial surgeons always have complained of temporalis atrophy following such procedure despite the protection of the main pedicles feeding the muscle and the protection of the nerve supply. Our three dimensional model have shown clearly the vascular relationship of the bone to the middle temporal artery via the perforating myo-osseus branch of the middle meningeal artery (Figure 48, 49). The striping of the muscle in that area away from the bone damages that communication and could explain the atrophy of temporalis muscle seen with this procedure.

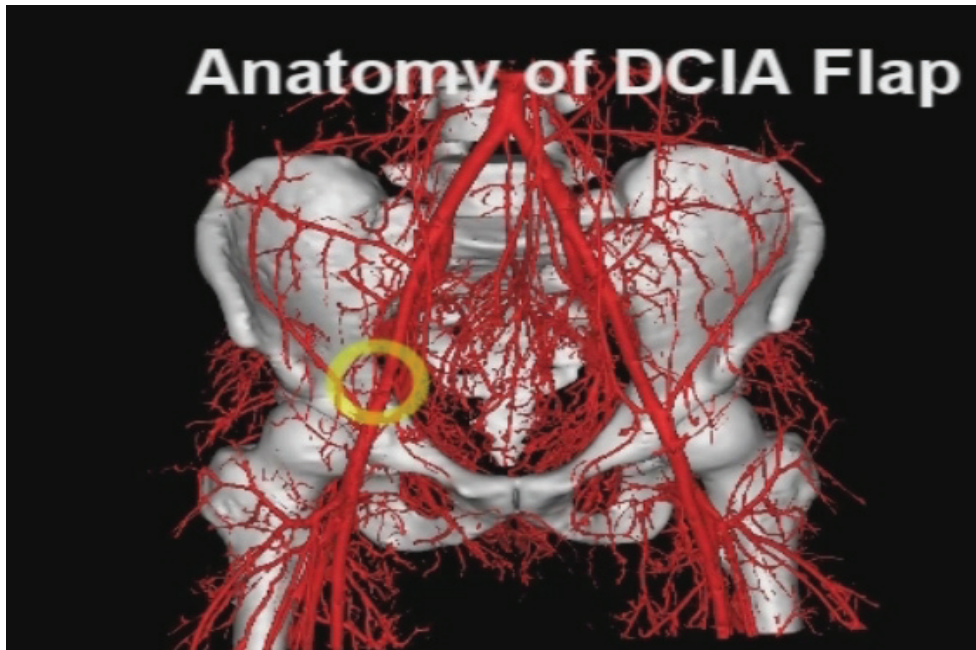


Figure 77: Anatomy of DCIA Bone Flap

DCIA = Deep circumflex iliac artery

The latissimus dorsi muscle can be used as a turnover flap to cover midline defects of the back. The blood supply is based on the thoracolumbar perforators. In our three dimensional studies we clearly demonstrate the dominance of the posterior intercostal perforators over the thoracolumbar perforators (Figure 56, 57). This when taken into consideration can help surgeons design their turnover flap with minimal injury to the medial row of the posterior intercostal perforators.

In hand surgery, thumb replantation is a great procedure and understanding the vascularity of the thenar muscle can help surgeons replant and anastomose the vascular pedicle to the thenar muscle. This is not common practice due to the feeling that these muscles vascular anatomy is not clear and that future opponensplasty procedure can substitute for thenar muscle function. We believe that revascularizing thenar muscles with vascular pedicles $\geq 0.5\text{mm}$ with nowadays advanced microsurgical technique is possible (Table 23), and could have some clinical implications in terms of return of function and strength of the replanted thumb. Currently there are no clinical studies to prove this theoretical claim, but with the data we provide, and with knowledge that the procedure could be executed by hand surgeons, future studies can be preformed to assess whether an impact on thumb function can be seen with repair of thenar muscles.

The weakness of most anatomical studies lies in the sample number, the quality of the vasculature, and the quality of the injection technique. Our study is no exception, our sample number is low, but we believe that this weakness can be improved by extending the principles founded in this project to future projects. The quality of vessels injected is a factor of cadaver

age, the presence of some degree of peripheral vascular disease, and premortal surgical procedures. Our mean age was 70 years old, this entailed a certain level of peripheral vascular disease (PVD) that weakened our anatomical findings despite our stringent criteria of excluding any cadaver exhibiting signs of PVD or having any documented past medical history related to PVD; such as myocardial infarction (MI), arterial ulcers, and strokes.

The injection technique has always been a major concern with most anatomical studies. Mathes and Nahai used barium sulphate which has a great safety profile but produces obscure images of the anatomy compared to the lead oxide technique.^{20,21,92} We also admit that the toxicity of lead oxide makes it a less favorable agent, which can only be used in cadavers. The problem with lead oxide's toxicity necessitates the need for a substitute agent that can produce similar quality angiograms with a higher safety profile.

In conclusion, we present results that show significant potential for transfer of smaller muscles based on smaller diameter and shorter pedicles. This hopefully will help microsurgeons target more muscles in the human body for potential harvest of all available donor muscles.

Bibliography

1. Bunnell, S. *Surgery of the Hand*: JB Lippincott Co, 1948.
2. McKee, N. H., and Kuzon, W. Functioning free muscle transplantation: making it work? What is known? Vol. 23: Lippincott Williams & Wilkins, pp. 249, 1989.
3. Ariyan, S., and Cuono, C. B. Myocutaneous flaps for head and neck reconstruction. *Head Neck Surg.* 2: 321, 1980.
4. Mathes, S. J., and Nahai, F. Classification of the vascular anatomy of muscles: experimental and clinical correlation. *Plast Reconstr Surg.* 67: 177, 1981.
5. Mathes, S. J., Alpert, B. S., and Chang, N. Use of the muscle flap in chronic osteomyelitis: experimental and clinical correlation. *Plast Reconstr Surg.* 69: 815, 1982.
6. Mathes, S. J., and Nahal, F. Vascular anatomy of muscle: Classification and application. In: clinical application for muscles and musculocutaneous flaps. 1st ED. St. Louis: CV Mosby. Pp. 20, 1982.
7. Tobin, G. R. Myocutaneous and muscle flaps: refinements and new applications. *Curr Probl Surg.* 23: 315, 1986.
8. Tobin, G. R., Schusterman, M., Peterson, G. H., Nichols, G., and Bland, K. I. The intramuscular neurovascular anatomy of the latissimus dorsi muscle: the basis for splitting the flap. *Plast Reconstr Surg.* 67: 637, 1981.
9. Zuker, R. M., and Manktelow, R. T. Functioning free muscle transfers. *Hand Clin.* 23: 57, 2007.
10. Manktelow, R. T., and Zuker, R. M. Muscle transplantation by fascicular territory. Vol. 73, pp. 751, 1984.
11. Manktelow, R. T., Zuker, R. M., and McKee, N. H. Functioning free muscle transplantation. *J Hand Surg [Am].* 9A: 32, 1984.
12. Manktelow, R. T., and McKee, N. H. Free muscle transplantation to provide active finger flexion. *J Hand Surg [Am].* 3: 416, 1978.
13. Cormack, G. C., and Lamberty, B. G. H. *The arterial anatomy of skin flaps*: Churchill Livingstone, 1986.
14. Taylor, G. I., and Palmer, J. H. The vascular territories (angiosomes) of the body: experimental study and clinical applications. *Br J Plast Surg.* 40: 113, 1987.

15. Taylor, G. I., Gianoutsos, M. P., and Morris, S. F. The neurovascular territories of the skin and muscles: anatomic study and clinical implications. *Plast Reconstr Surg.* 94: 1, 1994.
16. Shanghai Sixth Peoples Hospital. Free muscle transplantation by microsurgical neurovascular anastomoses. Report of a case. *Chin Med J (Engl).* 2: 47, 1976.
17. Harii, K., Ohmori, K., and Torii, S. Free gracilis muscle transplantation, with microneurovascular anastomoses for the treatment of facial paralysis. A preliminary report. *Plast Reconstr Surg.* 57: 133, 1976.
18. Kubo, T., Ikuta, Y., and Tsuge, K. Free muscle transplantation in dogs by microneurovascular anastomoses. *Plast Reconstr Surg.* 57: 495, 1996.
19. Haschek, E., Linderthal, a., and Ein, O. T. Beitrag zur praktischen Verwerthung der Photographie nach Rontgen. *Wien Klin.* 9, 1896.
20. Bergeron, L., Tang, M., and Morris, S. F. A review of vascular injection techniques for the study of perforator flaps. *Plast Reconstr Surg.* 117: 2050, 2006.
21. Tang, M., Geddes, C. R., Yang, D., and Morris, S. F. Modified lead oxide-gelatin injection technique for vascular studies. *J of Clin Anat.* 1: 73, 2002.
22. Rees, M. J., and Taylor, G. I. A simplified lead oxide cadaver injection technique. *Plast Reconstr Surg.* 77: 141, 1986.
23. Rozen, W. M., Stella, D. L., Ashton, M. W., Phillips, T. J., and Taylor, G. I. Three-dimensional CT angiography: a new technique for imaging microvascular anatomy. *Clin Anat.* 20: 1001, 2007.
24. Taylor, G. I. Invited discussion: "New approach to vascular injection in fresh cadaver dissection" (*J Reconstr Microsurg* 2004;20:311-315). *J Reconstr Microsurg.* 20: 457, 2004.
25. Zhang, Y. Z., Li, Y. B., Tang, M. L., Xie, L., Geddes, C. R., Zhong, S. Z., and Pei, G. X. Application of three-dimensional digitalized reconstruction of an anterolateral thigh flap and an arterial dorsalis pedis flap. *Microsurgery.* 27: 553, 2007.
26. Tregaskiss, A. P., Goodwin, A. N., Bright, L. D., Ziegler, C. H., and Acland, R. D. Three-dimensional CT angiography: a new technique for imaging microvascular anatomy. *Clin Anat.* 20: 116, 2007.
27. Rikimaru, H., Kiyokawa, K., Inoue, Y., and Tai, Y. Three-dimensional anatomical vascular distribution in the pectoralis major myocutaneous flap. *Plast Reconstr Surg.* 115: 1342, 2005.
28. Beer, G. M., and Manestar, M. Three-dimensional anatomical vascular distribution in the pectoralis major myocutaneous flap. *Plast Reconstr Surg.* 118: 280, 2006.

29. Tregaskiss, A. P., Goodwin, A. N., and Acland, R. D. The cutaneous arteries of the anterior abdominal wall: a three-dimensional study. *Plast Reconstr Surg.* 120: 442, 2007.
30. Schaverien, M., Saint-Cyr, M., Arbique, G., Hatef, D., Brown, S. A., and Rohrich, R. J. Three- and four-dimensional computed tomographic angiography and venography of the anterolateral thigh perforator flap. *Plast Reconstr Surg.* 121: 1685, 2008.
31. Saint-Cyr, M., Schaverien, M., Arbique, G., Hatef, D., Brown, S. A., and Rohrich, R. J. Three- and four-dimensional computed tomographic angiography and venography for the investigation of the vascular anatomy and perfusion of perforator flaps. *Plast Reconstr Surg.* 121: 772, 2008.
32. Schaverien, M., Saint-Cyr, M., Arbique, G., Brown, S. A., and Rohrich, R. J. Three- and four-dimensional arterial and venous anatomies of the thoracodorsal artery perforator flap. *Plast Reconstr Surg.* 121: 1578, 2008.
33. Grabherr, S., Djonov, V., Yen, K., Thali, M. J., and Dirnhofer, R. Postmortem angiography: review of former and current methods. *AJR Am J Roentgenol.* 188: 832, 2007.
34. Mathes, S. J., and Nahai, F. *Reconstructive surgery: principles, anatomy & technique*: New York: Churchill Livingstone; St. Louis: Quality Medical Pub., 1997.
35. Houseman, N. D., Taylor, G. I., and Pan, W. R. The angiosomes of the head and neck: anatomic study and clinical applications. *Plast Reconstr Surg.* 105: 2287, 2000.
36. Cheung, L. K. The vascular anatomy of the human temporalis muscle: implications for surgical splitting techniques. *Int J Oral Maxillofac Surg.* 25: 414, 1996.
37. Kawai, K., Imanishi, N., Nakajima, H., Aiso, S., Kakibuchi, M., and Hosokawa, K. Arterial anatomical features of the upper palpebra. *Plast Reconstr Surg.* 113: 479, 2004.
38. Pinar, Y. A., and Govsa, F. Anatomy of the superficial temporal artery and its branches: its importance for surgery. *Surg Radiol Anat.* 28: 248, 2006.
39. Marinho, L. H., Shanahan, D. A., Langdon, J. D., and Sinnatamby, C. S. The inferiorly based masseter muscle flap: anatomical basis for its use in head and neck reconstructive surgery. *Int J Oral Maxillofac Surg.* 20: 100, 1991.
40. Lopez, R., Lauwers, F., Paoli, J. R., Boutault, F., and Guitard, J. Vascular territories of the tongue: anatomical study and clinical applications. *Surg Radiol Anat.* 29: 239, 2007.
41. Shangkuan, H., Xinghai, W., Zengxing, W., Shizhen, Z., Shiyang, J., and Yishi, C. *Anatomic bases of tongue flaps*. Vol. 20: Springer, pp. 83, 1998.
42. Aszmann, O. C., Ebmer, J. M., and Dellon, A. L. The anatomic basis for the innervated mylohyoid/digastric flap in facial reanimation. *Plast Reconstr Surg.* 102: 369, 1998.

43. Aktekin, M., Kurtoglu, Z., and Ozturk, A. H. A bilateral and symmetrical variation of the anterior belly of the digastric muscle. *Acta Med Okayama*. 57: 205, 2003.
44. Alagoz, M. S., Uysal, A. C., Tuccar, E., and Sensoz, O. The vascular anatomy of the digastric muscle. *J Craniofac Surg*. 15: 114, 2004.
45. Karcher, H., Radner, H., and Anderhuber, F. [The pedicled transposition of the digastric and stylohyoid muscles in the treatment of velopharyngeal incompetence. Anatomic basis and clinical application]. *Acta Anat (Basel)*. 144: 145, 1992.
46. Magden, O., Edizer, M., Tayfur, V., and Atabey, A. Anatomic study of the vasculature of the submental artery flap. *Plast Reconstr Surg*. 114: 1719, 2004.
47. Yilmaz, M., Menderes, A., and Barutcu, A. Submental artery island flap for reconstruction of the lower and mid face. *Ann Plast Surg*. 39: 30, 1997.
48. Hongshi Wang, J. S. D. M. J. W. A. T. The infrahyoid myocutaneous flap for reconstruction after resection of head and neck cancer. Vol. 57, pp. 663, 1986.
49. Su, T., Zhao, Y. F., Liu, B., Hu, Y. P., and Zhang, W. F. Clinical review of three types of platysma myocutaneous flap. *Int J Oral Maxillofac Surg*. 35: 1011, 2006.
50. Imanishi, N., Nakajima, H., Kishi, K., Chang, H., and Aiso, S. Is the platysma flap musculocutaneous? Angiographic study of the platysma. *Plast Reconstr Surg*. 115: 1018, 2005.
51. Uehara, M., Helman, J. I., Lillie, J. H., and Brooks, S. L. Blood supply to the platysma muscle flap: an anatomic study with clinical correlation. *J Oral Maxillofac Surg*. 59: 642, 2001.
52. Hu, K. S., Song, W. C., Kim, S. H., Choi, S. W., Han, S. H., Paik, D. J., Kim, H. J., and Koh, K. S. Branching patterns of the arterial branches supplying the middle vascular pedicle of the sternocleidomastoid muscle: a topographic anatomical study with surgical applications for the use of pedicles osteomuscular flaps. *Surg Radiol Anat*. 28: 7, 2006.
53. Alagoz, M. S., Cagri Uysal, A., Tuccar, E., and Sensoz, O. How cranial could the sternocleidomastoid muscle be split? *J Craniofac Surg*. 16: 201, 2005.
54. Ariyan, S. Further experience with the sternocleidomastoid myocutaneous flap. *Plast Reconstr Surg*. 111: 381, 2003.
55. Yang, C., Cui, L., Wang, W., and Liu, Q. [Transposition of pedicled sternocleidomastoid muscle for repair of facial paralysis in late stage]. *Zhongguo Xiu Fu Chong Jian Wai Ke Za Zhi*. 16: 48, 2002.

56. Zhao, Y. F., Zhang, W. F., and Zhao, J. H. Reconstruction of intraoral defects after cancer surgery using cervical pedicle flaps. *J Oral Maxillofac Surg.* 59: 1142, 2001.
57. Losken, A., Rozycki, G. S., and Feliciano, D. V. The use of the sternocleidomastoid muscle flap in combined injuries to the esophagus and carotid artery or trachea. *J Trauma.* 49: 815, 2000.
58. Strek, P., Olszewski, E., Modrzejewski, M., Skawina, A., Skladzien, J., and Zawilinski, J. [Changes in vascularization of sternocleidomastoid myocutaneous flaps]. *Otolaryngol Pol.* 51: 176, 1997.
59. Yugueros, P., and Woods, J. E. The sternocleidomastoid myocutaneous flap: a reappraisal. *Br J Plast Surg.* 49: 93, 1996.
60. Rojananin, S., Igarashi, T., Ratanavichitrasin, A., Lertakayamane, N., and Ruksamane, A. Experimental study of the facial artery: relevance to its reverse flow competence and cutaneous blood supply of the neck for clinical use as a new flap. *Head Neck.* 18: 17, 1996.
61. Dogliotti, P. L., and Bennun, R. D. Occipitoparietal bone flap for mandibular reconstruction. *J Craniofac Surg.* 6: 249, 1995.
62. Cadenat, H., Combelles, R., Clouet, M., and Fabert, G. [Cervical and cervicodorsal flaps. Vascularisation. Surgical applications (author's transl)]. *Rev Stomatol Chir Maxillofac.* 79: 227, 1978.
63. Jabaley, M. E., Heckler, F. R., Wallace, W. H., and Knott, L. H. Sternocleidomastoid regional flaps: a new look at an old concept. *Br J Plast Surg.* 32: 106, 1979.
64. Marx, R. E., and McDonald, D. K. The sternocleidomastoid muscle as a muscular or myocutaneous flap for oral and facial reconstruction. *J Oral Maxillofac Surg.* 43: 155, 1985.
65. Rabson, J. A., Hurwitz, D. J., and Futrell, J. W. The cutaneous blood supply of the neck: relevance to incision planning and surgical reconstruction. *Br J Plast Surg.* 38: 208, 1985.
66. Hurwitz, D. J., Rabson, J. A., and Futrell, J. W. The anatomic basis for the platysma skin flap. *Plast Reconstr Surg.* 72: 302, 1983.
67. Eliachar, I., and Moscona, A. R. Reconstruction of the laryngotracheal complex in children using the sternocleidomastoid myocutaneous flap. *Head Neck Surg.* 4: 16, 1981.
68. Ariyan, S. The sternocleidomastoid myocutaneous flap. *Laryngoscope.* 90: 676, 1980.
69. Ariyan, S. Further experiences with the sternocleidomastoid myocutaneous flap: a clinical appraisal of 31 cases. *Plast Reconstr Surg.* 99: 61, 1997.

70. Kierner, A. C., Aigner, M., Zelenka, I., Riedl, G., and Burian, M. The blood supply of the sternocleidomastoid muscle and its clinical implications. *Arch Surg.* 134: 144, 1999.
71. Kierner, A. C., Zelenka, I., and Gstoettner, W. The sternocleidomastoid flap--its indications and limitations. *Laryngoscope.* 111: 2201, 2001.
72. Ariyan, S. The pectoralis major myocutaneous flap. A versatile flap for reconstruction in the head and neck. *Plast Reconstr Surg.* 63: 73, 1979.
73. Ariyan, S. Further experiences with the pectoralis major myocutaneous flap for the immediate repair of defects from excisions of head and neck cancers. *Plast Reconstr Surg.* 64: 605, 1979.
74. Palmer, J. H., and Taylor, G. I. The vascular territories of the anterior chest wall. *Br J Plast Surg.* 39: 287, 1986.
75. MacQuillan, A., Horlock, N., Grobbelaar, A., and Harrison, D. Arterial and venous anatomical features of the pectoralis minor muscle flap pedicle. *Plast Reconstr Surg.* 113: 872, 2004.
76. Cuadros, C. L., Driscoll, C. L., and Rothkopf, D. M. The anatomy of the lower serratus anterior muscle: a fresh cadaver study. *Plast Reconstr Surg.* 95: 93, 1995.
77. Percival, N. J., and Earley, M. J. Anomalous blood supply to the serratus anterior/rib composite flap. *Br J Plast Surg.* 42: 98, 1989.
78. Boustred, M. The Rectus Abdominis Flap for Closure of Difficult Perineal Wounds. *Operative Techniques in General Surgery.* 8: 216, 2006.
79. Schlenz, I., Burggasser, G., Kuzbari, R., Eichberger, H., Gruber, H., and Holle, J. External oblique abdominal muscle: a new look on its blood supply and innervation. *Anat Rec.* 255: 388, 1999.
80. Kuzbari, R., Worsseg, A., Burggasser, G., Schlenz, I., Kuderna, C., Vinzenz, K., Gruber, H., and Holle, J. The external oblique muscle free flap. *Plast Reconstr Surg.* 99: 1338, 1997.
81. Urken, M. L., Weinberg, H., Vickery, C., Buchbinder, D., Lawson, W., and Biller, H. F. The internal oblique-iliac crest free flap in composite defects of the oral cavity involving bone, skin, and mucosa. *Laryngoscope.* 101: 257, 1991.
82. Urken, M. L., Vickery, C., Weinberg, H., Buchbinder, D., Lawson, W., and Biller, H. F. The internal oblique-iliac crest osseomyocutaneous free flap in oromandibular reconstruction. Report of 20 cases. *Arch Otolaryngol Head Neck Surg.* 115: 339, 1989.

83. Konerding, M. A., Gaumann, A., Shumsky, A., Schlenger, K., and Hockel, M. The vascular anatomy of the inner anterior abdominal wall with special reference to the transversus and rectus abdominis musculoperitoneal (TRAMP) composite flap for vaginal reconstruction. *Plast Reconstr Surg.* 99: 705, 1997.
84. Chen, R. S., Liu, Y. X., Liu, C. B., Hu, Y. S., Xu, D. C., Zhong, S. Z., and Li, Z. H. Anatomic basis of iliac crest flap pedicled on the iliolumbar artery. *Surg Radiol Anat.* 21: 103, 1999.
85. Rowsell, A. R., Davies, D. M., Eisenberg, N., and Taylor, G. I. The anatomy of the subscapular-thoracodorsal arterial system: study of 100 cadaver dissections. *Br J Plast Surg.* 37: 574, 1984.
86. Taylor, G. I., Corlett, R. J., Caddy, C. M., and Zelt, R. G. An anatomic review of the delay phenomenon: II. Clinical applications. *Plast Reconstr Surg.* 89: 408, 1992.
87. Feneis, H., and Dauber, W. Pocket atlas of human anatomy: based on the international nomenclature: Georg Thieme Verlag, 2000.
88. Huelke, D. The dorsal scapular artery—a proposed term for the artery to the rhomboid muscles. *The Anatomical Record.* 142: 57, 1962.
89. Huelke, D. F. A study of the transverse cervical and dorsal scapular arteries. *The Anatomical Record.* 132: 233, 1958.
90. Mathes, S. J., and Nahai, F. Clinical Atlas of Muscle and Musculocutaneous Flaps. St. Louis, C.V.: Mosby, 1979.
91. Mathes, S., and Nahai, F. General principles. Reconstructive surgery: Principles, anatomy & technique. New York: Quality Medical Publishing and Churchill Livingstone, 1997.
92. Mathes, S., and Nahai, F. Clinical atlas of muscle and musculocutaneous flaps. *St Louis, CV Mosby.* 291, 1979.
93. Hallock, G. G. The hemideltoid muscle flap. *Ann Plast Surg.* 44: 18, 2000.
94. Hong, T. C., Kumar, V. P., and Nather, A. The posterior neuromuscular compartment of the deltoid. *Plast Reconstr Surg.* 115: 1660, 2005.
95. Hue, E., Gagey, O., Mestdagh, H., Fontaine, C., Drizenko, A., and Maynou, C. The blood supply of the deltoid muscle. Application to the deltoid flap technique. *Surg Radiol Anat.* 20: 161, 1998.
96. Russell, R. C., Guy, R. J., Zook, E. G., and Merrell, J. C. Extremity reconstruction using the free deltoid flap. *Plast Reconstr Surg.* 76: 586, 1985.

97. Godfrey, P. M., Godfrey, N. V., Romita, M. C., and Guthrie, R. H. The teres major muscle flap in breast reconstruction. *Ann Plast Surg.* 25: 402, 1990.
98. Giessler, G. A., Doll, S., and Germann, G. Macroscopic and microangiographic anatomy of the teres major muscle: a new free functional muscle flap? *Plast Reconstr Surg.* 119: 941, 2007.
99. Taylor, G. I., and Razaboni, R. Salmon's arteries of the muscles of the extremities and the trunk, and the arterial anastomotic pathways of the extremities. *St Louis:Quality medical publishers.:* 51, 1994.
100. Har-Shai, Y., Kaufman, T., Hashmonai, M., Hirshowitz, B., and Schramek, A. External longitudinal splitting of the biceps brachii muscle for coverage of repaired brachial vessels: an anatomical study and clinical application. *Ann Plast Surg.* 21: 158, 1988.
101. Hentz, V. R., Pearl, R. M., and Kaplan, E. N. Use of the medial upper arm skin as an arterialised flap. *Hand.* 12: 241, 1980.
102. Kaplan, E. N., and Pearl, R. M. An arterial medial arm flap--vascular anatomy and clinical applications. *Ann Plast Surg.* 4: 205, 1980.
103. Taylor, G. I., Cichowitz, A., Ang, S. G., Seneviratne, S., and Ashton, M. Comparative anatomical study of the gracilis and coracobrachialis muscles: implications for facial reanimation. *Plast Reconstr Surg.* 112: 20, 2003.
104. Salmon, M. Arteries of the Muscles of the extremities and Trunk. Book 1, 1994.
105. Parry, S. W., Ward, J. W., and Mathes, S. J. Vascular anatomy of the upper extremity muscles. *Plast Reconstr Surg.* 81: 358, 1988.
106. Sanger, J. R., Ye, Z., Yousif, N. J., and Matloub, H. S. The brachioradialis forearm flap: anatomy and clinical application. *Plast Reconstr Surg.* 94: 667, 1994.
107. Leversedge, F. J., Casey, P. J., Payne, S. H., and Seiler, J. G. Vascular anatomy of the brachioradialis rotational musculocutaneous flap. *The Journal of Hand Surgery.* 26: 711, 2001.
108. Schmidt, C. C., Kohut, G. N., Greenberg, J. A., Kann, S. E., Idler, R. S., and Kiefhaber, T. R. The anconeus muscle flap: its anatomy and clinical application. *J Hand Surg [Am].* 24: 359, 1999.
109. Uysal, A. Ç., ri, Alagöz, M. S., Tüccar, E., Sensöz, Ö., and Tekdemir, I. The vascular anatomy of the abductor digiti minimi and the flexor digiti minimi brevis muscles. *The Journal of Hand Surgery.* 30: 172, 2005.

110. Gregory, H., Heitmann, C., and Germann, G. The evolution and refinements of the distally based dorsal metacarpal artery (DMCA) flaps. *J Plast Reconstr Aesthet Surg.* 60: 731, 2007.
111. Uysal, A. C., Alagoz, M. S., Tuccar, E., and Sensoz, O. Vascular anatomy of the metacarpal bones and the interosseous muscles. *Ann Plast Surg.* 51: 63, 2003.
112. Bertelli, J. A., Pagliei, A., and Lassau, J. P. Role of the first dorsal metacarpal artery in the construction of pedicled bone grafts (27.3.92). *Surg Radiol Anat.* 14: 275, 1992.
113. Olave, E., Prates, J. C., Gabrielli, C., and Mandiola, E. Perforating branches: important contribution to the formation of the dorsal metacarpal arteries. *Scand J Plast Reconstr Surg Hand Surg.* 32: 221, 1998.
114. Earley, M. J. The second dorsal metacarpal artery neurovascular island flap. *J Hand Surg [Br].* 14: 434, 1989.
115. Weinzweig, N., Starker, I., Sharzer, L. A., and Fleegler, E. J. Revisitation of the vascular anatomy of the lumbrical and interosseous muscles. *Plast Reconstr Surg.* 99: 785, 1997.
116. Yang, D., and Morris, S. F. Reversed dorsal digital and metacarpal island flaps supplied by the dorsal cutaneous branches of the palmar digital artery. *Ann Plast Surg.* 46: 444, 2001.
117. Earley, M. J. The arterial supply of the thumb, first web and index finger and its surgical application. *J Hand Surg [Br].* 11: 163, 1986.
118. Song, W. C., Bae, S. M., Han, S. H., and Koh, K. S. Anatomical and radiological study of the superior and inferior gluteal arteries in the gluteus maximus muscle for musculocutaneous flap in Koreans. *J Plast Reconstr Aesthet Surg.* 59: 935, 2006.
119. Ramirez, O. M. Blood supply to the gluteus maximus flap. *Plast Reconstr Surg.* 105: 812, 2000.
120. Minami, R. T., Mills, R., and Pardoe, R. Gluteus maximus myocutaneous flaps for repair of pressure sores. *Plast Reconstr Surg.* 60: 242, 1977.
121. Perez-Gurri, J. A., Temple, W. J., and Ketcham, A. S. Gluteus maximus myocutaneous flap for the treatment of recalcitrant pilonidal disease. *Dis Colon Rectum.* 27: 262, 1984.
122. Ramirez, O. M., Orlando, J. C., and Hurwitz, D. J. The sliding gluteus maximus myocutaneous flap: its relevance in ambulatory patients. *Plast Reconstr Surg.* 74: 68, 1984.
123. Schefflan, M., Nahai, F., and Bostwick, J., 3rd. Gluteus maximus island musculocutaneous flap for closure of sacral and ischial ulcers. *Plast Reconstr Surg.* 68: 533, 1981.
124. Yang, D., and Morris, S. F. Neurovascular anatomy of the rectus femoris muscle related to functioning muscle transfer. *Plast Reconstr Surg.* 104: 102, 1999.

125. Lin, C. H., Wei, F. C., Lin, Y. T., Yeh, J. T., Rodriguez Ede, J., and Chen, C. T. Lateral circumflex femoral artery system: warehouse for functional composite free-tissue reconstruction of the lower leg. *J Trauma*. 60: 1032, 2006.
126. Mathes, S., and Nahai, F. Clinical applications for muscle, musculocutaneous flaps. St. Louis: CV Mosby, 1982.
127. Yousif, N. J., Matloub, H. S., Kolachalam, R., Grunert, B. K., and Sanger, J. R. The transverse gracilis musculocutaneous flap. *Ann Plast Surg*. 29: 482, 1992.
128. Reddy, V. R., Stevenson, T. R., and Whetzel, T. P. 10-year experience with the gracilis myofasciocutaneous flap. *Plast Reconstr Surg*. 117: 635, 2006.
129. Lasso, J. M., Rosado, J., Perez Luengo, E., Jimenez, E., and Perez Cano, R. Gracilis flap: a variation of the main vascular pedicle. *Plast Reconstr Surg*. 114: 597, 2004.
130. Hayashi, A., and Maruyama, Y. Lateral intermuscular septum of the thigh and short head of the biceps femoris muscle: an anatomic investigation with new clinical applications. *Plast Reconstr Surg*. 108: 1646, 2001.
131. Hayashi, A., and Maruyama, Y. The lateral genicular artery flap. *Ann Plast Surg*. 24: 310, 1990.
132. Cavadas, P. C., Sanz-Jimenez-Rico, J. R., Landin, L., and Correa, J. Biceps femoris perforator free flap for upper extremity reconstruction: anatomical study and clinical series. *Plast Reconstr Surg*. 116: 145, 2005.
133. Mairesse, J. L., Mestdagh, H., Bailleul, J. P., Letendart, J., and Dabrowski, A. [The arterial blood supply of the skin flap of the dorsal foot]. *Acta Anat (Basel)*. 115: 296, 1983.
134. Baltensperger, M. M., Ganzoni, N., Jirecek, V., and Meyer, V. E. The extensor digitorum brevis island flap: possible applications based on anatomy. *Plast Reconstr Surg*. 101: 107, 1998.
135. Pai, C. H., Lin, G. T., Lin, S. Y., Lin, S. D., and Lai, C. S. Extensor digitorum brevis rotational muscle flap for lower leg and ankle coverage. *J Trauma*. 49: 1012, 2000.
136. Skef, Z., Ecker, H. A., Jr., and Graham, W. P., 3rd. Heel coverage by a plantar myocutaneous island pedicle flap. *J Trauma*. 23: 466, 1983.
137. Ikuta, Y., Murakami, T., Yoshioka, K., and Tsuge, K. Reconstruction of the heel pad by flexor digitorum brevis musculocutaneous flap transfer. *Plast Reconstr Surg*. 74: 86, 1984.
138. Sakai, N., Yoshida, T., and Okumura, H. Distal plantar area reconstruction using a flexor digitorum brevis muscle flap with reverse-flow lateral plantar artery. *Br J Plast Surg*. 54: 170, 2001.

139. Attinger, C. E., Ducic, I., Cooper, P., and Zelen, C. M. The role of intrinsic muscle flaps of the foot for bone coverage in foot and ankle defects in diabetic and nondiabetic patients. *Plast Reconstr Surg.* 110: 1047, 2002.
140. Al-Qattan, M. M. Harvesting the abductor digiti minimi as a muscle plug with the lateral calcaneal artery skin flap. *Ann Plast Surg.* 46: 651, 2001.
141. Yoshimura, Y., Nakajima, T., and Kami, T. Distally based abductor digiti minimi muscle flap. *Ann Plast Surg.* 14: 375, 1985.
142. Schwabegger, A. H., Shafiqhi, M., and Gurunluoglu, R. Versatility of the abductor hallucis muscle as a conjoined or distally-based flap. *J Trauma.* 59: 1007, 2005.
143. Macchi, V., Tiengo, C., Porzionato, A., Stecco, C., Parenti, A., Mazzoleni, F., Ger, R., and De Caro, R. Correlation between the course of the medial plantar artery and the morphology of the abductor hallucis muscle. *Clin Anat.* 18: 580, 2005.
144. Ortak, T., Ozdemir, R., Ulusoy, M. G., Tiftikcioglu, Y. O., Karaaslan, O., Kocer, U., and Sensoz, O. Reconstruction of heel defects with a proximally based abductor hallucis muscle flap. *J Foot Ankle Surg.* 44: 265, 2005.
145. Schwabegger, A. H., Shafiqhi, M., Harpf, C., Gardetto, A., and Gurunluoglu, R. Distally based abductor hallucis muscle flap: anatomic basis and clinical application. *Ann Plast Surg.* 51: 505, 2003.
146. Karacalar, A. A pedicle-lengthening technique for abductor hallucis muscle flap. *Plast Reconstr Surg.* 105: 2275, 2000.
147. Zhang, G. M., Syed, S. A., and Tsai, T. M. Anatomic study of a new axial skin flap based on the cutaneous branch of the medial plantar artery. *Microsurgery.* 16: 144, 1995.
148. Xu, S. T., and Shi, S. S. [Repair of a skin defect of the heel with abductor hallucis and flexor digitorum brevis myocutaneous flap]. *Zhonghua Zheng Xing Shao Shang Wai Ke Za Zhi.* 2: 192, 1986.
149. Orbay, H., Kerem, M., Unlu, R. E., Esmer, A. F., Comert, A., Tuccar, E., and Sensoz, O. Vascular anatomy of plantar muscles. *Ann Plast Surg.* 58: 420, 2007.
150. Reiffel, R. S., and McCarthy, J. G. Coverage of heel and sole defects: a new subfascial arterialized flap. *Plast Reconstr Surg.* 66: 250, 1980.
151. Kalin, P. J., and Hirsch, B. E. The origins and function of the interosseous muscles of the foot. *J Anat.* 152: 83, 1987.
152. Gabrielli, C., Olave, E., Mandiola, E., Rodrigues, C. F., and Prates, J. C. The deep plantar arch in humans: constitution and topography. *Surg Radiol Anat.* 23: 253, 2001.

153. Mehmet Asim Ozer, F. G. O. B. Anatomic study of the deep plantar arch. Vol. 18, pp. 434, 2005.
154. Taylor, G. I. The angiosomes of the body and their supply to perforator flaps. *Clin Plast Surg.* 30: 331, 2003.
155. Taylor, G. I., and Pan, W. R. Angiosomes of the leg: anatomic study and clinical implications. *Plast Reconstr Surg.* 102: 599, 1998.
156. R.A. Derbin. Volume rendering. *Computer Graphics, Proc. SIGGRAPH.* 22: 65, 1988.
157. Krüger, J., and Westermann, R. Acceleration Techniques for GPU-based Volume Rendering. 14th IEEE Visualization, pp. 287, 2003.
158. Mavili, M. E., Canter, H. I., Saglam-Aydinatay, B., Kamaci, S., and Kocadereli, I. Use of Three-Dimensional Medical Modeling Methods for Precise Planning of Orthognathic Surgery. *J Craniofac Surg.* 18: 740, 2007.
159. Liu, Y., Gong, Z., He, L., Zhao, J., Yu, B., and Zhang, H. [Individual digital design and functional reconstruction of large mandibular defect with computer-aided design/computer aided manufacture technique]. *Zhongguo Xiu Fu Chong Jian Wai Ke Za Zhi.* 19: 803, 2005.
160. Ding, H. M., Yin, Z. X., Zhou, X. B., Li, Y. B., Tang, M. L., Chen, S. H., Xu, D. C., and Zhong, S. Z. Three-dimensional visualization of pelvic vascularity. *Surg Radiol Anat.* 30: 437, 2008.
161. Tregaskiss, A. P., Goodwin, A. N., and Acland, R. D. The Cutaneous Arteries of the Anterior Abdominal Wall: A Three-Dimensional Study. Vol. 120: WILLIAMS & WILKINS, pp. 442, 2007.
162. Gelaude, F., Vander Sloten, J., and Lauwers, B. Accuracy assessment of CT-based outer surface femur meshes. *Computer Aided Surgery.* 13: 188, 2008.
163. Gelaude, F., Vander Sloten, J., and Lauwers, B. Semi-automated segmentation and visualisation of outer bone cortex from medical images. *Computer Methods in Biomechanics and Biomedical Engineering.* 9: 65, 2006.
164. Adam, F., Hammer, D., Pape, D., and Kohn, D. Femoral anatomy, computed tomography and computer-aided design of prosthetic implants. *Archives of orthopaedic and trauma surgery.* 122: 262, 2002.
165. Wurm, G., Tomancok, B., Pogady, P., Holl, K., and Trenkler, J. Cerebrovascular stereolithographic biomodeling for aneurysm surgery. *Journal of neurosurgery.* 100: 139, 2004.

166. Salmon, M., and Dor, J. Les artères des muscles des membres et du tronc. Paris: Masson, 1933.
167. Brooks, B. Intra-arterial injection of sodium iodide. *JAMA*. 82: 1016, 1924.
168. Krasuski, R. A., Sketch Jr, M. H., and Harrison, J. K. Contrast Agents for Cardiac Angiography: Osmolality and Contrast Complications. *Curr Interv Cardiol Rep*. 2: 258, 2000.
169. Cademartiri, F., Mollet, N. R., van der Lugt, A., McFadden, E. P., Stijnen, T., de Feyter, P. J., and Krestin, G. P. Intravenous Contrast Material Administration at Helical 16–Detector Row CT Coronary Angiography: Effect of Iodine Concentration on Vascular Attenuation. *Radiology*. 236: 661, 2005.
170. Schoellnast, H., Deutschmann, H. A., Fritz, G. A., Stessel, U., Schaffler, G. J., and Tillich, M. MDCT angiography of the pulmonary arteries: influence of iodine flow concentration on vessel attenuation and visualization. *American Journal of Roentgenology*. 184: 1935, 2005.
171. Hinman, F., Morison, D. M., and Lee-Brown, R. K. Methods of demonstrating the circulation in general. *JAMA*. 81: 177, 1923.
172. Burggasser, G., Happak, W., Gruber, H., and Freilinger, G. The temporalis: blood supply and innervation. *Plast Reconstr Surg*. 109: 1862, 2002.
173. Cormack, G. C., and Lamberty, B. G. Cadaver studies of correlation between vessel size and anatomical territory of cutaneous supply. *Br J Plast Surg*. 39: 300, 1986.
174. Quinodoz, P., Quinodoz, M., Nussbaum, J. L., Montandon, D., and Pittet, B. Barium sulphate and soft-tissue radiology: allying the old and the new for the investigation of animal cutaneous microcirculation. *Br J Plast Surg*. 55: 664, 2002.
175. Mathes, S. J., and Alpert, B. S. Advances in muscle and musculocutaneous flaps. *Clin Plast Surg*. 7: 15, 1980.
176. Kerwin, W., Hooker, A., Spilker, M., Vicini, P., Ferguson, M., Hatsukami, T., and Yuan, C. Quantitative magnetic resonance imaging analysis of neovasculature volume in carotid atherosclerotic plaque. *Circulation*. 107: 851, 2003.
177. Gilfeather, M., Holland, G. A., Siegelman, E. S., Schnall, M. D., Axel, L., Carpenter, J. P., and Golden, M. A. Gadolinium-enhanced ultrafast three-dimensional spoiled gradient-echo MR imaging of the abdominal aorta and visceral and iliac vessels. *Radiographics*. 17: 423, 1997.

178. Anderson, V. C., Berryhill, P. C., Sandquist, M. A., Ciaverella, D. P., Nesbit, G. M., and Burchiel, K. J. High-resolution three-dimensional magnetic resonance angiography and three-dimensional spoiled gradient-recalled imaging in the evaluation of neurovascular compression in patients with trigeminal neuralgia: a double-blind pilot study. *Neurosurgery*. 58: 666, 2006.
179. Bruening, R., Kuettner, A., and Flohr, T. Protocols for Multislice CT. Vol. 179: Springer Verlag, 2006.
180. Alberico, R. A., Loud, P., Pollina, J., Greco, W., Patel, M., and Klufas, R. Thick-Section Reformatting of Thinly Collimated Helical CT for Reduction of Skull Base-Related Artifacts. *American Journal of Roentgenology*. 175: 1361, 2000.
181. Barrett, J. F., and Keat, N. Artifacts in CT: Recognition and Avoidance¹. *Radiographics*. 24: 1679, 2004.
182. Anderson, L. M., and Gibbons, G. H. Notch: a mastermind of vascular morphogenesis. *J Clin Invest*. 117: 299, 2007.
183. Yalovine, S. Procédé de cloture plastique de l'orbit après l'extenteration. *Arch d'Ophthalmol*. 18: 679, 1989.
184. Pereira, M. D., Marques, A. F., Brenda, E., and de Castro, M. Immediate reconstruction of the central segment of the mandible using the masseter osteomuscular flap. *Plast Reconstr Surg*. 99: 1749, 1997.
185. Baek, S. M., Biller, H. F., Krespi, Y. P., and Lawson, W. The lower trapezius island myocutaneous flap. *Ann Plast Surg*. 5: 108, 1980.
186. Hobar, P. C., Rohrich, R. J., and Mickel, T. J. The coracobrachialis muscle flap for coverage of exposed axillary vessels: a salvage procedure. *Plast Reconstr Surg*. 85: 801, 1990.
187. Mahakkanukrauh, P., and Somsarp, V. Dual innervation of the brachialis muscle. *Clin Anat*. 15: 206, 2002.
188. Omokawa, S., Takaoka, T., Shigematsu, K., Inada, Y., Tanaka, Y., Yajima, H., and Takakura, Y. Reverse-flow island flap from the thenar area of the hand. *J Reconstr Microsurg*. 18: 659, 2002.
189. Omokawa, S., Mizumoto, S., Fukui, A., Inada, Y., and Tamai, S. Innervated radial thenar flap combined with radial forearm flap transfer for thumb reconstruction. *Plast Reconstr Surg*. 107: 152, 2001.
190. Omokawa, S., Ryu, J., Tang, J. B., and Han, J. Vascular and neural anatomy of the thenar area of the hand: its surgical applications. *Plast Reconstr Surg*. 99: 116, 1997.

191. Nahai, F., Silverton, J. S., Hill, H. L., and Vasconez, L. O. The tensor fascia lata musculocutaneous flap. *Ann Plast Surg.* 1: 372, 1978.
192. Khalil, I. M., and Sudarsky, L. Sartorius muscle "twist" rotation flap: an answer to flap necrosis. *J Vasc Surg.* 6: 93, 1987.
193. Markee, J. E., Logue Jr, J. T., Williams, M., Stanton, W., Wrenn, R., and Walker, L. Two-joint muscles of the thigh. *The Journal of Bone and Joint Surgery (American).* 37: 125, 1955.
194. Kadir, S., and Brothers, M. F. Atlas of normal and variant angiographic anatomy. Vol. 57: Saunders, 1991.
195. Rohen, J. W., Yokochi, C., Lütjen-Drecoll, E., and Romrell, L. J. Color atlas of anatomy: Lippincott Williams & Wilkins, 1998.
196. Frank, H. N., and Netter, M. Atlas of human anatomy: Elsevier Books, 2006.
197. Netter, F. H. Atlas of human anatomy: Saunders Title, 2010.
198. Vazquez, M., Murillo, J., Maranillo, E., Parkin, I., and Sanudo, J. Patterns of the circumflex femoral arteries revisited. *Clinical Anatomy.* 20: 180, 2007.
199. Gautier, E., Ganz, K., Krugel, N., Gill, T., and Ganz, R. Anatomy of the medial femoral circumflex artery and its surgical implications. *Journal of Bone and Joint Surgery-British Volume.* 82: 679, 2000.
200. Massoud, T., and Fletcher, E. Anatomical variants of the profunda femoris artery: an angiographic study. *Surgical and Radiologic Anatomy.* 19: 99, 1997.
201. Tobin, G. R. Hemisoleus and reversed hemisoleus flaps. *Plast Reconstr Surg.* 76: 87, 1985.
202. Dubreuil-Chambardel, L. Variation des Arteres du Pelvis et du Membre Inferieur. Paris: Mason, 1925.